



MODERN FLIGHT CONTROL DESIGN,
IMPLEMENTATION, AND FLIGHT TEST

THESIS
Phillip T. Edwards
Captain, USAF

AFIT/GAE/ENY/97M-01

DISTRIBUTION STATEMENT A

Approved for public release
Distribution Unlimited

DEPARTMENT OF THE AIR FORCE
AIR UNIVERSITY
AIR FORCE INSTITUTE OF TECHNOLOGY

Wright-Patterson Air Force Base, Ohio

DTIC QUALITY INSPECTED 1

AFIT/GAE/ENY/97M-01

MODERN FLIGHT CONTROL DESIGN,
IMPLEMENTATION, AND FLIGHT TEST

THESIS
Phillip T. Edwards
Captain, USAF

AFIT/GAE/ENY/97M-01

19970402 089

The views expressed in this thesis are those of the author and do not reflect the official policy or position of the Department of Defense or the U.S. Government

AFIT/GAE/ENY/97M-01

MODERN FLIGHT CONTROL DESIGN, IMPLEMENTATION, AND FLIGHT TEST

THESIS

Presented to the Faculty of the School of Engineering
of the Air Force Institute of Technology

Air University

In Partial Fulfillment of the
Requirements for a Degree of
Master of Science

Phillip T. Edwards, B.S.

Captain, USAF

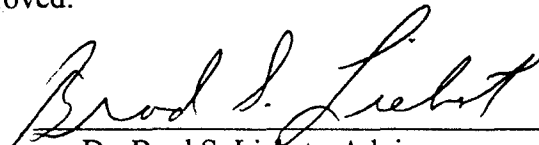
March 1997

Approved for public release; distribution unlimited

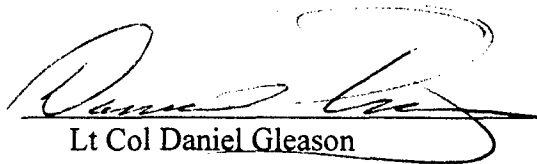
MODERN FLIGHT CONTROL DESIGN, IMPLEMENTATION, AND FLIGHT TEST

Phillip T. Edwards, B.S.
Captain, USAF

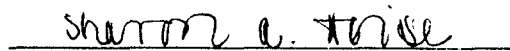
Approved:


Dr. Brad S. Liebst - Advisor

24 FEB 97
Date


Lt Col Daniel Gleason

11 Feb 97
Date


Capt Sharon Heise

24 FEB 97
Date

Acknowledgments

This research could never have been completed without the help and support from a number of people. I would first like to thank my fellow Test Pilot School classmates, specifically the Have Infinity test team: Tony Deliberato, Phil Fittante, Steve Snyder, and Tom Yarger. Not only were these four individuals instrumental in preparing and conducting the flight test, but they helped minimize my TPS workload prior to the flight test so I could complete the flight control system designs and work on the implementation problems that faced this project. My fellow Joint AFIT/TPS students, Pat Peters and Roger Vincent were helpful throughout the entire program, guiding my way, taking care of me and setting an example of excellence. This thesis would never have reached completion without all of their help and support.

I would like to thank the pilots, engineers, and support personnel from Calspan corporation. They provided the test-bed for the flight test and worked hard to ensure all the sorties were successfully completed. I owe an unmeasurable level of gratitude to Russ Easter. He provided me with encouragement, insights, and motivation by working overtime to conquer the implementation problems and provide the proper simulated aircraft dynamics in the Variable Stability System II Learjet. The designs' implementation and flight test success was a direct result of Russ Easter's dedication and expertise.

I wish to thank my advisor, Dr. Brad Liebst for accepting the position so late in the process and for remaining at AFIT through my defense, unlike my first two advisors. I would also like to thank the members of my research committee, Dr. Sharon Heise, and LTC Dan Gleason, for joining the team and being willing to review my research

I would never have completed this thesis without the support and encouragement of Melissa, thank you for just being in my life during a very challenging period. Finally, I would like to thank God for leading me and providing the strength to continue when the task seemed impossible.

Table of Contents

	Page
Acknowledgments.....	iii
List of Figures.....	vii
List of Tables.....	x
List of Abbreviations, Acronyms, and Symbols	xi
Abstract.....	xv
I. Introduction.....	1-1
1.1. Background/Motivation.....	1-1
1.2. Research Objectives	1-2
1.3. Thesis Outline	1-3
II. Preliminaries	2-1
2.1. Control Theory	2-1
2.1.1. Classical Control Theory.....	2-1
2.1.2. H_2 Control Theory	2-2
2.1.3. H_∞ Control Theory	2-6
2.1.4. Mixed H_2/H_∞ Control Theory.....	2-9
2.2. Handling Qualities Analysis	2-17
2.2.1. Bandwidth Criteria	2-17
2.2.2. Ralph Smith Criteria.....	2-19
2.3. TPS Project.....	2-22
2.4. CALSPAN Variable Stability Simulator II Learjet	2-24
2.5. Summary.....	2-26
III. Model Set-up and Design.....	3-1
3.1. Aircraft Plant Model.....	3-1
3.2. Wind and Sensor Noise Model / Intensity Determination	3-3
3.3. Evaluation Models.....	3-4

3.3.1.	Time Domain Evaluation	3-5
3.3.2.	Handling Qualities Evaluation.....	3-6
3.4.	Design Models and Resulting Designs	3-6
3.4.1.	Classical Design Set-up and Resulting Design	3-6
3.4.2.	H ₂ Design Set-up and Resulting Design	3-9
3.4.3.	H _∞ Design Set-up and Resulting Design	3-13
3.4.4.	Mixed H ₂ /H _∞ Design Set-up and Resulting Design	3-17
3.5.	Summary	3-21
VI.	Implementation	4-1
4.1.	Implementation Model.....	4-1
4.1.1.	VSS II System Limitations	4-1
4.1.2.	Final H ₂ , H _∞ , and Mixed H ₂ / H _∞ Implementation Model	4-3
4.2.	Verification and Validation Testing	4-6
V.	Flight Test Results	5-1
5.1.	Test Objective	5-1
5.2.	Test Procedures	5-2
5.2.1.	Methods and Conditions.....	5-2
5.2.2.	Offset Landing Task:.....	5-3
5.2.2.1.	Landing Zone	5-4
5.2.2.2.	Landing Task Evaluation.....	5-4
5.3.	Results and Analysis.....	5-5
5.3.1.	Classical Flight Control Configuration.....	5-5
5.3.2.	H ₂ Flight Control Configuration.....	5-6
5.3.3.	H _∞ Flight Control Configuration	5-6
5.3.4.	Mixed H ₂ /H _∞ Flight Control Configuration.....	5-7
5.3.5.	Overall Results:	5-7
VI.	Conclusions and Recommendations.....	6-1

6.1.	Summary.....	6-1
6.2.	Recommendations.....	6-3
Appendix A	Aircraft Model Data	A-1
Appendix B	Design Evaluation Script Files	B-1
Appendix C	Design Phase Time Histories	C-1
Appendix D	Data Acquisition Parameters	D-1
Appendix E	Data Analysis Plots	E-1
Appendix F	Test Card and Rating Scales.....	F-1
Appendix G	Pilot Comments Data Base.....	G-1
Appendix H	Flight Test Data.....	H-1
Bibliography	BIB-1
Vita	VITA-1

List of Figures

Figure	Page
2.1. Block Diagram.....	2-1
2.2. General H_2 Feedback System.....	2-3
2.3. H_2 System with Parametrized Controller	2-4
2.4. General H_∞ Feedback System	2-6
2.5. H_∞ System with Parametrized Controller.....	2-8
2.6. General Mixed H_2/H_∞ Design Diagram	2-10
2.7. Typical Mixed H_2/H_∞ α Versus γ Curve	2-17
2.8. Definition of Bandwidth Frequency ω_{BW} from Open Loop Frequency Response	2-18
2.9. Bandwidth Requirements, Category C Flight Phase	2-19
2.10. Criterion Phase Angle Versus Cooper-Harper Rating.....	2-21
2.11. Predicted Pitch Axis PIO Rating for Conventional Flight Control Systems	2-22
2.12. TPS FCS Design Option 1 (Nominal).....	2-23
2.13. Example SIMULINK Block Diagram for a VSS II Acceptable System.....	2-26
3.1. General Evaluation System	3-4
3.2. Classical Evaluation Model	3-5
3.3. Classical Design Model Block Diagram	3-6
3.4. Category C Bandwidth Requirements: Classical Design	3-7
3.5. H_2 Design Model Block Diagram	3-9
3.6. Category C Bandwidth Requirements: H_2 Design.....	3-12
3.7. H_∞ Design Model Block Diagram.....	3-13
3.8. Category C Bandwidth Requirements: H_∞ Design.....	3-16
3.9. Mixed H_2/H_∞ α Versus γ Curve	3-18
3.10. Category C Bandwidth Requirements: Mixed Design	3-20
3.11. Category C Bandwidth Requirements: All Designs	3-21
4.1. Initial Implementation Model	4-3

4.2.	Implementation Block Diagram	4-4
5.1.	Landing Zone Markings and Dimensions	5-4
C.1.	Classical Design Time Histories (Set 1 of 2)	C-1
C.2.	Classical Design Time Histories (Set 2 of 2)	C-2
C.3.	H ₂ Design Time Histories (Set 1 of 2)	C-3
C.4.	H ₂ Design Time Histories (Set 2 of 2)	C-4
C.5.	H _∞ Design Time Histories (Set 1 of 2)	C-5
C.6.	H _∞ Design Time Histories (Set 2 of 2)	C-6
C.7.	Mixed Design Time Histories (Set 1 of 2)	C-7
C.8.	Mixed Design Time Histories (Set 2 of 2)	C-8
C.9.	All Designs Time Histories (Set 1 of 2)	C-9
C.10.	All Designs Time Histories (Set 2 of 2)	C-10
C.11.	All Designs Singular Value Plots	C-11
E.1.	Classical Design Bode Plot, Closed Loop, Alpha/PTI Sweep	E-1
E.2.	Classical Design Bode Plot, Closed Loop, Pitch Rate/PTI Sweep	E-2
E.3.	H ₂ Design Bode Plot, Closed Loop, Alpha/PTI Sweep	E-3
E.4.	H ₂ Design Bode Plot, Closed Loop, Pitch Rate/PTI Sweep	E-4
E.5.	H _∞ Design Bode Plot, Closed Loop, Alpha/PTI Sweep	E-5
E.6.	H _∞ Design Bode Plot, Closed Loop, Pitch Rate/PTI Sweep	E-6
E.7.	Mixed Design Bode Plot, Closed Loop, Alpha/PTI Sweep	E-7
E.8.	Mixed Design Bode Plot, Closed Loop, Pitch Rate/PTI Sweep	E-8
E.9.	Step Input Time Histories, Classical Design	E-9
E.10.	Step Input Time Histories; H ₂ Design	E-10
E.11.	Step Input Time Histories; H _∞ Design	E-11
E.12.	Step Input Time Histories; Mixed Design	E-12
F.1.	Sample Test Card	F-1
F.2.	Cooper Harper Rating Scale	F-2

F.3.	PIO Rating Decision Tree.....	F-3
H.1.	Classical Flight Control Design Handling Quality Ratings.....	H-1
H.2.	Classical Flight Control Design Pilot Induced Oscillation Ratings.....	H-2
H.3.	H ₂ Flight Control Design Handling Quality Ratings.....	H-3
H.4.	H ₂ Flight Control Design Pilot Induced Oscillation Ratings.....	H-4
H.5.	H _∞ Flight Control Design Handling Quality Ratings	H-5
H.6.	H _∞ Flight Control Design Pilot Induced Oscillation Ratings	H-6
H.7.	Mixed Flight Control Design Handling Quality Ratings.....	H-7
H.8.	Mixed Flight Control Design Pilot Induced Oscillation Ratings.....	H-8

List of Tables

Table	Page
2.1. TPS FCS Design Option 1, Nominal Gains and Ranges	2-23
2.2. Learjet Limitations	2-25
3.1. RSmith Handling Qualities Predicted Level for the Classical Design.....	3-8
3.2. Classical Design Vector Stability Margins.....	3-8
3.3. H ₂ Design Weighting.....	3-11
3.4. RSmith Handling Qualities Predicted Level for the H ₂ Design.....	3-13
3.5. H ₂ Design Vector Stability Margins.....	3-13
3.6. RSmith Handling Qualities Predicted Level for the H _∞ Design	3-16
3.7. H _∞ Design Vector Stability Margins	3-16
3.8. Design Weighting for the Mixed H ₂ Sub-Problem.....	3-18
3.9. RSmith Handling Qualities Predicted Level for the Mixed Design.....	3-20
3.10. Mixed Design Vector Stability Margins.....	3-20
3.11. RSmith Handling Qualities Predicted Level Summary	3-21
3.12. Vector Stability Margin Summary.....	3-22
4.1. Reduced Order Controllers	4-2
5.1. Evaluation Pilots' Flying Experience.....	5-2
D.1. Data Aquisition Parameters Recorded During Testing.....	D-1

List of Abbreviations, Acronyms, and Symbols

<u>Abbreviation</u>	<u>Definition</u>
AFB	Air Force Base
AFFTC	Air Force Flight Test Center
AGL	above ground level
ARE	Algebraic Ricatti Equation
B+	Lack of recognition, injustice
CH	Cooper-Harper
d	bounded (but unknown) energy input
dB	decibel(s)
deg	degree(s)
dom(Ric)	domain of the Riccati operator
e	H_∞ controlled system outputs
FAA	Federal Aviation Administration
FBW	fly-by-wire
FCS	flight control system
F_{es}	elevator stick force
FRA	frequency response analyses
ft	foot, feet
g	acceleration due to gravity
G	aircraft plant transfer function
gpm	gallons per minute
Hz	hertz
ILS	instrument landing system
in	inch(es)
K	controller transfer function

List of Abbreviations, Acronyms, and Symbols (Continued)

<u>Abbreviation</u>	<u>Definition</u>
K_a	angle of attack gain
KAS	knots airspeed
KCAS	knots calibrated airspeed
KIAS	knots indicated airspeed
K_q	pitch rate gain
kt	knot(s)
lb	pound(s)
LFT	lower fractional transformation
LQG	linear quadratic gaussian
MIL-STD	military standard
MIMO	multiple-input-multiple-output
MSL	mean sea level
No.	number
n_z	normal acceleration
P	linear, time invariant aircraft plant model
PC-FRA	personal computer-frequency response analyses
PIO	pilot induced oscillation
PTI	programmed test inputs
q	pitch rate
Q	constrained freedom parameter
r	commanded input
rad/sec	radians per second
Ric	Riccati operator - Ric : $M \rightarrow X$ or $X=Ric(M)$
RSmith	Ralph Smith handling qualities criteria

List of Abbreviations, Acronyms, and Symbols (Continued)

<u>Abbreviation</u>	<u>Definition</u>
S	slope parameter
S	sensitivity function
S/N	serial number
sec	second(s)
SISO	single-input-single-output
T	complementary sensitivity function
T_{ed}	closed loop transfer function in H_{∞} optimization problems
TPS	USAF Test Pilot School
T_{zw}	closed loop transfer function in H_2 optimization problems
USAF	United States Air Force
USN	United States Navy
UWGN	unit intensity white gaussian noise
v	forward true velocity
VHF	very high frequency
VSS II	Variable Stability Simulator II
w	H_2 exogenous inputs
x_{act}	actuator state
y	system outputs
z	H_2 controlled system outputs
α	two-norm
$\underline{\alpha}$	minimum attainable two-norm
γ	∞ - norm
$\underline{\gamma}$	minimum attainable ∞ - norm
ω	frequency

List of Abbreviations, Acronyms, and Symbols (Continued)

<u>Abbreviation</u>	<u>Definition</u>
ϕ	phase angle
θ	pitch angle
γ	glide-path angle
α	angle of attack
Γ	process noise distribution matrix
ζ	damping ratio
$\bar{\sigma}$	maximum singular value
σ	natural frequency
$\Theta(j\omega)$	normal acceleration phase angle parameter
ω_c	criterion frequency
δ_e	elevator deflection
τ_p	equivalent time delay

Abstract

This thesis addresses the application issues raised implementing flight control designs derived from optimal control theory and the challenges in obtaining acceptable handling qualities when using these techniques. Using the USAF TPS FCS project as the controller architecture, four controllers were designed using classical methods, and H_2 , H_∞ , and mixed H_2/H_∞ optimal control theory. These designs were implemented in the Calspan VSS II Learjet, simulating unstable aircraft longitudinal dynamics and a limited handling qualities flight test evaluation was performed. The design phase found the optimal control techniques, as applied, difficult to design to handling qualities specifications. The H_2 , H_∞ , and mixed H_2/H_∞ controllers were unstable and often contained high frequency poles, which were difficult to implement. The flight test rated the designs acceptable on approach, but no handling qualities level for approach was determined.

MODERN FLIGHT CONTROL DESIGN, IMPLEMENTATION AND FLIGHT TEST

I. Introduction

1.1. Background/Motivation

Flight controller designs for piloted aircraft have become increasingly more complex in the past few years with the advent of fly-by-wire control systems [Ber88]. Modern aircraft now have the capability to use both conventional and innovative control surfaces and systems to increase performance and reduce drag and radar cross section. While these systems greatly enhance capabilities, the challenges to the flight control designer have grown exponentially. Single-input-single-output (SISO) systems become multiple-input-multiple-output (MIMO) systems. Modeling the aircraft dynamics, which has never been an exact science [DFT92], is more complex. To simplify the design process, a linear, time invariant system model is developed about an operating point or nominal condition. The primary purpose of a flight control system for piloted aircraft is to provide acceptable handling qualities to accomplish a mission flight phase [TPS95]. Embedded in this requirement for good handling qualities is the objective to obtain nominal and robust stability and performance. Ultimately the pilot completes the flight control system, and as handling qualities degrade, the pilot becomes unable to perform piloting duties. Stability and performance alone are not sufficient if a pilot cannot control the aircraft.

There has been considerable research developing design techniques to optimize flight control systems to reduce noise introduced into the system, and provide robust stability to the system [Gan86]. These techniques include H_2 control theory, H_∞ control theory, and a Mixed H_2/H_∞ control theory [RW95]. H_2 optimization minimizes the system's output energy when the system is faced with white Gaussian noise inputs. The H_2 design technique targets noise rejection as its main objective. H_∞ optimization minimizes the system's output energy to unknown, bounded energy inputs, which results in a highly robust system. The H_∞ design technique targets system stability margins and also provides good tracking. Mixed H_2/H_∞ optimization combines the objectives of H_2 and H_∞ optimization by limiting the H_2 problem with an H_∞ constraint. The Mixed H_2/H_∞ design technique optimally trades off noise rejection with the tracking and

robust stability objectives to obtain a system targeting all of these goals. All of these design methods are capable of handling both SISO and MIMO systems. These techniques do not directly provide assurances of acceptable handling qualities in the flight control systems designed by these methods. The previous research on these methods has focused on improving the numeric solutions of these techniques. Although example applications of these techniques have been analyzed for robustness and some measures of performance, little has been done to investigate the resulting design's handling qualities.

There are several handling qualities design criteria for evaluating flight control designs described in the Department of Defense MIL-STD-1797A, *Flying Qualities of Piloted Aircraft* [Mil90]. These criteria are used to predict an aircraft's handling qualities based on historical pilot evaluations. Of these criteria, Hoh's Bandwidth Criteria [Hoh81] and Ralph Smith Criteria [SG79] are accepted as predictors of an aircraft's handling qualities. The USAF Test Pilot School (TPS), as part of its curriculum, uses these criteria to evaluate student designed flight control systems during the Flight Control System (FCS) design project. This project then implements the FCS in the CALSPAN Variable Stability Simulator II (VSS II) Learjet [Bal93] to allow the TPS students to evaluate the handling qualities of their design. This project is well suited for implementation and a limited handling qualities evaluation of augmented longitudinal flight control systems designed with optimization techniques.

1.2 Research Objectives

The purpose of this thesis is to investigate the implementation of flight control systems designed using H_2 , H_∞ , and Mixed H_2/H_∞ design techniques and evaluate the resulting handling qualities of these designs. This research applies modern optimal control theory to the USAF TPS FCS design project, used in the TPS curriculum from 1994 through 1995. These designs, as well as a classically designed flight control system, were implemented in the CALSPAN VSS II Learjet and evaluated for handling qualities during flight test. The classically designed flight control system served as a control case for comparison and was used to help verify proper implementation of the un-augmented aerodynamics simulated by the VSS II system. The classical design serves as a base-line and is not intended to be compared to the optimal control theory designs to determine which method can achieve a "better" controller. This thesis addresses the

application issues raised implementing flight control designs derived from optimal control theory and the challenges in obtaining acceptable handling qualities when using these techniques.

1.3 Thesis Outline

This thesis is divided into six chapters, including this introductory chapter. The second chapter presents the necessary groundwork for this research. The control theory used to develop the flight control designs is discussed in the first section of Chapter II. An explanation of the handling qualities criteria used to evaluate the designs is then presented. The third section of this chapter addresses the TPS FCS project on which this research is based. Finally, a description of the CALSPAN VSS II Learjet and its limitations is presented.

In Chapter III, the various models used in this research are developed. The aircraft aerodynamic model, in both transfer function and state space form, is derived from the stability derivatives of the intended target aircraft. The models for wind gust noise and sensor noise, used in the design and computer evaluation, are then developed. The third section addresses the structure of the closed loop system used in each of the designs. It also explains the model used in the computer simulations to evaluate the designs and in the handling qualities predictions. The fourth section describes the set-up for each design method, comments on the design process and presents the resulting designs.

Chapter IV describes the implementation of the flight control designs. It discusses the controller model used in implementation and the issues raised developing this model. This chapter also presents the results of the ground and flight verification and validation testing.

The fifth chapter addresses the flight test. It describes the flight test objectives, and the methods and procedures used during the flight test. The flight test results are presented and then analyzed. The flight test analysis focuses on the handling qualities ratings determined during the test, and on the conclusions that can be drawn based on these results.

The final chapter summarizes the findings of this study, presents some conclusions and provides recommendations for areas of future research.

II. Preliminaries

2.1. Control Theory

The control theory and the optimization techniques presented in this section are all well developed processes. This section will summarize the basic principles and assumptions made by the design methods used for each of the flight controllers examined in this thesis. A very general description of the classical control theory used to design the classical controller will first be discussed. The remaining subsections present the basic development of H_2 , H_∞ , and Mixed H_2/H_∞ optimization.

2.1.1. Classical Control Theory

Flight control designs have classically used single loop frequency response and root locus design techniques to solve the control problem. When multiple feedback loops are required to achieve the desired stability and performance objectives, classical control theory predominantly relies on one-loop-at-time frequency response and root locus design techniques [Gan86]. While classical control theory encompasses a broader range of techniques than presented here, this discussion will be limited to the techniques specified in the TPS project outlined later in this chapter.

The classical design method starts with a block diagram like that shown in Figure 2.1. Here G represents the linearized aircraft modeled dynamics and K the designed controller. The commanded input is labeled r , and the outputs of interest are depicted by y . Transfer function representations for G and K are commonly used, as is a negative feedback sign convention. The controller can be a simple gain,

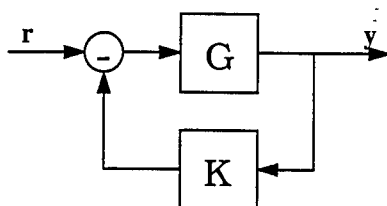


Figure 2.1. Block Diagram

or a dynamic filter. A root locus of all possible closed loop root locations for a given loop transfer function as loop gain is varied is then plotted for the system and gains are chosen to place the closed loop poles in a desired region of the plot. Frequency response plots, or Bode plots are used to analyze the loop transfer function gain magnitude and phase angle to determine the system loop shape. The feedback gains and controller dynamics are varied until the desired system response is obtained. As multiple loop closures and higher order controller dynamics are used, this iterative process requires significant engineering insight and experience [Gan86].

2.1.2. H_2 Control Theory

The objective of an H_2 design is to synthesize a controller which minimizes the energy of a system output faced with a zero-mean, Unit intensity White Gaussian Noise (UWGN) input. H_2 optimization is a generalization of the standard Linear Quadratic Gaussian (LQG) problem [Doy89]. The feedback system used for H_2 optimization can be depicted in general form, shown in Figure 2.2. The linear, time-invariant aircraft model is defined by P . The block represented by P also includes parameter weightings used to obtain the desired H_2 controller design. The controller developed by the design techniques is represented by K_2 . The exogenous inputs to the system are shown as w , and the controlled system outputs are represented as z . The measured outputs from the system are shown as y and are input to the controller. The controller output signal is labeled u and is fed back into the system. The symbol T_{zw} represents the closed loop system.

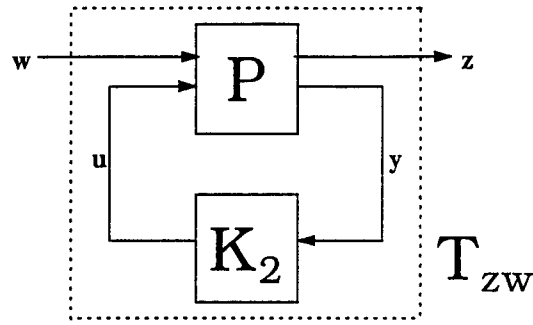


Figure 2.2. General H_2 Feedback System

The plant P can be partitioned into separate input and output transfer functions

$$P = \begin{bmatrix} P_{zw} & P_{zu} \\ P_{yw} & P_{yu} \end{bmatrix} \quad (2.1)$$

where

$$\begin{aligned} z &= P_{zw}w + P_{zu}u \\ y &= P_{yw}w + P_{yu}u \end{aligned} \quad (2.2)$$

A state space realization of P can be written as

$$\begin{aligned} \dot{x}_2 &= A_2 x_2 + B_w w + B_{u_2} u \\ z &= C_z x_2 + D_{zw} w + D_{zu} u \\ y &= C_{y_2} x_2 + D_{yw} w + D_{yu} u \end{aligned} \quad (2.3)$$

where the 2 subscript indicates the problem setup for H_2 optimization. Minimizing the energy of the system output to a UWGN input is equivalent to minimizing the 2-norm of the closed-loop transfer function, T_{zw} [RW95]. This minimal value of the 2-norm, $\underline{\alpha}$, is defined to be [Wal94]:

$$\underline{\alpha} = \inf_{K(s) \text{ Stabilizing}} \|z\|_2 \quad (2.4)$$

$$= \inf_{K(s) \text{ Stabilizing}} \|T_{zw}\|_2 \quad (2.5)$$

$$= \inf_{K(s) \text{ Stabilizing}} \|P_{zw} + P_{zu} K(I - P_{yu} K)^{-1} P_{yw}\|_2 \quad (2.6)$$

The following assumptions are made:

- i. $D_{zw} = 0$
- ii. $D_{yu} = 0$
- iii. (A, B_u) is stabilizable and (C_y, A) is detectable
- iv. $D_{zu}^T D_{zu} = I$ and $D_{yw} D_{yw}^T = I$
- v. $\begin{bmatrix} A - j\omega I & B_u \\ C_z & D_{zu} \end{bmatrix}$ has full column rank
- vi. $\begin{bmatrix} A - j\omega I & B_w \\ C_y & D_{yw} \end{bmatrix}$ has full row rank

Assumption (i) assures that the closed loop two-norm of the system is finite. Condition (ii) makes the development easier but can be removed completely. Condition (iii) is necessary for the existence of stabilizing solutions. Assumption (iv) is a regularity condition which insures that there is a direct penalty on all controls and no perfect measurements. Finally, requirements (v) and (vi) are required to ensure the existence of stabilizing solutions to the two Algebraic Riccati Equations (ARE) in the H_2 solution.

All stabilizing H_2 controllers can be parametrized by a family of lower fractional transformations (LFT) of a transfer function J and a constrained freedom parameter $Q \in H_2$ [Wal94], shown in Figure 2.3.

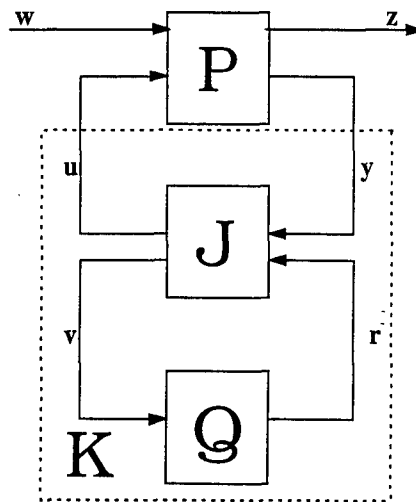


Figure 2.3. H_2 System with Parametrized Controller

The freedom parameter is used to identify sub-optimal H_2 controllers, which are useful for computing designs that trade off H_2 performance for H_∞ performance. One particular form of J is given by

$$J(s) = \begin{bmatrix} J_{uy} & J_{ur} \\ J_{vy} & J_{vr} \end{bmatrix} = \left[\begin{array}{c|cc} A_j & K_f & K_{fl} \\ \hline -K_c & 0 & I \\ K_{cl} & I & 0 \end{array} \right] \quad (2.7)$$

(2.8)

where

$$A_j = A - K_f C_{y_2} - B_{u_2} K_c \quad (2.9)$$

$$K_c = B_{u_2}^T X_2 + D_{zu}^T C_z \quad (2.10)$$

$$K_f = Y_2 C_{y_2}^T + B_w D_{yw}^T \quad (2.11)$$

$$K_{cl} = -C_{y_2} \quad (2.12)$$

$$K_{fl} = B_{u_2} \quad (2.13)$$

X_2 and Y_2 are the real, unique, symmetric positive semi-definite solutions to the AREs

$$(A - B_{u_2} D_{zu}^T C_z)^T X_2 + X_2 (A - B_{u_2} D_{zu}^T C_z) - X_2 B_{u_2} B_{u_2}^T X_2 + \hat{C}_z^T \hat{C}_z = 0 \quad (2.14)$$

where

$$\hat{C}_z = (I - D_{zu} D_{zu}^T) C_z \quad (2.15)$$

and

$$(A - B_w D_{yw}^T C_{y_2}) Y_2 + Y_2 (A - B_w D_{yw}^T C_{y_2})^T - Y_2 C_{y_2}^T C_{y_2} Y_2 + \hat{B}_w \hat{B}_w^T = 0 \quad (2.16)$$

where

$$\hat{B}_w = B_w (I - D_{yw}^T D_{yw}) \quad (2.17)$$

The controller is unique and optimal if $Q = 0$, otherwise the set of all controllers such that $\|T_{zw}\| \leq \alpha$ is

parametrized by any $Q \in H_2$ such that

$$\|Q\|_2^2 \leq \alpha^2 - \underline{\alpha}^2 \quad (2.18)$$

When Q is chosen to be identically equal to zero, the resulting optimal controller is

$$K_{2_{opt}} = \left[\begin{array}{c|c} A_j & K_f \\ \hline -K_c & 0 \end{array} \right] \quad (2.19)$$

2.1.3. H_∞ Control Theory

The objective of an H_∞ design is to synthesize a stabilizing controller which minimizes the maximum energy of the output e , given a bounded energy input, d [Dec94]. The feedback system used for H_∞ optimization is depicted in Figure 2.4 and is identical to the H_2 block diagram with the input and output re-labeled for distinction between the design methods.

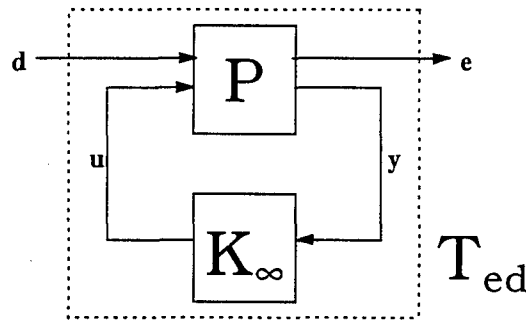


Figure 2.4. General H_∞ Feedback System

The plant P can be partitioned into separate input and output transfer functions

$$P = \begin{bmatrix} P_{ed} & P_{eu} \\ P_{yd} & P_{yu} \end{bmatrix} \quad (2.20)$$

where

$$\begin{aligned} e &= P_{ed}w + P_{eu}u \\ y &= P_{yd}w + P_{yu}u \end{aligned} \quad (2.21)$$

A state space realization of P can be written as

$$\begin{aligned} \dot{x}_\infty &= A_\infty x_\infty + B_d d + B_u u \\ e &= C_e x_\infty + D_{ed} d + D_{eu} u \\ y &= C_y x_\infty + D_{yd} d + D_{yu} u \end{aligned} \quad (2.22)$$

where the ∞ subscript indicates the problem setup for H_∞ optimization. Minimizing the energy of the output to an exogenous, bounded energy input is equivalent to minimizing the ∞ - norm of the closed-loop transfer function, T_{ed} [RW95]. This minimum achievable value of the ∞ - norm, γ , is defined to be

$$\underline{\gamma} = \inf_{K \text{ Stabilizing}} \sup_{\|d\|_2 \leq 1} \|e\|_2 = \inf_{K \text{ Stabilizing}} \|T_{ed}\|_\infty \quad (2.23)$$

where the infinity-norm of T_{ed} is

$$\|T_{ed}\|_\infty = \sup_\omega \bar{\sigma}[T_{ed}] \quad (2.24)$$

and $\bar{\sigma}$ denotes the maximum singular value.

The following assumptions are made:

- i. $D_{ed} = 0$
- ii. $D_{yu} = 0$
- iii. (A, B_u) is stabilizable and (C_y, A) is detectable
- iv. $D_{eu}^T D_{eu} = I$ and $D_{yd} D_{yd}^T = I$
- v. $\begin{bmatrix} A - j\omega I & B_u \\ C_e & D_{eu} \end{bmatrix}$ has full column rank
- vi. $\begin{bmatrix} A - j\omega I & B_d \\ C_y & D_{yd} \end{bmatrix}$ has full row rank

Assumption (i) and (ii) are not required for a solution to exist, but reduce the complexity of the solution. Condition (iii) is necessary for the existence of stabilizing solutions. Assumption (iv) is a regularity condition which insures that there is a direct penalty on all controls and that no perfect measurements are allowed. Finally, requirements (v) and (vi) are required to ensure the existence of stabilizing solutions to the two AREs in the H_∞ solution.

The H_∞ optimal controller found by the optimization process is not unique. This process is iterative and is based on the parametrization of all sub-optimal controllers where

$$\|T_{ed}\|_\infty < \gamma \quad (2.25)$$

The family of all admissible controllers which satisfy (2.25) is given by the LFT (Figure 2.5)

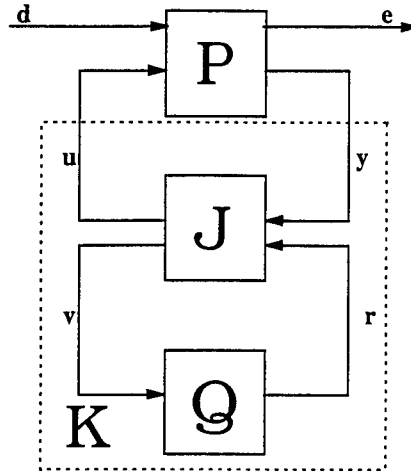


Figure 2.5. H_∞ System with Parametrized Controller

where

$$J(s) = \begin{bmatrix} J_{uy} & J_{ur} \\ J_{vy} & J_{vr} \end{bmatrix} = \begin{bmatrix} A_j & K_f & K_{fl} \\ -K_c & 0 & I \\ K_{cl} & I & 0 \end{bmatrix} \quad (2.26)$$

and

$$A_j = A - K_f C_{y\infty} - B_{u\infty} K_c + \gamma^{-2} Y_\infty C_e^T (C_e - D_{eu} K_c) \quad (2.27)$$

$$K_c = (B_{u\infty}^T X_\infty + D_{eu}^T C_e) (I - \gamma^{-2} Y_\infty X_\infty)^{-1} \quad (2.28)$$

$$K_f = Y_\infty C_{y\infty}^T + B_d D_{yd}^T \quad (2.29)$$

$$K_{cl} = -(\gamma^{-2} D_{yd} B_d^T X_\infty + C_{y\infty}) (I - \gamma^{-2} Y_\infty X_\infty)^{-1} \quad (2.30)$$

$$K_{fl} = \gamma^{-2} Y_\infty C_e^T D_{eu} + B_{u\infty} \quad (2.31)$$

The matrices X_∞ and Y_∞ are solutions to the AREs

$$(A - B_{u\infty} D_{eu}^T C_e)^T X_\infty + X_\infty (A - B_{u\infty} D_{eu}^T C_e) + X_\infty (\gamma^{-2} B_d B_d^T - B_{u\infty} B_{u\infty}^T) X_\infty + \hat{C}_e^T \hat{C}_e = 0 \quad (2.32)$$

where

$$\hat{C}_e = (I - D_{eu} D_{eu}^T) C_e \quad (2.33)$$

and

$$(A - B_d D_{yd}^T C_{y_-}) Y_\infty + Y_\infty (A - B_d D_{yd}^T C_{y_-})^T + Y_\infty (\gamma^{-2} C_e^T C_e - C_{y_-}^T C_{y_-}) Y_\infty + \hat{B}_d \hat{B}_d^T = 0 \quad (2.34)$$

where

$$\hat{B}_d = B_d (I - D_{yd}^T D_{yd}) \quad (2.35)$$

With that stated, Q can be chosen to be any $Q \in H_\infty$ such that

$$\|Q\|_\infty < \gamma \quad (2.36)$$

This parametrization of a controller K is valid if and only if the following three conditions hold :

- i. $H_X \in \text{dom}(\text{Ric})$ with $X_\infty = \text{Ric}(H_X) \geq 0$
- ii. $H_Y \in \text{dom}(\text{Ric})$ with $Y_\infty = \text{Ric}(H_Y) \geq 0$
- iii. $\rho(Y_\infty X_\infty) < \gamma^2$

where H_X and H_Y are the Hamiltonians associated with (2.32) and (2.34) [Wal94].

As previously stated, the process of finding a controller with a closed-loop infinity-norm close to γ is iterative. A value for γ is selected, then the above three conditions are checked. If any one of the conditions fail, increase γ and repeat the check. If all three conditions are met, decrease γ until the desired accuracy is obtained.

2.1.4. Mixed H_2/H_∞ Control Theory

The objective of mixed H_2/H_∞ optimization is to achieve the robustness of H_∞ control with the noise rejection properties of H_2 control. The mixed H_2/H_∞ diagram is shown in Figure 2.6. This method, described by Ridgely [Rid91] and Walker [Wal94], poses the H_2 problem, to minimize α with an H_∞ constraint that is constraining the infinity-norm. The final mixed design goal is to determine an admissible controller that meets the following:

$$\inf_{K_{adm}} \|T_{zw}\|_2, \text{ subject to the constraint } \|T_{ed}\|_\infty \leq \gamma \quad (2.37)$$

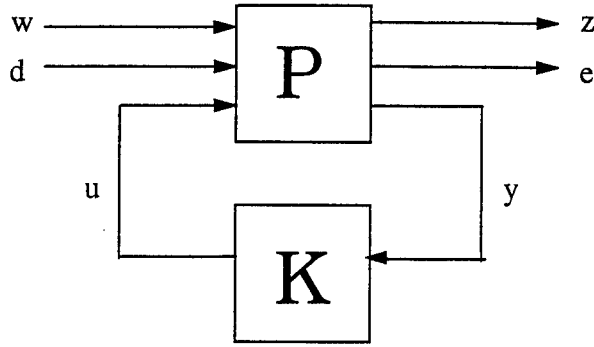


Figure 2.6. General Mixed H_2/H_∞ Design Diagram

The mixed system can be written in general form as

$$\begin{bmatrix} e \\ z \\ y \end{bmatrix} = \begin{bmatrix} P_{ed} & P_{ew} & P_{eu} \\ P_{zd} & P_{zw} & P_{zu} \\ P_{yd} & P_{yw} & P_{yu} \end{bmatrix} \begin{bmatrix} d \\ w \\ u \end{bmatrix} \quad (2.38)$$

A state space representation is given by

$$\dot{x} = \tilde{A}x + \tilde{B}_d d + \tilde{B}_w w + \tilde{B}_u u \quad (2.39)$$

$$e = \tilde{C}_e x + \tilde{D}_{ed} d + \tilde{D}_{ew} w + \tilde{D}_{eu} u \quad (2.40)$$

$$z = \tilde{C}_z x + \tilde{D}_{zd} d + \tilde{D}_{zw} w + \tilde{D}_{zu} u \quad (2.41)$$

$$y = \tilde{C}_y x + \tilde{D}_{yd} d + \tilde{D}_{yw} w + \tilde{D}_{yu} u \quad (2.42)$$

The closed loop transfer functions T_{ed} and T_{zw} for the mixed problem are defined as

$$T_{zw} = C_z (sI - A_2)^{-1} B_w + D_{zw} \quad (2.43)$$

$$T_{ed} = C_e (sI - A_\infty)^{-1} B_d + D_{ed} \quad (2.44)$$

The mixed H_2/H_∞ controller to be developed, in state space form is defined as

$$\dot{x}_c = A_c x_c + B_c y \quad (2.45)$$

$$u = C_c x_c \quad (2.46)$$

Closing the loop of the individual H_2 and H_∞ problems with the above mixed controller results in the following closed-loop state space representations

$$\dot{\mathbf{x}}_2 = \mathbf{A}_2 \mathbf{x}_2 + \mathbf{B}_w w \quad (2.47)$$

$$z = \mathbf{C}_z \mathbf{x}_2 + \mathbf{D}_{zw} w \quad (2.48)$$

and

$$\dot{\mathbf{x}}_\infty = \mathbf{A}_\infty \mathbf{x}_\infty + \mathbf{B}_d d \quad (2.49)$$

$$e = \mathbf{C}_e \mathbf{x}_\infty + \mathbf{D}_{ed} d \quad (2.50)$$

where

$$\mathbf{x}_2 = \begin{bmatrix} x_2 \\ x_c \end{bmatrix} \quad (2.51)$$

$$\mathbf{x}_\infty = \begin{bmatrix} x_\infty \\ x_c \end{bmatrix} \quad (2.52)$$

$$\mathbf{A}_2 = \begin{bmatrix} A_2 & B_{u_2} C_c \\ B_c C_{y_2} & A_c \end{bmatrix} \quad (2.53)$$

$$\mathbf{A}_\infty = \begin{bmatrix} A_\infty & B_{u_\infty} C_c \\ B_c C_{y_\infty} & A_c \end{bmatrix} \quad (2.54)$$

$$\mathbf{B}_w = \begin{bmatrix} B_w \\ B_c D_{yw} \end{bmatrix} \quad (2.55)$$

$$\mathbf{B}_d = \begin{bmatrix} B_d \\ B_c D_{yd} \end{bmatrix} \quad (2.56)$$

$$\mathbf{C}_z = [\mathbf{C}_z \quad D_{zu} \mathbf{C}_c] \quad (2.57)$$

$$\mathbf{C}_e = [\mathbf{C}_e \quad D_{eu} \mathbf{C}_c] \quad (2.58)$$

$$\mathbf{D}_{zw} = 0 \quad (2.59)$$

$$\mathbf{D}_{ed} = D_{ed} \quad (2.60)$$

The assumptions for the mixed problem are a combination of the assumptions for the individual H_2 and H_∞ problems. Walker [Wal94] reduced the assumption list to just those required by the H_2 problem, so the assumptions become

- i. $D_{zw} = 0$

- ii. $D_{yu} = 0$
- iii. (A, B_u) is stabilizable and (C_y, A) is detectable
- iv. $D_{zu}^T D_{zu} = I$ and $D_{yw} D_{yw}^T = I$
- v. $\begin{bmatrix} A - j\omega I & B_u \\ C_z & D_{zu} \end{bmatrix}$ has full column rank
- vi. $\begin{bmatrix} A - j\omega I & B_w \\ C_y & D_{yw} \end{bmatrix}$ has full row rank

Walker found that the H_∞ assumptions could be relaxed since conditions (i-vi) guarantee a strictly proper, admissible controller. A non-zero D_{ed} does not significantly complicate the mixed development. Singular and non-strictly proper H_∞ constraints are also allowed, so no assumptions need be made on the ranks of D_{ed} and D_{yd} .

The following definitions are made to simplify the development:

$$\underline{\gamma} \equiv \inf_{K \text{ admissible}} \|T_{ed}\|_\infty \quad (2.61)$$

$$\underline{\alpha} \equiv \inf_{K \text{ admissible}} \|T_{zw}\|_2 \quad (2.62)$$

$$K_{2_{opt}} \equiv \text{the unique } K(s) \text{ that makes } \|T_{zw}\|_2 = \underline{\alpha} \quad (2.63)$$

$$\bar{\gamma} \equiv \|T_{ed}\|_\infty \text{ when } K(s) = K_{2_{opt}} \quad (2.64)$$

$$K_{mix} \equiv \text{a solution to the } H_2 / H_\infty \text{ problem for some } \gamma > \underline{\gamma} \quad (2.65)$$

$$\gamma^* \equiv \|T_{ed}\|_\infty \text{ when } K(s) = K_{mix} \quad (2.66)$$

$$\alpha^* \equiv \|T_{zw}\|_2 \text{ when } K(s) = K_{mix} \quad (2.67)$$

where the admissible set of controllers is the set of all stabilizing controllers.

The mixed H_2/H_∞ problem can now be restated as follows: determine a $K(s)$ such that

1. the underlying H_2 and H_∞ problems are stable, i.e., A_2 and A_∞ are stable
2. $\gamma^* \leq \gamma$ for some given $\gamma > \underline{\gamma}$
3. $\|T_{zw}\|_2$ is minimized.

Walker [Wal94] introduced the following theorem to further refine the H_2/H_∞ problem setup.

Theorem 1. Let (A_c, B_c, C_c) be given and assume there exists a $Q_\infty = Q_\infty^T \geq 0$ satisfying

$$A_\infty Q_\infty + Q_\infty A_\infty^T + (Q_\infty C_e^T + B_d D_{ed}^T) R^{-1} (Q_\infty C_e^T + B_d D_{ed}^T)^T + B_d B_d^T = 0 \quad (2.68)$$

where $R = (\gamma^2 I - D_{ed} D_{ed}^T) > 0$. Then the following are equivalent:

- (i) (A_∞, B_d) is stabilizable
- (ii) A_∞ is stable
- (iii) A_2 is stable

Moreover, if the above hold then the following are true:

- (iv) $\|T_{ed}\|_\infty \leq \gamma$
- (v) the two-norm of the transfer function T_{zw} is given by

$$\|T_{zw}\|_2^2 = \text{tr}[C_z Q_2 C_z^T] = [Q_2 C_z^T C_z]$$

where $Q_2 = Q_2^T \geq 0$ is the solution to the Lyapunov equation

$$A_2 Q_2 + Q_2 A_2^T + B_w B_w^T = 0$$

- (vi) all real symmetric solutions Q_∞ of (2.68) are positive semidefinite
- (vii) there exists a unique minimal solution Q_∞ to (2.68) in the class of real symmetric solutions
- (viii) Q_∞ is the minimal solution of (2.68) iff

$$\text{Re}[\lambda_i (A_\infty + B_d D_{ed}^T R^{-1} C_e + Q_\infty C_e^T R^{-1} C_e)] \leq 0 \text{ for all } i$$

- (ix) $\|T_{ed}\|_\infty < (\leq) \gamma$ iff $\text{Re}[\lambda_i (A_\infty + B_d D_{ed}^T R^{-1} C_e + Q_\infty C_e^T R^{-1} C_e)] < (\leq) 0$ where Q_∞ is the minimal solution to (2.68).

This theorem allows the mixed problem to be stated as: Determine the $K(s)$ which minimizes the cost function

$$J(A_c, B_c, C_c) = \|T_{zw}\|_2^2 = \text{tr}[Q_2 C_z^T C_z] \quad (2.69)$$

where Q_2 is the real symmetric, positive semi-definite solution to

$$\mathbf{A}_2 \mathbf{Q}_2 + \mathbf{Q}_2 \mathbf{A}_2^T + \mathbf{B}_w \mathbf{B}_w^T = 0 \quad (2.70)$$

and such that

$$\mathbf{A}_\infty \mathbf{Q}_\infty + \mathbf{Q}_\infty \mathbf{A}_\infty^T + (\mathbf{Q}_\infty \mathbf{C}_e^T + \mathbf{B}_d \mathbf{D}_{ed}^T) \mathbf{R}^{-1} (\mathbf{Q}_\infty \mathbf{C}_e^T + \mathbf{B}_d \mathbf{D}_{ed}^T)^T + \mathbf{B}_d \mathbf{B}_d^T = 0 \quad (2.71)$$

has a real, symmetric, positive semi-definite solution.

The minimization problem can now be posed as a cost function (2.69) subject to two equality constraints (2.70) and (2.71). To solve this minimization problem a Lagrange multiplier approach is used.

The Lagrangian is

$$\begin{aligned} L = & \text{tr}[\mathbf{Q}_2 \mathbf{C}_z^T \mathbf{C}_z] + \text{tr}\{[\mathbf{A}_2 \mathbf{Q}_2 + \mathbf{Q}_2 \mathbf{A}_2^T + \mathbf{B}_w \mathbf{B}_w^T] \mathbf{X}\} \\ & + \text{tr}\{[\mathbf{A}_\infty \mathbf{Q}_\infty + \mathbf{Q}_\infty \mathbf{A}_\infty^T + (\mathbf{Q}_\infty \mathbf{C}_e^T + \mathbf{B}_d \mathbf{D}_{ed}^T) \mathbf{R}^{-1} (\mathbf{Q}_\infty \mathbf{C}_e^T + \mathbf{B}_d \mathbf{D}_{ed}^T)^T + \mathbf{B}_d \mathbf{B}_d^T] \mathbf{Y}\} \end{aligned} \quad (2.72)$$

where X and Y are symmetric Lagrange multiplier matrices. The first order necessary conditions for the minimum of this Lagrangian are:

$$\frac{\partial L}{\partial \mathbf{A}_c} = \mathbf{X}_{12}^T \mathbf{Q}_{12} + \mathbf{X}_2 \mathbf{Q}_2 + \mathbf{Y}_{12}^T \mathbf{Q}_{ab} + \mathbf{Y}_2 \mathbf{Q}_b = 0 \quad (2.73)$$

$$\begin{aligned} \frac{\partial L}{\partial \mathbf{B}_c} = & \mathbf{X}_{12}^T \mathbf{Q}_{12} \mathbf{C}_1^T + \mathbf{X}_2 \mathbf{Q}_{12}^T \mathbf{C}_{y_2}^T + \mathbf{X}_{12}^T \mathbf{V}_{12} + \mathbf{X}_2 \mathbf{B}_c \mathbf{V}_2 + \mathbf{Y}_{12}^T \mathbf{Q}_a \mathbf{C}_{y_a}^T + \mathbf{Y}_2 \mathbf{Q}_{ab}^T \mathbf{C}_{y_a}^T \\ & + \mathbf{Y}_{12}^T \mathbf{V}_{ab} + \mathbf{Y}_2 \mathbf{B}_c \mathbf{V}_b + (\mathbf{Y}_{12}^T \mathbf{Q}_a + \mathbf{Y}_2 \mathbf{Q}_{ab}^T) \mathbf{C}_e^T \mathbf{M} + (\mathbf{Y}_{12}^T \mathbf{Q}_{ab} + \mathbf{Y}_2 \mathbf{Q}_b) \mathbf{C}_c^T \mathbf{D}_{eu}^T \mathbf{M} = 0 \end{aligned} \quad (2.74)$$

$$\begin{aligned} \frac{\partial L}{\partial \mathbf{C}_c} = & \mathbf{B}_{u_2}^T \mathbf{X}_1 \mathbf{Q}_{12} + \mathbf{B}_{u_2}^T \mathbf{X}_{12} \mathbf{Q}_2 + \mathbf{R}_{12}^T \mathbf{Q}_{12} + \mathbf{R}_2 \mathbf{C}_c \mathbf{Q}_2 + \mathbf{B}_{u_a}^T \mathbf{Y}_1 \mathbf{Q}_{ab} + \mathbf{B}_{u_a}^T \mathbf{Y}_{12} \mathbf{Q}_b \\ & + \mathbf{R}_{ab}^T \mathbf{Q}_a \mathbf{Y}_1 \mathbf{Q}_{ab} + \mathbf{R}_{ab}^T \mathbf{Q}_a \mathbf{Y}_{12} \mathbf{Q}_b + \mathbf{R}_{ab}^T \mathbf{Q}_{ab} \mathbf{Y}_{12}^T \mathbf{Q}_{ab} + \mathbf{R}_{ab}^T \mathbf{Q}_{ab} \mathbf{Y}_2 \mathbf{Q}_b \\ & + \mathbf{R}_b \mathbf{C}_c \mathbf{Q}_{ab}^T \mathbf{Y}_1 \mathbf{Q}_{ab} + \mathbf{R}_b \mathbf{C}_c \mathbf{Q}_b \mathbf{Y}_{12}^T \mathbf{Q}_{ab} + \mathbf{R}_b \mathbf{C}_c \mathbf{Q}_{ab}^T \mathbf{Y}_{12} \mathbf{Q}_b + \mathbf{R}_b \mathbf{C}_c \mathbf{Q}_b \mathbf{Y}_2 \mathbf{Q}_b \\ & + \mathbf{P}_1 (\mathbf{Y}_1 \mathbf{Q}_{ab} + \mathbf{Y}_{12} \mathbf{Q}_b) + \mathbf{P}_2 (\mathbf{Y}_{12}^T \mathbf{Q}_{ab} + \mathbf{Y}_2 \mathbf{Q}_b) = 0 \end{aligned} \quad (2.75)$$

$$\frac{\partial L}{\partial \mathbf{X}} = \mathbf{A}_2 \mathbf{Q}_2 + \mathbf{Q}_2 \mathbf{A}_2^T + \mathbf{B}_w \mathbf{B}_w^T = 0 \quad (2.76)$$

$$\frac{\partial L}{\partial \mathbf{Q}_2} = \mathbf{A}_2^T \mathbf{X} + \mathbf{X} \mathbf{A}_2 + \mathbf{C}_z^T \mathbf{C}_z = 0 \quad (2.77)$$

$$\frac{\partial L}{\partial \mathbf{Y}} = \mathbf{A}_\infty \mathbf{Q}_\infty + \mathbf{Q}_\infty \mathbf{A}_\infty^T + (\mathbf{Q}_\infty \mathbf{C}_e^T + \mathbf{B}_d \mathbf{D}_{ed}^T) \mathbf{R}^{-1} (\mathbf{Q}_\infty \mathbf{C}_e^T + \mathbf{B}_d \mathbf{D}_{ed}^T)^T + \mathbf{B}_d \mathbf{B}_d^T = 0 \quad (2.78)$$

$$\frac{\partial L}{\partial Q_\infty} = (A_\infty + B_d D_{ed}^T R^{-1} C_e + Q_\infty C_e^T R^{-1} C_e)^T Y$$

$$+ Y (A_\infty + B_d D_{ed}^T R^{-1} C_e + Q_\infty C_e^T R^{-1} C_e) = 0 \quad (2.79)$$

where

$$M = R^{-1} D_{ed} D_{yd}^T \quad (2.80)$$

$$P_1 = D_{eu}^T R^{-1} D_{ed} B_d^T \quad (2.81)$$

$$P_2 = D_{eu}^T M B_c^T \quad (2.82)$$

$$Q_2 = \begin{bmatrix} Q_1 & Q_{12} \\ Q_{12}^T & Q_2 \end{bmatrix} \quad (2.83)$$

$$X = \begin{bmatrix} X_1 & X_{12} \\ X_{12}^T & X_2 \end{bmatrix} \quad (2.84)$$

$$Q_\infty = \begin{bmatrix} Q_a & Q_{ab} \\ Q_{ab}^T & Q_b \end{bmatrix} \quad (2.85)$$

$$Y = \begin{bmatrix} Y_1 & Y_{12} \\ Y_{12}^T & Y_2 \end{bmatrix} \quad (2.86)$$

$$B_w B_w^T = \begin{bmatrix} B_w \\ B_c D_{yw} \end{bmatrix} \begin{bmatrix} B_w^T & D_{yw}^T B_c^T \end{bmatrix}$$

$$= \begin{bmatrix} V_1 & V_{12} B_c^T \\ B_c V_{12}^T & B_c V_2 B_c^T \end{bmatrix} \quad (2.87)$$

$$B_d (D_{ed}^T R^{-1} D_{ed} + I) B_d^T = \begin{bmatrix} B_d \\ B_c D_{yd} \end{bmatrix} (D_{ed}^T R^{-1} D_{ed} + I) \begin{bmatrix} B_d^T & D_{yd}^T B_c^T \end{bmatrix}$$

$$= \begin{bmatrix} V_a & V_{ab} B_c^T \\ B_c V_{ab}^T & B_c V_b B_c^T \end{bmatrix} \quad (2.88)$$

$$C_z^T C_z = \begin{bmatrix} C_z^T \\ C_c^T D_{zu}^T \end{bmatrix} \begin{bmatrix} C_z & D_{zu} C_c \end{bmatrix}$$

$$= \begin{bmatrix} R_1 & R_{12} C_c \\ C_c^T R_{12}^T & C_c^T R_2 C_c \end{bmatrix} \quad (2.89)$$

$$\begin{aligned} \mathbf{C}_e^T \mathbf{R}^{-1} \mathbf{C}_e &= \begin{bmatrix} \mathbf{C}_e^T \\ \mathbf{C}_c^T \mathbf{D}_{eu}^T \end{bmatrix} \mathbf{R}^{-1} \begin{bmatrix} \mathbf{C}_e & \mathbf{D}_{eu} \mathbf{C}_c \end{bmatrix} \\ &= \begin{bmatrix} \mathbf{R}_a & \mathbf{R}_{ab} \mathbf{C}_c \\ \mathbf{C}_c^T \mathbf{R}_{ab}^T & \mathbf{C}_c^T \mathbf{R}_b \mathbf{C}_c \end{bmatrix} \end{aligned} \quad (2.90)$$

Equations (2.76) and (2.78) are the original constraint functions, equations (2.70) and (2.71). There are two possible solutions to (2.79). One solution to (2.79) is that $\mathbf{Y} = 0$; the other possibility is that

$(\mathbf{A}_\infty + \mathbf{B}_d \mathbf{D}_{ed}^T \mathbf{R}^{-1} \mathbf{C}_e + \mathbf{Q}_\infty \mathbf{C}_e^T \mathbf{R}^{-1} \mathbf{C}_e)$ is neutrally stable. The first solution, $\mathbf{Y} = 0$, corresponds to the an inactive H_∞ constraint. The second solution implies that solution lies on the boundary of the H_∞ constraint and \mathbf{Q}_∞ is the neutrally stabilizing solution for the H_∞ Riccati equation (2.71). When $\mathbf{Y} = 0$, the Lagrangian reduces to

$$L = \text{tr}[\mathbf{Q}_2 \mathbf{C}_z^T \mathbf{C}_z] + \text{tr}\{[\mathbf{A}_2 \mathbf{Q}_2 + \mathbf{Q}_2 \mathbf{A}_2^T + \mathbf{B}_w \mathbf{B}_w^T] \mathbf{X}\} \quad (2.91)$$

which is the same as the H_2 Lagrangian. Therefore, for $\mathbf{Y} = 0$, $\mathbf{K}_{\text{mix}} = \mathbf{K}_{2\text{opt}}$. Walker [Wal94] developed the following theorem:

Theorem 2 Assume $n_c \geq n_2$, where n_c is the order of the controller and n_2 is the order of the plant for the H_2 problem. Then the following hold:

1. If $\underline{\gamma} < \underline{\gamma}$, no solution to the mixed H_2/H_∞ problem exists
2. If $\underline{\gamma} < \gamma \leq \bar{\gamma}$, \mathbf{K}_{mix} is such that $\gamma^* = \gamma$
3. If $\gamma \geq \bar{\gamma}$, $\mathbf{K}_{2\text{opt}}$ is the solution to the mixed H_2/H_∞ problem.

When the order of the controller is chosen greater than or equal to that of the H_2 problem, the solution to the mixed H_2/H_∞ problem will lie on the H_∞ constraint boundary. Theorem 2 implies that each point on the mixed H_2/H_∞ curve occurs on the H_∞ constraint boundary, $\gamma^* = \gamma$, for $\underline{\gamma} < \gamma \leq \bar{\gamma}$. In this region, α^* is a monotonically decreasing function of γ . A typical α versus γ curve is shown in Figure 2.7.

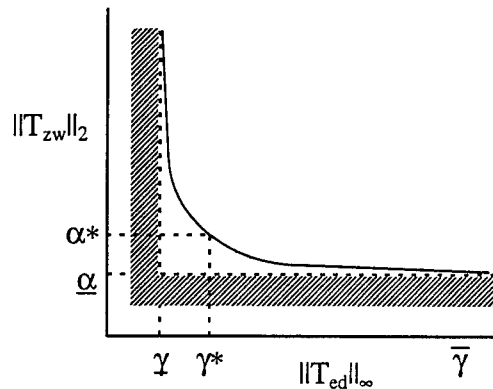


Figure 2.7. Typical Mixed H_2/H_∞ α Versus γ Curve

2.2. Handling Qualities Analysis

There are several handling qualities prediction criteria commonly used to evaluate flight control systems. These criteria are based on historical data of pilot ratings, and are outlined in the Department of Defense MIL-STD-1797A, *Flying Qualities of Piloted Aircraft* [Mil90]. Two criteria were used to evaluate the flight control systems designed by the various methods in this thesis. The primary criteria used was Hoh's bandwidth criteria. The TPS project this thesis was based on, uses this criteria. The Ralph Smith (RSmith) criteria was also considered, and is the criteria TPS is currently using on an updated flight control system project [TPS95]. The next two subsections briefly describe these handling qualities criteria. For a full description see the [MIL90], [Hoh96] and [SG78].

2.2.1. Bandwidth Criteria

The bandwidth requirement is based on the hypothesis that if the aircraft has good response characteristics over a sufficiently wide range of pilot control input frequencies, then the aircraft will have favorable handling qualities [Hoh81]. This evaluation method examines two parameters – an equivalent time delay, to account for the higher order dynamics of the aircraft, and the bandwidth of the pitch attitude to stick force (or displacement) transfer function.

The bandwidth is defined as the lesser of two frequencies, $\omega_{BW_{phase}}$ and $\omega_{BW_{gain}}$. The bandwidth due to phase margin, $\omega_{BW_{phase}}$, is defined as the frequency at a phase margin of 45 degrees. The frequency

where the phase angle is -180° , labeled ω_{180} , and the gain which corresponds to that frequency are determined. The bandwidth due to gain margin, $\omega_{BW_{gain}}$, is defined as the frequency at the gain which is 6 dB above the gain amplitude corresponding to ω_{180} . The bandwidth determination is graphically depicted in Figure 2.8.

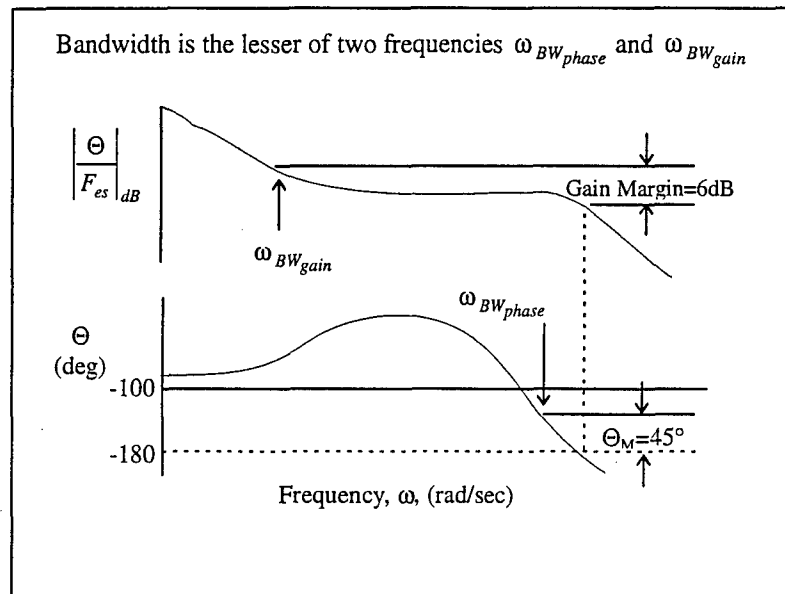


Figure 2.8. Definition of Bandwidth Frequency ω_{BW} from Open Loop Frequency Response

The second parameter needed to determine predicted handling qualities level is the equivalent time delay, τ_p . This parameter is computed using the formula

$$\tau_p = -\frac{(\phi_{2\omega_{180}} + 180)}{2(57.3)(\omega_{180})} \quad (2.92)$$

where ω_{180} is the frequency corresponding to -180° phase and $\phi_{2\omega_{180}}$ is the phase angle at a frequency twice as great as the frequency where -180 degrees of phase angle occurs.

These two parameters are plotted on the ω_{BW} versus τ_p Bandwidth requirements diagram to determine the predicted handling qualities level. There are separate diagrams for different flight phases.

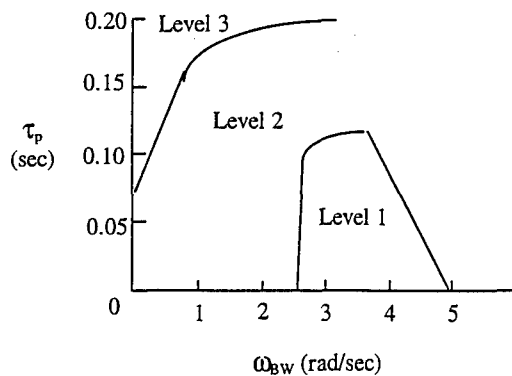


Figure 2.9. Bandwidth Requirements, Category C Flight Phase

Figure 2.9 depicts the level boundaries for the bandwidth criteria, for Category C Flight Phase. This thesis is only concerned with approach and landing, Category C Flight Phase, so only this diagram is reproduced here.

2.2.2. *Ralph Smith Criteria*

A pitch and roll axis handling qualities criteria was proposed by Ralph Smith and Norman Geddes [SG78]. The RSmith criteria predicts a pilot-vehicle cross-over frequency, a Cooper-Harper rating, and a pilot-induced oscillation (PIO) rating in both the pitch and roll axes. Only the pitch axis portion of this criteria will be presented here. The proposed pitch axis requirements are restricted to longitudinal mode, short period dynamics of Class IV aircraft (high-maneuverability - fighter type), Flight Phase Category A (non-terminal flight phases that require rapid maneuvering, precision tracking, precise flight-path control). The requirements proposed in [SG78] were derived from flight test data for a variety of flight control tasks; the power approach task, however, was not included in this data base. The Smith-Geddes paper does argue that this criteria is “sufficient to ensure acceptability of front-side power approach handling qualities...[but] may be too stringent for direct use as design specifications for the power approach condition.” [SG78:142] The test bed used for this research is a Class II aircraft, but it is simulating Class IV aircraft dynamics. Also, since TPS is currently using the RSmith criteria to evaluate the approach and landing task in the current TPS FCS project, the RSmith criteria was considered during design as a secondary prediction of handling qualities.

The RSmith criteria for the pitch axis can be summarized in a six step process [TPS95]. It requires measuring a slope, determining a criterion frequency, and obtaining two phase angles. Each of these parameters has an associated handling qualities requirement. The six steps and the associated requirements are as follows:

Step 1: From a pitch rate time history, determine the elapsed time to the first peak, t_q , resulting from a step input. The time to first peak must be:

$$\text{Level 1: } 0.2 \leq t_q \leq 0.9$$

Level 2: none proposed

Step 2: Determine the slope parameter, S , the slope of the Bode magnitude curve of $\left| \frac{\theta}{F_{es}}(j\omega) \right|$, in

dB/octave, between 1 and 6 rad/sec. In equation form, S is defined as

$$S \equiv \frac{d}{d\omega} \left| \frac{\theta}{F_{es}}(j\omega_c) \right| \text{ dB / octave} \quad (2.93)$$

The handling qualities requirement is

$$\text{Level 1: } S < -2 \text{ dB/octave}$$

Level 2: none proposed

Step 3: Determine the pilot-vehicle cross-over frequency, also called the criterion frequency, ω_c , using the formula:

$$\omega_c = 6.0 + 0.24 S \text{ (radians/second)} \quad (2.94)$$

where S is the slope of the Bode magnitude curve of $\left| \frac{\theta}{F_{es}}(j\omega_c) \right|$, determined in step 2.

Step 4: Determine the phase angle of $\frac{\theta}{F_{es}}(j\omega_c)$ at ω_c , and use Figure 2.10 to determine the predicted

Cooper-Harper rating.

Step 5: If $\angle \frac{\theta}{F_{es}}(j\omega_c) > -180^\circ$, susceptibility to pitch attitude PIO is not predicted. However, if

$\angle \frac{\theta}{F_{es}}(j\omega_c) \leq -180^\circ$, a PIO may result from pitch attitude tracking.

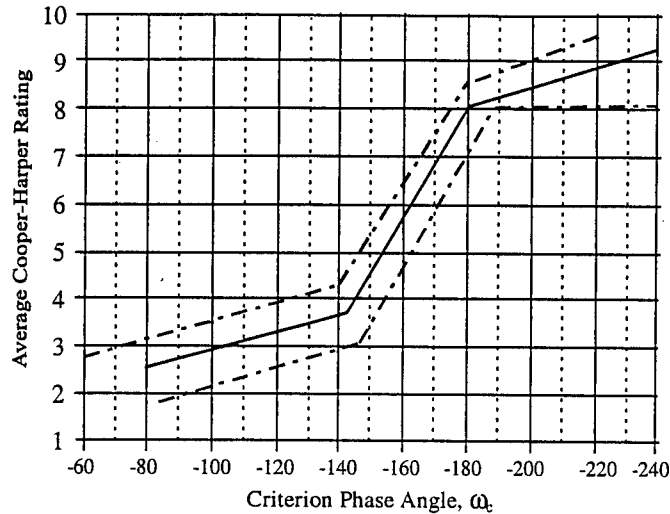


Figure 2.10. Criterion Phase Angle Versus. Cooper-Harper Rating

Step 6: Determine the normal acceleration phase angle parameter $\Phi(j\omega_c)$ from the following formula:

$$\Phi(j\omega_c) = \angle \frac{n_{z_p}}{F_{es}}(j\omega_c) - 14.3 \omega_c \quad (2.95)$$

where n_{z_p} is normal acceleration at the pilot's location in the airplane. The $-14.3\omega_c$ term is the phase lag introduced by typical pilot dynamics and is modeled by a transport delay of 0.25

seconds. The angle of $\frac{n_{z_p}}{F_{es}}(j\omega_c)$ is measured from a Bode phase angle curve. For conventional

flight control systems, the PIO rating can be predicted using $\Phi(j\omega_c)$ in Figure 2.11.

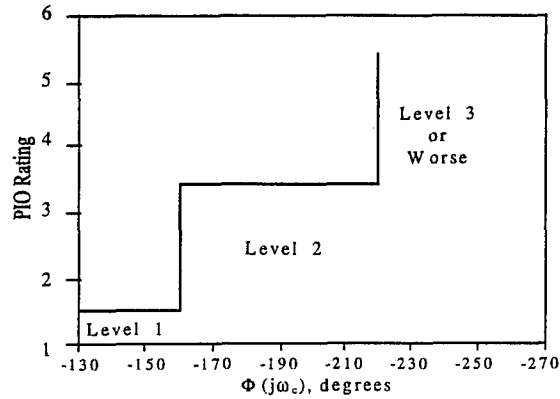


Figure 2.11. Predicted Pitch Axis PIO Rating for Conventional Flight Control Systems

These requirements should be considered a set of necessary conditions. Each must be satisfied at the Level 1 or 2 values for the overall handling qualities rating to be Level 1 or 2, respectively. If any one is violated, the overall rating is equal to the level for which the violation exists.

2.3. TPS Project

The US Air Force Test Pilot School (TPS), as part of its curriculum, requires the students to complete a Flight Control System (FCS) design project. This project includes a scenario involving analysis of a proposed contractor designed flight control system, then a redesign of the FCS based on two specified design structure options. The student test teams choose one of two design options. The structure of these design options (i.e. the designated feedback loops) is fixed, and the test team is limited to selecting FCS gains and stick characteristics. The FCS is for a Class IV type aircraft performing the approach and landing task. The project specifies evaluating the handling qualities of the design by applying Hoh's Bandwidth Criteria. The FCS design is then implemented in the Calspan Variable Stability Simulator (VSS) Learjet and the handling qualities are evaluated, using the Cooper-Harper rating scale, by the student test pilots performing a lateral offset approach to a spot landing. This project was used as a foundation for this thesis research. Only the portion of the TPS FCS project used for this research will be presented here. Design option one was chosen as the basic structure for the flight control systems designed in this thesis. The system was restricted further by fixing the stick dynamics used to the baseline stick dynamics and feel system presented in the TPS project.

The TPS FCS project strictly uses classical design methods (i.e. Root Locus, Bode frequency, and time response analysis) and transfer function models of the aircraft dynamics. The pitch angle to elevator deflection and the angle of attack to elevator deflection transfer functions specified in the TPS project are:

$$\frac{\theta(s)}{\delta(s)} = \frac{2.85(s+0.06)(s+0.87)}{(s+1.55)(s-0.38)(s+0.06 \pm 0.23j)} \quad (2.96)$$

$$\frac{\alpha(s)}{\delta(s)} = \frac{0.041(s+0.016 \pm 0.21j)(s+70.2)}{(s+1.55)(s-0.38)(s+0.06 \pm 0.23j)} \quad (2.97)$$

The structure of design Option 1, shown in Figure 2.12, is based on an inner angle of attack feedback loop (with feedback gain of KA, and a low pass noise filter), an outer pitch rate feedback loop (with feedback gain KQ), and a forward command gain (KFL). A nominal value and a range for these gains was also specified, and are shown in Table 2.1.

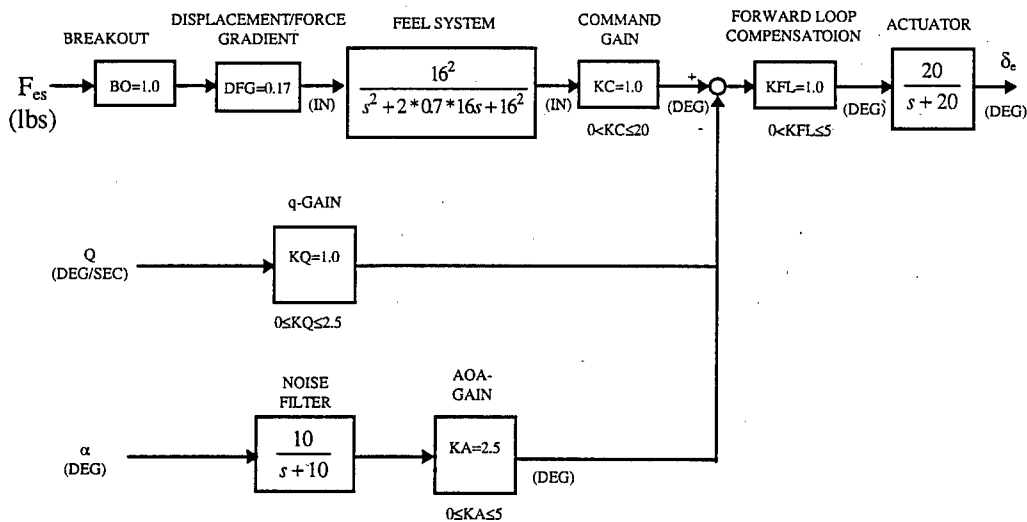


Figure 2.12. TPS FCS Design Option 1 (Nominal)

GAIN	NOMINAL VALUE	RANGE
KFL	1.0	$0 \leq KFL \leq 5$
KA	2.5	$0 \leq KA \leq 5$
KQ	1.0	$0 \leq KQ \leq 2.5$

Table 2.1. TPS FCS Design Option 1, Nominal Gains and Ranges

The general structure of this TPS FCS project was the foundation for the flight control systems designed in this thesis. The classically designed system followed this setup exactly. The modern designs (H_2 , H_∞ , and mixed H_2/H_∞ designs) only fed back pitch rate and angle of attack, like the TPS project, but used state space methods and did not limit the controller to simple gains and a low pass filter. The controller was also not limited to negative feedback, nor to the feedback path.

2.4. CALSPAN Variable Stability Simulator II Learjet

This thesis research implemented the FCS designs on the CALSPAN Variable Stability Simulator II (VSS II) Learjet, tail number N102VS. The VSS II is a modified Learjet Model 25 that functions as a three axis in-flight simulator [Bal93]. It is operated by CALSPAN under an experimental license from the FAA. The cockpit has a set of side-by-side controls. The control yoke at the left seat, for the safety pilot, maintains the Learjet's conventional flight control system. The evaluation pilot's center control stick in the right seat uses a fly-by-wire response feedback system. The variable stability and variable control system consist of: variable feel system, aircraft motion sensors and associated signal conditioning, control system simulation computer, control surface servos, digital configuration control system, engage/disengage and safety monitor logic, and recording/playback capability. The system can be disengaged by any of four manual disconnect switches which are installed on each of the three control sticks/yokes and on the glare shield. In addition, automatic safety trips are provided. In the event of incapacitation of the safety pilot or certain control cable failures, the aircraft can be flown by the evaluation pilot as a nearly normal Learjet using the VSS in the "Fly-by-Wire" (FBW) mode. All basic Learjet systems are available in the FBW mode except for nose gear steering. The handling qualities are those of the basic aircraft with the yaw damper on. There are no safety trips in the emergency FBW mode.

Hydraulic power for the variable stability actuators is obtained from the existing Learjet hydraulic system which provides four gallons per minute (gpm) per engine. Estimated maximum flow demand to operate all servo actuators is 3.35 gpm. Maximum demand for normal Learjet flaps, spoilers, gear and brakes is under four gpm. Solenoid operated valves to the variable stability actuators are designed fail safe to prevent hydraulic locks on the actuators.

Some operating limitations that apply to the Learjet are listed in Table 2.2.

	VSS OFF	VSS ON
SPEED LIMITATIONS	356 KIAS 0.82 Mach	325 KIAS
G LIMITATIONS	+4.4 to -1.0	+2.8 to +0.15

Table 2.2. Learjet Limitations

The control system simulation computer uses MATLAB[®] SIMULINK to modify the perceived aircraft dynamics. For the longitudinal axis, only short-period dynamics are simulated. While the system programming and inter-workings are proprietary to Calspan, the following guidance for implementing FCSs was provided:

1. Suggest use of MATLAB[®] version 4.2C.1 and SIMULINK 1.3 or later.
2. Recommend controllers be cast in pole/zero/gain form using scalar parameters and integrators. Do not use built in transfer function blocks unless the parameters will never change. An example block diagram is shown in Figure 2.13.
3. Do not use MATLAB[®] function blocks.
4. Setup file (MATLAB[®] script) must contain only constants, no expressions.
5. Do not use masked blocks with dummy parameters.
6. Do not use a^b , use $\text{pow}(a,b)$
7. Do not use matrix SIMULINK parameters unless they won't ever change
8. Use named scalar parameters for anything you might change and initialize it with your setup file.
9. Don't forget initialization of integrators. A "system engage" discrete is available for controlling reset integrators.
10. Use Euler integration, with a 0.01 step size.
11. Please make sure your top level interface is well defined including engineering units, etc. Inputs are generally pilot forces or stick displacements and engage status logicals and sensor signals. Outputs are generally just surface actuator commands.

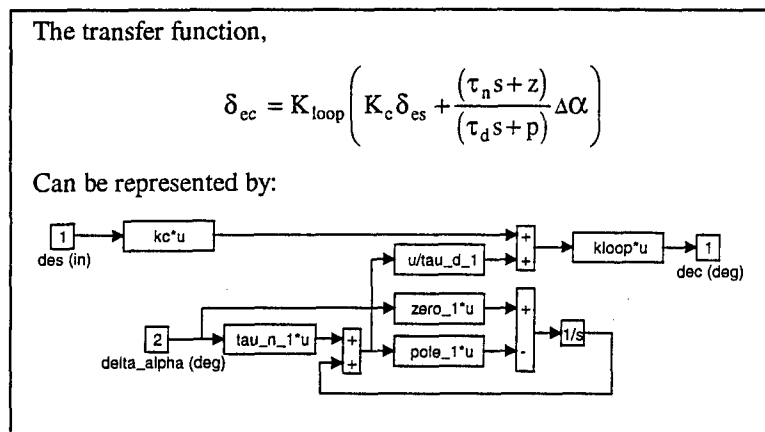


Figure 2.13. Example SIMULINK Block Diagram for a VSS II Acceptable System

From the list of guidelines provided by Calspan, the critical factors were that the system must be stable using Euler integration with a 0.01 seconds step size, and the integrators must be able to be initialized and zero-ized (reset) in-flight with the system running – therefore the SIMULINK state-space blocks were not directly implementable in the VSS II system. How this was accomplished will be covered in Chapter 4, Implementation.

2.5. Summary

This chapter has covered the background theory used in this thesis and background information concerning the resources and the foundation design set-up on which this thesis is based. This chapter started with classical design theory fundamentals, and then described the basics of H_2 and H_∞ optimization. Next, mixed H_2/H_∞ optimization theory was briefly discussed. Two handling qualities design criteria were explained; specifically addressed were Hoh's Bandwidth criteria and RSmith criteria. The TPS project, which was the foundation for this research, was introduced. Finally the Calspan VSS II Learjet was described, including the design implementation guidelines specified by Calspan. The next chapter will address the set-up used to formulate the FCS designs.

III. Model Set-up and Design

3.1. Aircraft Plant Model

The TPS FCS project provided an aircraft plant model in transfer function form. This model only provided the pitch angle $\left(\frac{\theta(s)}{\delta_e(s)}\right)$ and angle of attack $\left(\frac{\alpha(s)}{\delta_e(s)}\right)$ dynamics (see equations 2.96 and 2.97). The modern control theory designs investigated in this thesis required a state-space description of the aircraft dynamics [RB86]. Calspan provided a set of stability derivatives and flight conditions for the aircraft model used in the TPS FCS project during the past few years. This list of stability derivatives and flight conditions and the MATLAB™ script file used to calculate the state-space model are shown in Appendix A. At the time the state-space model was created, the VSS II limitation of only simulating short period dynamics was not known. Therefore, since it is more complete, a full state-space model was determined based on the data provided by Calspan. The states used were: q - pitch rate (degrees/second), α - angle of attack (degrees), v - forward true velocity (feet/second), γ - glide-path angle (degrees), and once the actuator was included in the model, x_{act} - the actuator state. The sign convention for elevator deflection used by TPS is the NASA sign convention, a positive elevator deflection implies the trailing edge moves down and will produce a negative pitching motion [TPS95]. The actuator model used in the TPS project, $\frac{20}{s+20}$, was added to the aircraft plant model for the design and evaluation process. The variables considered for analysis, the output variables, were the states, α , q , γ , v , as well as θ - pitch angle (degrees), and n_z - normal acceleration (g's). The resulting state-space model was

$$\dot{x} = Ax + Bu \quad (3.1)$$

$$y = Cx + Du \quad (3.2)$$

where

$$x = \begin{bmatrix} q \\ \alpha \\ v \\ \gamma \\ x_{act} \end{bmatrix}$$

$$u = [\delta_{ec}]$$

$$y = \begin{bmatrix} \alpha \\ q \\ \theta \\ n_z \\ \gamma \\ v \\ \delta_e \end{bmatrix}$$

$$A = \begin{bmatrix} -0.38 & 0.78 & 0.00 & 0.00 & 2.86 \\ 1.00 & -0.85 & -0.08 & 0.00 & 0.04 \\ 0.00 & -0.44 & -0.05 & -0.56 & 0.00 \\ 0.00 & 0.85 & 0.08 & 0.00 & -0.04 \\ 0.00 & 0.00 & 0.00 & 0.00 & -20.00 \end{bmatrix}$$

$$B = \begin{bmatrix} 0.00 \\ 0.00 \\ 0.00 \\ 0.00 \\ 20.00 \end{bmatrix}$$

$$C = \begin{bmatrix} 0.000 & 1.000 & 0.000 & 0.000 & 0.000 \\ 1.000 & 0.000 & 0.000 & 0.000 & 0.000 \\ 0.000 & 1.000 & 0.000 & 1.000 & 0.000 \\ 0.000 & 0.098 & 0.009 & 0.000 & 0.005 \\ 0.000 & 0.000 & 0.000 & 1.000 & 0.000 \\ 0.000 & 0.000 & 1.000 & 0.000 & 0.000 \\ 0.000 & 0.000 & 0.000 & 0.000 & 1.000 \end{bmatrix}$$

$$D = \begin{bmatrix} 0.000 \\ 0.000 \\ 0.000 \\ 0.000 \\ 0.000 \\ 0.000 \\ 0.000 \end{bmatrix}$$

This state-space model can be transformed back to transfer function form to verify accuracy of the model (compared to the transfer functions given in the TPS project) and for use in the classical design as well as evaluation of the designs. The transfer function representation of this state-space model is

$$\frac{\theta(s)}{\delta(s)} = \frac{2.86(20)(s+0.06)(s+0.84)}{(s+20)(s+1.53)(s-0.39)(s+0.07 \pm 0.23j)} \quad (3.3)$$

$$\frac{\alpha(s)}{\delta(s)} = \frac{0.041(20)(s+0.024 \pm 0.21j)(s+70.2)}{(s+20)(s+1.53)(s-0.39)(s+0.07 \pm 0.23j)} \quad (3.4)$$

When compared to (2.96) and (2.97), the differences are small.

3.2. Wind and Sensor Noise Model / Intensity Determination

One of the objectives of the flight control designs is to provide stability and performance in the face of noises acting on the system. Both for design and analysis, the noises needed to be categorized and modeled. The two types of noise considered were wind gust noise and sensor noise. The limited nature of the flight test prevented the noise rejection characteristics of the designs to be quantified during the flight test. Prior to flight test, computer analysis was performed to evaluate each design's noise rejection characteristics.

The wind gust noise can be characterized as a random low frequency disturbance in angle of attack, α . It is modeled as an angle of attack perturbation by inserting the deviation directly into the core plant (bypassing the actuator), see Figure 3.1. This is done by multiplying the filtered wind times the second column of the A matrix of the aircraft plant and adding this to the states. The second column of A will be denoted by Γ . For the purposes of design, the wind noise is modeled as a zero-mean, Unit intensity White Gaussian Noise (UWGN), with no filtering or 'coloring' added since the filtering proves only to increase the order of the controller and not improve the controller's performance. The design process included weighting the noise input to obtain the desired noise rejection results. For evaluation of the designs, the UWGN with a sample time of 0.01 seconds, was passed through a low pass filter, represented by

$$W_g = \frac{0.1}{s+0.5} \quad (3.5)$$

This filter removes the high frequency component of the UWGN to result in a 'wind like' disturbance of reasonable intensity for approach and landing. However, when comparing designs, to accentuate the differences in designs caused by the 'wind noise', the intensity was increased by a multiple of five. This proved beneficial for analysis.

time history plots presented in Appendix C. The latter two considerations were used to expedite the design process, and were accomplished by a simple series of MATLAB™ commands. The MATLAB™ script files used are presented in Appendix B. The next two sub-sections present the set-up for the time history and the handling qualities analysis.

3.3.1. Time Domain Evaluation

The MATLAB™ SIMULINK simulation program was used to obtain time histories of the feedback control systems designed. The same SIMULINK diagram, shown in Figure 3.1, was used for all the modern design methods to obtain the simulated time histories. The classical design used the SIMULINK diagram shown in Figure 3.2, to obtain the simulated time histories. Different diagrams were used to accommodate the location of the controller in the feedback path.

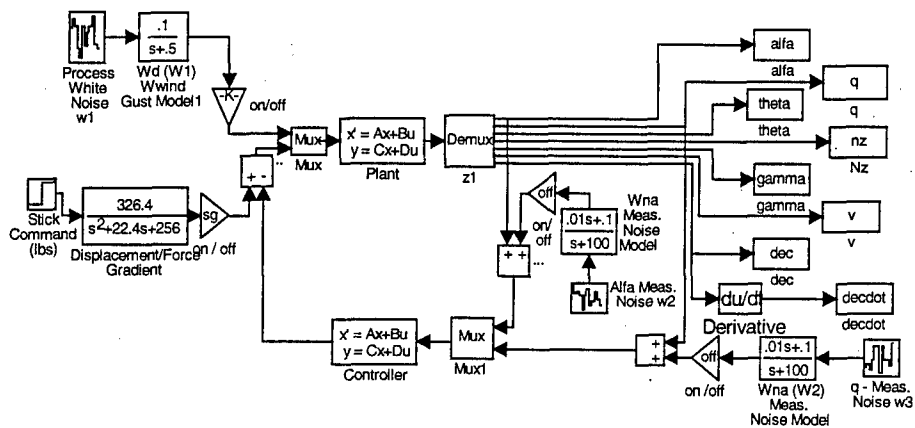


Figure 3.2. Classical Evaluation Model

All the SIMULINK simulations used the LINSIM numerical integration routine, a time step of 0.01 seconds, and for a duration of 10 seconds. Both a step input and an initial condition of 5° angle of attack were considered, with no-noise introduced and with five times the nominal noise intensity. The step input was used to evaluate the tracking response of the system and the initial condition was used to evaluate the perturbation rejection characteristics of the system. Both input types were used to consider the noise rejection properties of the designs.

3.3.2. Handling Qualities Evaluation

The handling qualities rating of the flight control systems designed were predicted using Hoh's Bandwidth criteria as primary evaluation method and RSmith's criteria as a secondary evaluation method. The *Interactive Flying Qualities Toolbox for Matlab*, version 0.01 Beta, February 1995 was used to predict the handling qualities of the systems. This toolbox takes as its input the pitch angle to stick force transfer function. The nominal stick dynamics defined in the TPS FCS project were used to define this closed loop transfer function.

3.4. Design Models and Resulting Designs

3.4.1. Classical Design Set-up and Resulting Design

The classical design was included in this thesis as a control case for the flight test and as a means to validate the bare airframe aerodynamics simulated by the Calspan VSS II Learjet. The set-up and structure was based on Design Option One of the TPS FCS project described in Chapter II. The system can be represented by the block diagram shown in Figure 3.3. The state-space aircraft dynamics model shown in Figure 3.3 incorporates the actuator specified by the TPS project. It used negative feedback of angle of attack and pitch rate, with the controller gains in the feedback path and the alpha channel incorporating a low pass filter. The ranges on the three variable gains were set by the TPS project.

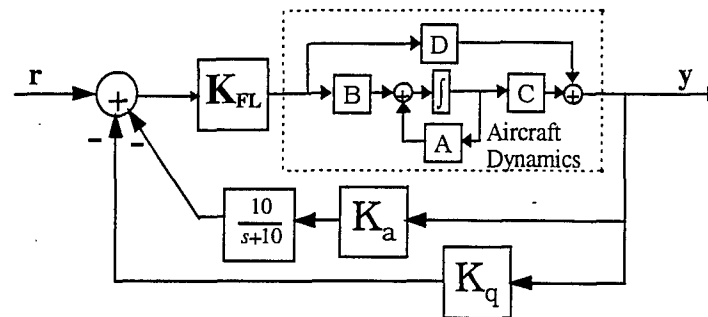


Figure 3.3. Classical Design Model Block Diagram

This made a vary iterative process manageable to an inexperienced designer. The nice aspect of the classical design method with this simple structure is the physical interpretation of the variables and

feedback loop gains. Increasing K_a will generally increase the natural frequency and decrease the damping ratio of the second-order aircraft response modes. Increasing K_q generally will increase the damping ratio of the system [Bal93]. Determining the balance of the two which meets the desired handling qualities and performance constraints is the challenge to the designer. There is no way to determine if the gains chosen provide either the highest stability margins possible, or the best noise rejection characteristics obtainable, for a given performance objective and handling qualities rating. The controller gains or states do maintain their physical interpretation throughout the process. The gains chosen were

$$K_a = 3.4$$

$$K_q = 2.3$$

$$K_{FL} = 1.0$$

or written in state-space form, the controller can be represented by

$$A_K = [-10.0] \quad B_K = [1.0 \ 0.0]$$

$$C_K = [34.0] \quad D_K = [0.0 \ 2.3]$$

The time histories are shown in Appendix C. The handling qualities analysis results for the Bandwidth criteria are shown in Figure 3.4. and the results for the RSmith criteria are shown in Table 3.1.

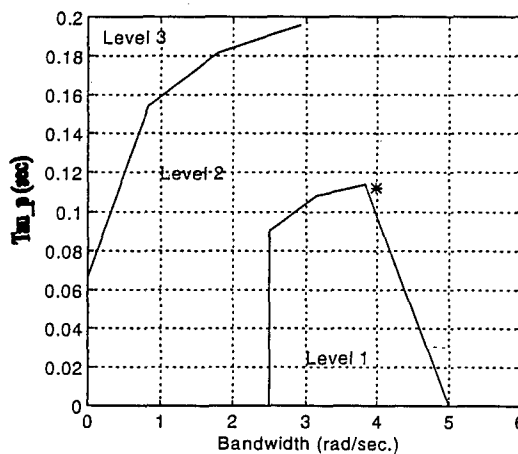


Figure 3.4. Category C Bandwidth Requirements: Classical Design

Parameter	Value	Level
S (dB/octave)	-3.97	1
ω_c (rad/sec)	5.05	
Φ_{oc} (deg)	-150.84	2
t_{q-peak} (sec)	0.48	1

Table 3.1. RSmith Handling Qualities Predicted Level for the Classical Design

The structure of this system contains two feedback loops, α and q , but only one input, δ_e . To fully describe the stability margins, four types of vector stability margins were calculated. The first three are single-input-single-output (SISO) methods, considering perturbations in one-loop-at-a-time, closing the remaining feedback loop. Input vector margins and output vector margins were determined in this way. It should be emphasized that vector margins are conservative bounds on the allowable system perturbations, and that conventional stability margins are guaranteed to be as good or better. The fourth type of vector stability margin determined was a MIMO vector margin. It considers breaking both loops simultaneously and is the most conservative bound on the vector gain and phase margins. For a more complete discussion of vector stability margins in general, see [FPE94:422-425] and for a derivation of MIMO vector margin calculations see [RB86]. Table 3.2 presents the vector stability margins for the classical design. It should be noted that the TPS FCS project did not address or specify stability

Margin Type	Vector Gain Margin (dB)	Vector Phase Margin (degrees)
Input Margin	[5.86 - ∞]	± 60.84
Output Margin (α loop 'broken')	[11.70 -8.03]	± 43.43
Output Margin (q loop 'broken')	[6.87 -8.66]	± 36.78
MIMO Margins (sensitivity)	[3.03 -2.24]	± 17.93
MIMO Margins (complementary sensitivity)	[2.36 -3.24]	

Table 3.2. Classical Design Vector Stability Margins

margins of any kind. Therefore there were no minimum acceptable margin levels targeted. The MIL-STD [Mil90] refers to conventional stability margins of ± 6 dB gain margin and $\pm 45^\circ$ phase margin. Since vector

margins are conservative, values approaching those in the MIL-STD were considered safe to flight test. The MIMO vector margins were considered only for comparison between designs.

3.4.2. H_2 Design Set-up and Resulting Design

The H_2 design problem was set-up as a one degree of freedom, angle of attack command controller in the feed-forward loop with output weightings to influence the resulting controller and a weight on the input to penalize the control power of the system. Figure 3.5 depicts the block diagram of the H_2 problem

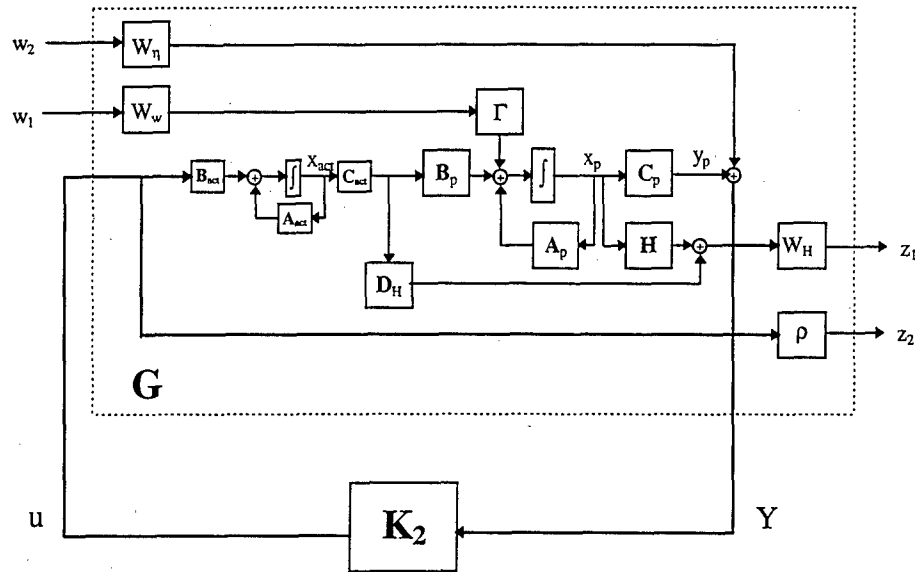


Figure 3.5. H_2 Design Model Block Diagram

set-up. Here the actuator is separate from the aircraft plant, and the matrix H represents the outputs of interest, $[\alpha, q, \theta, n_z, \gamma, v]$, while C_p relates to the outputs fed back, α and q . Input weights, W_n and W_w , represent sensor noise intensities and wind gust noise intensities respectively, and are set to anticipated levels and altered in the design process to obtain the desired noise rejection characteristics. The Γ is the second column of A , the α column, thereby affecting the states as an α perturbation. The output weight W_H , is a diagonal matrix with weighting factors on each of the outputs of H . The ρ is a penalty on control power. The H_2 problem can be expressed in equation form as

$$\begin{bmatrix} \dot{x}_p \\ \dot{x}_{act} \end{bmatrix} = \overbrace{\begin{bmatrix} A_p & B_p C_{act} \\ 0 & A_{act} \end{bmatrix}}^{A_2} \begin{bmatrix} x_p \\ x_{act} \end{bmatrix} + \overbrace{\begin{bmatrix} \Gamma W_w & 0 \\ 0 & 0 \end{bmatrix}}^{B_w} \begin{bmatrix} w_1 \\ w_2 \end{bmatrix} + \overbrace{\begin{bmatrix} 0 \\ B_{act} \end{bmatrix}}^{B_u} u \quad (3.7)$$

$$\begin{bmatrix} z_1 \\ z_2 \end{bmatrix} = \overbrace{\begin{bmatrix} W_H H & W_H D_H C_{act} \\ 0 & 0 \end{bmatrix}}^{C_z} \begin{bmatrix} x_p \\ x_{act} \end{bmatrix} + \overbrace{\begin{bmatrix} 0 & 0 \\ 0 & 0 \end{bmatrix}}^{D_{zw}} \begin{bmatrix} w_1 \\ w_2 \end{bmatrix} + \overbrace{\begin{bmatrix} 0 \\ \rho \end{bmatrix}}^{D_{zu}} u \quad (3.8)$$

$$y = \overbrace{\begin{bmatrix} C_y \\ C_p & 0 \end{bmatrix}}^{C_y} \begin{bmatrix} x_p \\ x_{act} \end{bmatrix} + \overbrace{\begin{bmatrix} 0 & W_\eta \end{bmatrix}}^{D_{yw}} \begin{bmatrix} w_1 \\ w_2 \end{bmatrix} + \overbrace{\begin{bmatrix} 0 \end{bmatrix}}^{D_{yu}} u \quad (3.9)$$

From this set-up, the designer sets the weights based on expected intensities and relative importance of the variables, then tunes the weights to obtain the controller that exhibits the desired objectives.

One of the desired objectives is to design a controller so the closed loop system will track a given commanded input. Since H_2 optimization does not target tracking as an objective, a pseudo-integrator was originally placed prior to the actuator. This pseudo-integrator would be joined with the controller for implementation to help improve tracking. It was found that the pseudo-integrator acted like a dynamic weight on u , which only increased the order of the controller, complicated the numerics, and did not improve the tracking. The H_2 synthesis created a controller state that inverted and canceled the pseudo-integrator state. When the H_2 controller was designed without the pseudo-integrator, the steady state response could be scaled with an input gain to obtain the desired outcome. Therefore, the H_2 controller was designed without the pseudo-integrator, as shown in Figure 3.5.

The process of designing an H_2 controller was fairly straight forward when the only objective was to reject noise. Even when the two types of noise introduced into the system resulted in competing objectives, the designer could quickly determine acceptable levels of each disturbance and trade off weightings to find an acceptable controller. However, designing an H_2 controller, based on this structure, that met the handling qualities criteria was extremely difficult. It should be pointed out that this method, as well as the other state-space optimization methods, are far more powerful with full state feedback. The process of designing an H_2 controller was just as iterative as the classical method, but more complex. For the classical method, the designer chooses a solution based on engineering judgment, evaluates the design to determine if the desired objectives were met, then refines the design. For the H_2 controller, the designer varies the

problem set-up via the weightings, solves the optimization problem, then evaluates the design to determine if the desired objectives were met. The designer then refines the weightings, resolves the problem, and hopes the 'refined' controller is an improvement. Unfortunately, the physical interpretation of the controller states is lost in the optimization process. So, although choosing which weighting to change to increase the noise rejection properties on a given output variable is not difficult, knowing which weighting would effect the closed loop damping or natural frequency was not intuitive. There was no predictable, direct relation between output weightings and improving predicted handling qualities ratings. The design chosen for implementation was found after numerous, almost random iterations. The difficulty in achieving the desired handling qualities objective by this design method, with the model structure set-up used in this research, raises serious questions concerning the utility of this design method, as applied, as the sole source for designing a manned aircraft flight control system. Since noise rejection typically is not the primary objective of a flight control system, H_2 optimization methods are well suited for mixed design methods which combine other objectives with noise rejection.

Despite the difficulties in obtaining level 1 handling qualities using H_2 design techniques with the set-up applied in this thesis, a controller design was chosen to flight test. The weightings used are shown in Table 3.3, with the penalty on control power set at $\rho=0.40$.

Input Weights	Value	Output Weights	Value
W_w	1000	w_α	5.0
N_α	10	w_q	1.0
N_a	10	w_θ	1.0
$W_\eta = \begin{bmatrix} N_\alpha & 0 \\ 0 & N_a \end{bmatrix}$		w_y	0.1
		w_{nz}	1.0
		w_γ	1.0

Table 3.3. H_2 Design Weightings

The resulting controller, in state-space form was

$$A_2 = \begin{bmatrix} -53.52 & 57.02 & 0.00 & 0.00 & 2.86 \\ 57.24 & -62.35 & -0.08 & 0.00 & 0.04 \\ 31.54 & -31.40 & -0.05 & -0.56 & 0.00 \\ -57.97 & 61.66 & 0.08 & 0.00 & -0.04 \\ -76.96 & -210.86 & 5.01 & -43.33 & -29.22 \end{bmatrix} \quad (3.10)$$

$$B_2 = \begin{bmatrix} -56.24 & 53.13 \\ 61.50 & -56.24 \\ 30.96 & -31.54 \\ -60.81 & 57.97 \\ 0.00 & 0.00 \end{bmatrix} \quad (3.11)$$

$$C_2 = [-3.85 \quad -10.54 \quad 0.25 \quad -2.17 \quad -0.46] \quad (3.12)$$

$$D_2 = [0.00 \quad 0.00] \quad (3.13)$$

and in transfer function form, the controller can be expressed in short-hand notation as

$$\frac{\delta_{ek}}{\alpha} = \frac{-292.46(20.00)(2.56)[0.28, 0.22]}{(116.71)[0.74, 19.52](-0.33)(0.04)} \quad (3.14)$$

$$\frac{\delta_{ek}}{q} = \frac{255.02(20.00)(-4.75)[0.30, 0.25]}{(116.71)[0.74, 19.52](-0.33)(0.04)} \quad (3.15)$$

where (x) represents (s+x), and $[\zeta, \sigma]$ represents $(s^2+2\zeta\sigma s+\sigma^2)$.

The time histories resulting from the SIMULINK simulation are shown in Appendix C. The handling qualities analysis results for the Bandwidth criteria are shown in Figure 3.6. and the results for the RSmith criteria are shown in Table 3.4.

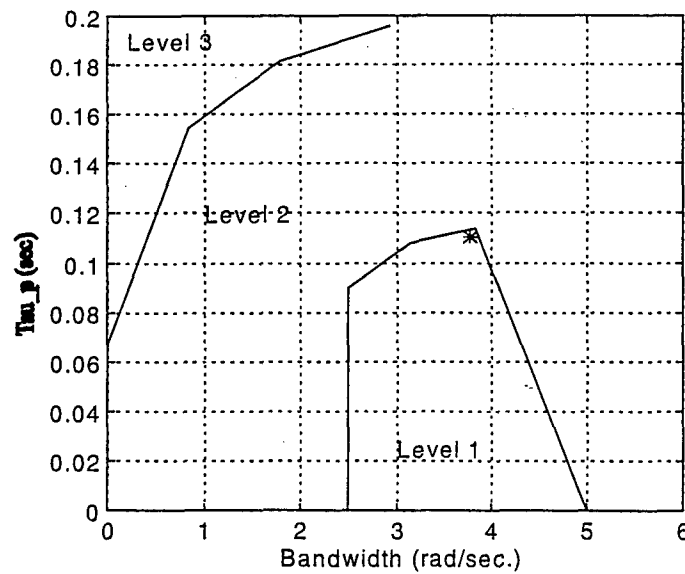


Figure 3.6. Category C Bandwidth Requirements: H₂ Design

Parameter	Value	Level
S (dB/octave)	-5.54	1
ω_c (rad/sec)	4.67	
Φ_{mc} (deg)	-143.11	2
t_{q-peak} (sec)	0.46	1

Table 3.4. RSmith Handling Qualities Predicted Level for the H_2

The stability vector margins for the H_2 design system are listed in Table 3.5.

Margin Type	Vector Gain Margin (dB)	Vector Phase Margin (degrees)
Input Margin	[7.41 -5.32]	± 33.35
Output Margin (α loop 'broken')	[24.61 - ∞]	± 77.17
Output Margin (q loop 'broken')	[7.92 -8.05]	± 35.16
MIMO Margins (sensitivity)	[6.50 -3.68]	± 30.55
MIMO Margins (complementary sensitivity)	[3.27 -5.32]	

Table 3.5. H_2 Design Vector Stability Margins

3.4.3. H_∞ Design Set-up and Resulting Design

The H_∞ design problem was set-up as a one degree of freedom, angle of attack command controller in the feed-forward loop with dynamic weightings on the system sensitivity and complementary sensitivity and a weight on the input to penalize the control power of the system. Figure 3.7 depicts the block diagram of the H_∞ problem set-up.

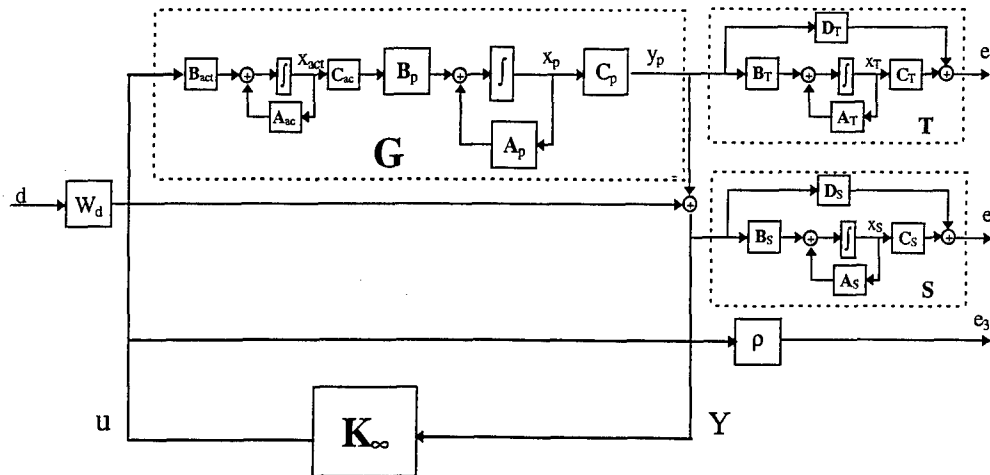


Figure 3.7. H_∞ Design Model Block Diagram

As with the H_2 set-up, the actuator is separate from the aircraft plant, and C_p contains the outputs fed back, α and q . The input weight, W_d , represents a weight on the bounded energy exogenous input, d . The dynamic weights on S and T are simply the inverse of the desired loop shapes of the system's sensitivity and complementary sensitivity functions. The ρ is a penalty on control power. The H_∞ problem can be expressed in equation form as

$$\begin{bmatrix} \dot{x}_p \\ \dot{x}_{act} \\ \dot{x}_S \\ \dot{x}_T \end{bmatrix} = \overbrace{\begin{bmatrix} A_p & B_p C_{act} & 0 & 0 \\ 0 & A_{act} & 0 & 0 \\ B_S C_p & 0 & A_S & 0 \\ B_T C_p & 0 & 0 & A_T \end{bmatrix}}^{A_\infty} \begin{bmatrix} x_p \\ x_{act} \\ x_S \\ x_T \end{bmatrix} + \overbrace{\begin{bmatrix} 0 \\ 0 \\ B_S W_d \\ 0 \end{bmatrix}}^{B_d} d + \overbrace{\begin{bmatrix} 0 \\ B_{act} \\ 0 \\ 0 \end{bmatrix}}^{B_u} u \quad (3.16)$$

$$\begin{bmatrix} e_1 \\ e_2 \\ e_3 \end{bmatrix} = \overbrace{\begin{bmatrix} D_S C_p & 0 & C_S & 0 \\ D_T C_p & 0 & 0 & C_T \\ 0 & 0 & 0 & 0 \end{bmatrix}}^{C_e} \begin{bmatrix} x_p \\ x_{act} \\ x_S \\ x_T \end{bmatrix} + \overbrace{\begin{bmatrix} D_S W_d \\ 0 \\ 0 \end{bmatrix}}^{D_{ed}} d + \overbrace{\begin{bmatrix} 0 \\ 0 \\ \rho \end{bmatrix}}^{D_{eu}} u \quad (3.17)$$

$$y = \overbrace{\begin{bmatrix} C_y \\ C_p & 0 & 0 & 0 \end{bmatrix}}^{C_y} \begin{bmatrix} x_p \\ x_{act} \\ x_S \\ x_T \end{bmatrix} + \overbrace{\begin{bmatrix} D_{yd} \\ W_d \end{bmatrix}}^{D_{yd}} d + \overbrace{\begin{bmatrix} D_{yu} \\ 0 \end{bmatrix}}^{D_{yu}} u \quad (3.18)$$

The process of designing an H_∞ controller is similar to the design process for the H_2 controller. The weightings are set to initial values, the controller is solved for, then the resulting controller is evaluated against some criteria. Although the process is similar, the choice of weights is more intuitive. The weights are based on the desired loop shape of the system, then tweaked to obtain the desired objectives. Constant weights, as well as first and second order weights on sensitivity, and constant and first order weights on complementary sensitivity were extensively investigated, including combinations of each type of weight. Poles in the sensitivity weights ranged from 0.0001 - 10.0 radians, and the zeros investigated ranged from 1.0 - 10,000 radians. The complementary sensitivity weights considered contained poles ranging from 1.0 - 10,000 radians, and zeros ranging from 0.0001 - 1.0 radians. Based on this problem set-up, with the aerodynamic model used, and types and ranges of weights considered, the best resulting design for handling

qualities, time response, and stability margins was determined. The weights chosen for sensitivity, S, and complementary sensitivity, T, in transfer function form were

$$W_{S\alpha} = \frac{5(s+100)}{(s+0.001)} \quad W_{T\alpha} = \frac{(s+0.001)}{(s+100)}$$

$$W_{Sq} = \frac{5(s+100)}{(s+0.001)} \quad W_{Tq} = 1$$

The resulting controller, in state-space form was

$$A_{\infty} = \begin{bmatrix} -7.80e-1 & 3.87e-1 & 0 & 0 & 2.86e+0 & 0 & 0 & 1.57e-6 \\ 6.05e-1 & -1.24e+0 & -8.04e-2 & 0 & 4.09e-2 & 0 & 0 & 1.57e-6 \\ 1.17e+0 & -7.20e-1 & -4.81e-2 & -5.62e-1 & 0 & 0 & 0 & -4.62e-6 \\ -6.09e-1 & 2.40e-1 & 8.04e-2 & 0 & -4.09e-2 & 0 & 0 & 2.42e-6 \\ -5.75e+2 & -2.79e+3 & 6.53e-2 & -9.90e+2 & -6.20e+1 & -2.49+3 & 6.82e+0 & 4.78e+1 \\ 0 & 0 & 0 & 0 & 0 & -1.00e-3 & 0 & 0 \\ 0 & 0 & 0 & 0 & 0 & 0 & -1.00e-3 & 0 \\ -3.94e-3 & 9.96e-1 & 0 & 0 & 0 & 0 & 0 & -1.00e+2 \end{bmatrix} \quad (3.19)$$

$$B_{\infty} = \begin{bmatrix} 1.78e-1 & 1.78e-1 \\ 1.77e-1 & 1.77e-1 \\ -5.22e-1 & -5.24e-1 \\ 2.73e-1 & 2.74e-1 \\ 0 & 0 \\ 4.45e-1 & 0 \\ 0 & 4.49e-1 \\ 1.76e-3 & 1.77e-3 \end{bmatrix} \quad (3.20)$$

$$C_{\infty} = [-6.40e+1 \quad -3.11e+2 \quad 7.26e+1 \quad -1.10e+2 \quad -4.67e+0 \quad -2.77e+2 \quad 7.59e-1 \quad 5.32e+0] \quad (3.21)$$

$$D_{\infty} = [0 \quad 0] \quad (3.22)$$

and in transfer function form, the controller can be expressed in short-hand notation as

$$\frac{\delta_{ek}}{\alpha} = \frac{-258.72(20.00)(1.53)[0.29, 0.24](0.19)}{[0.75, 41.63](3.03)(-1.18)(0.064)(0.001)} \quad (3.23)$$

$$\frac{\delta_{ek}}{q} = \frac{-134.49(20.00)(1.53)[0.29, 0.24](-2.95e-7)}{[0.75, 41.63](3.03)(-1.18)(0.064)(0.001)} \quad (3.24)$$

The time histories resulting from the SIMULINK simulation are shown in Appendix C. The handling qualities analysis results for the Bandwidth criteria are shown in Figure 3.8, and the results for the RSmith criteria are shown in Table 3.6.

Parameter	Value	Level
S (dB/octave)	-6.54	1
ω_c (rad/sec)	4.43	
Φ_{oc} (deg)	-155.11	2
t_{q-peak} (sec)	0.58	1

Table 3.6. RSmith Handling Qualities Predicted Level for the H_∞ Design

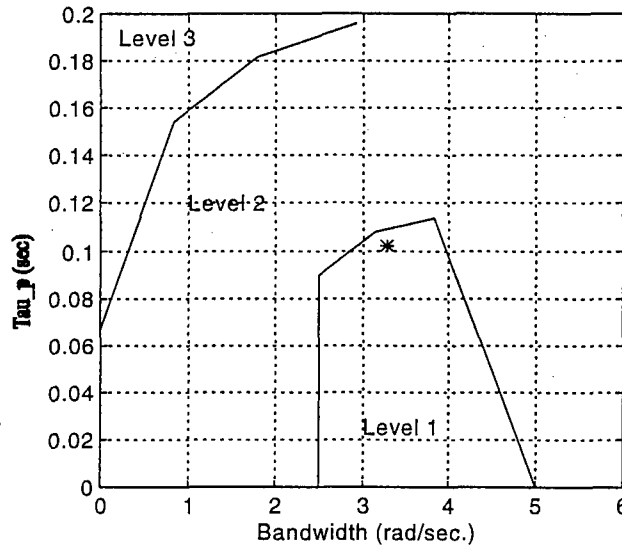


Figure 3.8. Category C Bandwidth Requirements: H_∞ Design

The stability vector margins for the H_∞ design system are listed in Table 3.7.

Margin Type	Vector Gain Margin (dB)	Vector Phase Margin (degrees)
Input Margin	[17.05 -7.60]	± 50.91
Output Margin (α loop 'broken')	[15.57 -16.78]	± 50.62
Output Margin (q loop 'broken')	[12.15 $-\infty$]	± 68.78
MIMO Margins (sensitivity)	[5.74 -3.42]	± 27.97
MIMO Margins (complementary sensitivity)	[3.26 -5.27]	

Table 3.7. H_∞ Design Vector Stability Margins

3.4.4. Mixed H_2/H_∞ Design Set-up and Resulting Design

The purpose of the mixed design technique is to design a controller that optimally trades off the objectives of both the H_2 design and the H_∞ design. Upon inspection of the time histories of the H_2 design and the H_∞ design discussed in previous sections, due to the handling qualities objective, there is little difference between the noise rejection properties of the two designs. Therefore, determining a tradeoff between these two designs, as proposed, would not demonstrate the strengths of the mixed method. The H_2 portion of the mixed set-up was therefore redone to pose the H_2 problem as a pure noise rejection problem. The nominal H_2 controller used in the mixed problem was not constrained by being implementable as an independent design, that is, it did not have to track commands, have stability margins, nor meet any handling qualities criteria. Although applying this same logic to the mixed design's H_∞ sub-problem might result in a mixed H_2/H_∞ controller with the best tradeoff between stability margins and noise rejection, there would be no guarantee that any of the resulting controllers would meet the handling qualities criteria. The H_∞ sub-problem used was required to meet both the stability margin requirements and the handling qualities objective, but no restriction on noise rejection properties or other implementation issues were made.

Initially the H_∞ design set-up described in the previous section was used for the mixed H_2/H_∞ synthesis. Unfortunately, the complexity of a single H_∞ constraint with dynamic weightings on both sensitivity and complementary sensitivity prevented a solution to the mixed control problem as posed. A new H_∞ sub-problem set-up, only weighting the system complementary sensitivity function, was derived. The resulting H_∞ controller's handling qualities ratings are shown in Figure 3.10, and Table 3.9. The H_∞ controller expressed in shorthand notation is

$$\frac{\delta_{ek}}{\alpha} = \frac{-2.07e+7(1000.00)(20.00)(1.53)[0.29, 0.24]}{(2.11e+5)[0.97, 762.38](2.92)(-1.07)(0.060)} \quad (3.25)$$

$$\frac{\delta_{ek}}{q} = \frac{-2.08e+7(1000.00)(20.00)(1.53)[0.29, 0.24]}{(2.11e+5)[0.97, 762.38](2.92)(-1.07)(0.060)} \quad (3.26)$$

This design was not implementable due to the second order high frequency poles which could not be eliminated without resulting in an improper controller or effecting the design characteristics. The implementation issues of the various controllers are addressed in the next chapter.

The mixed design H_2 sub-problem used the same structure as the set-up used for the previous H_2 design. The weights chosen for the mixed design H_2 sub-problem resulted in a design that rejected the wind and sensor noise; specifically the focus was on minimizing the angle of attack perturbations, or wind gust noise. The weights used are shown in Table 3.8.

Input Weights	Value	Output Weights	Value
W_w	1000	w_α	200.00
N_α	1000	w_q	100.00
N_q	1000	w_θ	0.01
$W_\eta = \begin{bmatrix} N_\alpha & 0 \\ 0 & N_q \end{bmatrix}$		w_γ	0.01
		w_{pz}	1.00
		w_v	1.00
		ρ	1.0

Table 3.8. Design Weighting for Mixed H_2 Sub-problem

This design would have been considered a Cooper-Harper handling qualities rating 10 (uncontrollable).

The time histories for this design are shown in Appendix C.

The mixed H_2/H_∞ synthesis was performed with these two sub-problems. The initial controller used in the numerical mixed solution is the H_2 controller described in the previous paragraph. The resulting α versus γ curve is presented in Figure 3.9. Each of the points on the curve represent a controller determined to be on the optimal 2-norm versus ∞ -norm curve. Each of these controllers was then evaluated

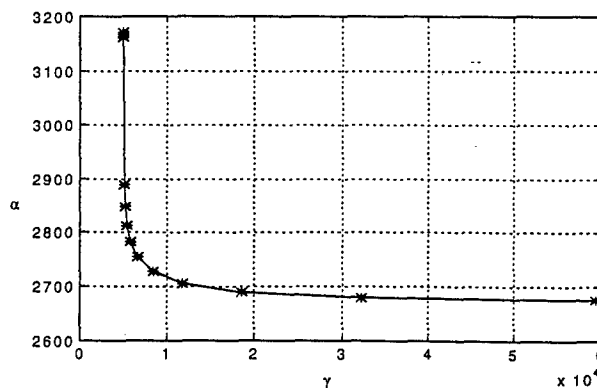


Figure 3.9. Mixed H_2/H_∞ α versus γ curve

for handling qualities, stability margins, and time history response. There did not seem to be any predictable pattern to the handling qualities rating resulting from the closed loop systems as successive controllers on the curve were analyzed. A few had acceptable handling qualities predictions, so the 'best' of those, considering all of the evaluation criteria, was chosen for flight test.

The resulting mixed controller, in state-space form, was

$$A_m = \begin{bmatrix} -5.00e+3 & -6.14e-1 & 0 & 0 & 0 & 0 & 0 \\ 6.13e-1 & -1.50e+3 & -4.81e-2 & 0 & 0 & 0 & 0 \\ 0 & 4.81e-2 & -8.35e+1 & 2.57e+0 & 0 & 0 & 0 \\ 0 & 0 & -2.57e+0 & -2.07e+1 & 3.49e+1 & 0 & 0 \\ 0 & 0 & 0 & -3.49e+1 & -2.42e+1 & 5.18e+0 & 0 \\ 0 & 0 & 0 & 0 & -5.18e+0 & 1.62e+0 & -2.78e-2 \\ 0 & 0 & 0 & 0 & 0 & 2.78e-2 & -8.52e-2 \end{bmatrix} \quad (3.27)$$

$$B_m = \begin{bmatrix} 9.55e-2 & -3.71e+0 \\ -3.01e-2 & 1.05e+0 \\ -3.01e+1 & 1.86e+2 \\ 3.83e+1 & 1.06e+2 \\ 6.46e+0 & 1.66e+2 \\ -1.73e+1 & -2.02e+1 \\ -5.83e+0 & 4.49e+1 \end{bmatrix} \quad (3.28)$$

$$C_m = [-1.50e+3 \quad -5.00e+3 \quad 2.60e+0 \quad -1.48e+0 \quad -3.68e-1 \quad 3.54e-1 \quad -1.61e-2] \quad (3.29)$$

$$D_m = [0 \quad 0] \quad (3.30)$$

and in transfer function form, the controller can be expressed in short-hand notation as

$$\frac{\delta_{ek}}{\alpha} = \frac{-139.01[0.54, 2815.28][0.84, 40.96][0.48, 0.26]}{(4999.94)(1500.29)(83.44)[0.54, 41.65](-1.29)(0.085)} \quad (3.31)$$

$$\frac{\delta_{ek}}{q} = \frac{581.82(-27623.10)[-0.093, 97.35](19.83)[0.23, 0.26]}{(4999.94)(1500.29)(83.44)[0.54, 41.65](-1.29)(0.085)} \quad (3.32)$$

The time histories resulting from the SIMULINK simulation are shown in Appendix C. The handling qualities analysis results for the Bandwidth criteria are shown in Figure 3.10. and the results for the RSmith criteria are shown in Table 3.9.

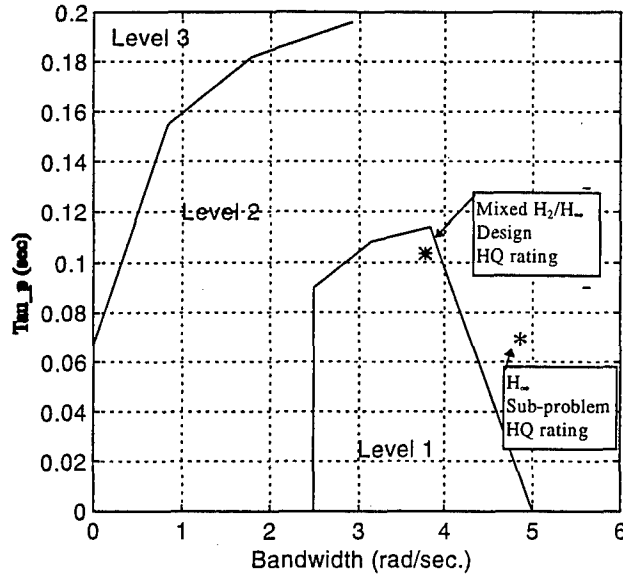


Figure 3.10. Category C Bandwidth Requirements: Mixed Design

	H_{∞} Sub-problem		Mixed H_2/H_{∞} Design	
Parameter	Value (Level)		Value (Level)	
S (dB/octave)	-5.79	(1)	-5.90	(1)
ω_c (rad/sec)	4.61		4.58	
Φ_{ω_c} (deg)	-132.22	(1)	-146.58	(2)
$t_{q\text{-peak}}$ (sec)	0.041	(1)	0.48	(1)

Table 3.9. RSmith Handling Qualities Predicted Level for the Mixed Design

The stability vector margins for the mixed design system are listed in Table 3.10.

Margin Type	H_{∞} Sub-problem		Mixed H_2/H_{∞} Design	
	VGM (dB)	VPM (degrees)	VGM (dB)	VPM (degrees)
Input Margin	[37.79 -11.78]	± 59.15	[10.77 -12.09]	± 44.13
Output Margin (α loop 'broken')	[28.09 - ∞]	± 61.14	[25.14 - ∞]	± 75.96
Output Margin (q loop 'broken')	[13.13 - ∞]	± 68.64	[11.04 -18.70]	± 52.45
MIMO Margins (sensitivity)	[7.25 -3.89]	± 42.05	[7.51 -3.97]	± 40.28
MIMO Margins (complementary sensitivity)	[4.70 -10.89]		[4.55 -10.13]	

Table 3.10. Mixed Design Vector Stability Margins

3.5. Summary

This chapter has described the steps taken to develop, design, and evaluate four longitudinal flight control systems, starting with stability derivatives describing the basic longitudinal modes of motion of a fictitious unstable fighter type aircraft. The methods used to design these flight control systems included classical methods, as well as modern state-space methods, specifically H_2 , H_∞ , and mixed H_2/H_∞ control synthesis. The performance of each design was not intended to be compared to the other designs. The designs offered here may not be the 'best' each of these design methods can create. The intent was merely to demonstrate the ability to implement these design methods from design model set-up through the flight test process. The practicality of these design methods was addressed in this chapter, and will be further addressed in Chapter 4, Implementation. With that said, the designs are summarized in the following figure and tables. Time history plots are in Appendix C.

	Classical	H_2 Design	H_∞ Design	H_∞ Sub-problem	Mixed H_2/H_∞
Parameter	Value (Lvl)	Value (Lvl)	Value (Lvl)	Value (Lvl)	Value (Lvl)
S (dB/octave)	-3.97 (1)	-5.54 (1)	-6.54 (1)	-5.79 (1)	-5.90 (1)
ω_c (rad/sec)	5.05	4.67	4.43	4.61	4.58
Φ_{oc} (deg)	-150.84 (2)	-143.11 (2)	-155.11 (2)	-132.22 (1)	-146.58 (2)
t_{q-peak} (sec)	0.48 (1)	0.46 (1)	0.58 (1)	0.041 (1)	0.48 (1)

Table 3.11. RSmith Handling Qualities Predicted Level Summary

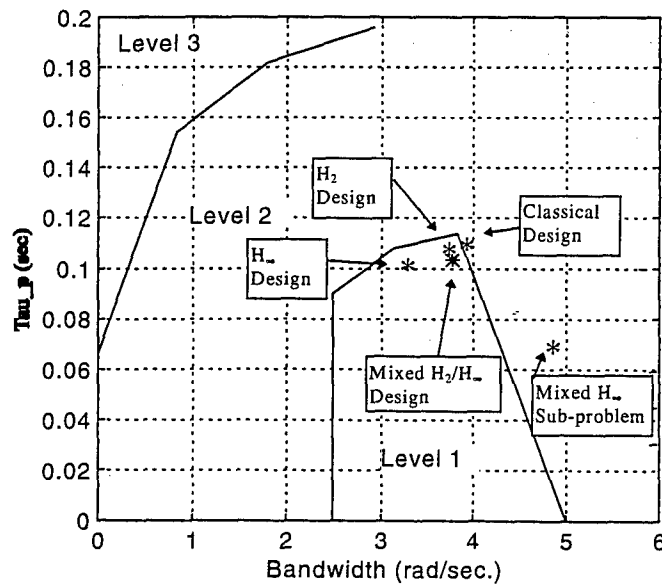


Figure 3.11. Category C Bandwidth Requirements: All Designs

	Classical		H ₂ Design		H _∞ Design		Mixed H _∞ Sub-problem		Mixed H ₂ /H _∞	
Margin Type	[VGM] (dB)	(VPM) (deg)	[VGM] (dB)	(VPM) (deg)	[VGM] (dB)	(VPM) (deg)	[VGM] (dB)	(VPM) (deg)	[VGM] (dB)	(VPM) (deg)
Input Margin	[6 -∞]	(±61)	[7 -5]	(±33)	[17 -8]	(±51)	[38 -12]	(±59)	[11 -12]	(±44)
Output Margin (α loop 'broken')	[12 -8]	(±43)	[25 -∞]	(±77)	[16 -17]	(±51)	[28 -∞]	(±61)	[25 -∞]	(±75)
Output Margin (q loop 'broken')	[7 -9]	(±37)	[8 -8]	(±35)	[12 -∞]	(±69)	[13 -∞]	(±69)	[11 -18]	(±52)
MIMO Margins (sensitivity)	[3 -2]	(±18)	[6 -4]	(±31)	[6 -3]	(±28)	[7 -4]	(±42)	[8 -4]	(±40)
MIMO Margins (comp sensitivity)	[2 -3]	(±18)	[3 -5]	(±31)	[3 -5]	(±28)	[5 -11]	(±42)	[5 -10]	(±40)

Table 3.12. Vector Stability Margin Summary

IV. Implementation

4.1. Implementation Model

The implementation issues raised in this chapter are directed at specific challenges resulting from the limitations of the Calspan VSS II Learjet. Some of the concerns are general in nature and would apply to any system designed with these methods, while other concerns are specific to the Calspan VSS II Learjet system and the flight test limitations for this project. This chapter addresses the factors that required major attention to ensure these flight control systems were successfully flight tested. The first problem was due to the VSS II simulation computer system's computing speed and the integration routine it uses. The second issue concerned the problems that result when implementing an unstable controller. The last major problem was due to the actuator model used in the design process. The last section of this chapter discusses the model verification and validation testing conducted on the implementation used for the actual flight test.

The architecture of the controller implemented needed to be general enough to accommodate all four designs. This requirement would allow designs to be quickly and efficiently switched in-flight, saving valuable flight test resources. Four separate set-up script files were used to initialize the system variables at the stroke of a button.

4.1.1. VSS II System Limitations

The implementation requirements for VSS II provided by Calspan are presented in Chapter II. The requirements that effected the implementation model most were: the integration routine (Euler) and step size (0.01sec) used; casting the controllers in pole/zero/gain form using scalar parameters and integrators, like in Figure 2.13; and ensuring that the integrators can be initialized and zero-ized (reset) in-flight with the system running.

The integration routine used by the VSS II computer was not known until after the design process was complete. It is recommended that the design phase use the integration routine implemented in the aircraft. Unfortunately, that was not known during the design phase. Once this limitation was discovered, the computer simulations were redone using Euler integration. These revised time histories were numerically unstable. The designs that had problems contained poles and/or zeros with a natural frequency

greater than 100 radians/second. Dynamics at those frequencies are beyond the range which affect aircraft dynamic modes of motion. Therefore, to eliminate the implementation problem, those poles and zeros were removed from the controller's transfer functions. The system norms, stability margins, handling qualities rating, and time histories were reevaluated to ensure this change did not significantly effect the properties of the controller. For the designs implemented, the evaluation criteria were unaffected by the reduced order controllers. The reduced transfer functions, in shorthand notation, chosen for implementation are shown in Table 4.1. Although the H_2 controller maintained a high frequency pole

	Alpha Controller, $\frac{\delta_{ek}}{\alpha}$	q Controller, $\frac{\delta_{ek}}{q}$
Classical Design	$\frac{34}{(10)}$	2.3
H_2 Design	$\frac{-292.46(20.00)(2.56)[0.28, 0.22]}{(116.71)[0.74, 19.52](-0.33)(0.04)}$	$\frac{255.02(20.00)(-4.75)[0.30, 0.25]}{(116.71)[0.74, 19.52](-0.33)(0.04)}$
H_∞ Design	$\frac{-258.72(20.00)(1.53)[0.29, 0.24](0.19)}{[0.75, 41.63](3.03)(-1.18)(0.064)(0.001)}$	$\frac{-134.49(20.00)(1.53)[0.29, 0.24](-2.95e-7)}{[0.75, 41.63](3.03)(-1.18)(0.064)(0.001)}$
Mixed H_2/H_∞ Design	$\frac{-146.88[0.84, 40.96][0.48, 0.26]}{(83.44)[0.54, 41.65](-1.29)(0.085)}$	$\frac{-2.14[0.84, 40.96][0.48, 0.26]}{(83.44)[0.54, 41.65](-1.29)(0.085)}$

Table 4.1. Reduced Order Controllers

at 116.7 rad/sec, which could have been discarded, the computer SIMULINK simulation time histories remained stable and appeared to meet the Calspan requirements.

The mixed H_∞ sub-problem design was eliminated from implementation since it could not be reduced to a lower order. It contained one zero and three poles with natural frequencies well above 100 rad/sec. Removing them would result in an improper system or significant changes to the properties of the controller. This limitation did not prevent this controller design from use in the mixed control synthesis. However, it does point out one concern of these methods, as applied. Controllers can be synthesized which are not implementable due to high frequency poles or zeros. Consideration should be given to adding a constraint to the problem which limits the frequency of the resulting controller.

The next task, in developing the implementation model, was to cast the controller model in pole/zero/gain form, like in Figure 2.13. This single controller architecture had to accommodate all four controller designs, even though each controller is of different order, and the classical controller is in the

feedback, rather than the feed-forward path. There are numerous ways to construct a system that meets the Calspan requirements, the controller model initially chosen is shown in Figure 4.1. This model met all of

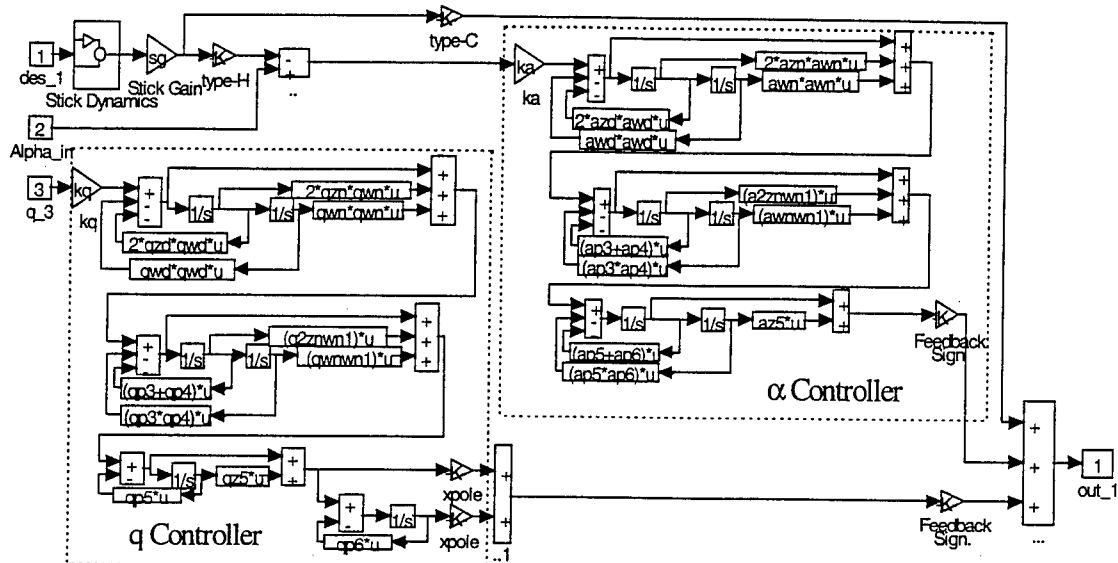


Figure 4.1. Initial Implementation Model

the requirements Calspan specified. The problems that occurred did not become apparent until the ground testing phase of the project.

4.1.2. Final H_2 , H_∞ and Mixed H_2/H_∞ Implementation Model

There were two major implementation issues discovered during the ground testing phase. The first was a result of the controllers designed by the modern methods being unstable; that is, they contained poles in the right half s-plane. The second concern resulted from simulating the first order design model actuator with the actual aircraft's fourth order actuator. The latter of these concerns was simply resolved, as described at the end of this section. The implementation of an unstable controller was more difficult.

When the controllers were implemented, as shown in Figure 4.1, during the ground testing, after approximately 23 seconds the system went unstable and diverged. Upon examining the controller integrator states, the individual integrators diverged upon activation of the controller. The closed loop system remained stable since the controller output was a small difference of large numbers. As the states grew exponentially, the numerics broke down and the system eventually went unstable. Therefore, the general architecture needed to be posed in a way that kept the integration states from growing exponentially. The

controllers were designed using state-space methods, so a state-space implementation architecture was attempted.

The implementation architecture redesign was accomplished by using a similarity transformation matrix on the state space representation of the reduced order controllers. The reduced order controllers were transformed into observer canonical form. The SIMULINK block diagram was then created to represent a general controller system. The block diagram that was implemented is shown in Figure 4.2.

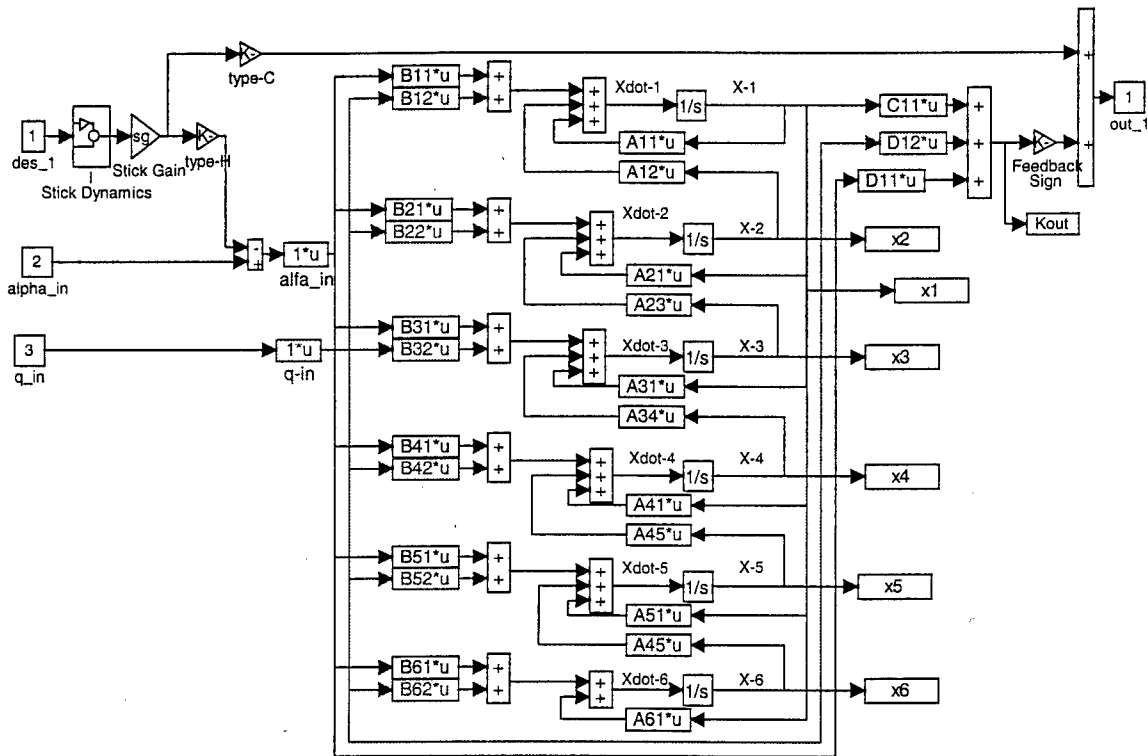


Figure 4.2. Implementation Block Diagram

where

$$A_c = \begin{bmatrix} A_{11} & 1 & 0 & 0 & 0 & 0 \\ A_{21} & 0 & 1 & 0 & 0 & 0 \\ A_{31} & 0 & 0 & 1 & 0 & 0 \\ A_{41} & 0 & 0 & 0 & 1 & 0 \\ A_{51} & 0 & 0 & 0 & 0 & 1 \\ A_{61} & 0 & 0 & 0 & 0 & 0 \end{bmatrix} \quad (4.1)$$

$$B_c = \begin{bmatrix} B_{11} & B_{12} \\ B_{21} & B_{22} \\ B_{31} & B_{32} \\ B_{41} & B_{42} \\ B_{51} & B_{52} \\ B_{61} & B_{62} \end{bmatrix} \quad (4.2)$$

$$C_c = [1 \ 0 \ 0 \ 0 \ 0 \ 0] \quad (4.3)$$

$$D_c = [D_{11} \ D_{12}] \quad (4.4)$$

and x1-x6 are the individual states. The 'type-C' and 'type-H' blocks select the appropriate feedback structure, and the 'feedback sign' block changes the polarity of the feedback loop. The off diagonal elements of the A_c matrix were left in variable form so controllers of lower order could be accommodated. This representation also meets the Calspan requirements, and remains numerically stable. The Calspan engineers added 'balance and hold' blocks and replaced the 1/s blocks with 'engage integrators'. These Calspan created blocks are simple functions that allow the integrators to be initialized and reset by the computer operator in-flight. It should be noted that this is just one way to solve the implementation problem resulting from unstable poles in the controller. It may not be the 'best' solution. Some of the states still gradually increased to fairly large numbers, but did not grow exponentially, and did not cause numerical problems for the duration the system was engaged during flight test (approximately 8 - 10 minutes per pattern). Although the unstable controllers were successfully implemented for this research, a flight control designer should approach unstable controllers with caution since the instability complicates implementation issues. It should be emphasized that this research was for a point design under controlled conditions, and not for a broad aircraft envelope or varying conditions.

The last major implementation issue concerned the actuator model used in the design. After the implementation model was finalized, the ground testing, as well as the initial verification and validation flight test revealed unpredicted oscillatory motion in some of the time histories. The Calspan VSS II system simulates different aircraft dynamics by varying computer gains to modify the elevator actuator command. The VSS II system's actuator is extremely fast (approximately 200 rad/sec) and can be modeled as a fourth order system. Modifying the fourth order dynamics down to first order dynamics with computer gains was not considered effective. The simulation would have been more accurate if a second order actuator model

had been used for design. The VSS II's actuator was considered fast enough that the resulting aircraft response should not have been adversely effected, and the added $\frac{20}{s + 20}$ dynamics would accurately represent the aircraft targeted by the designs. However, when the $\frac{20}{s + 20}$ dynamics were removed the unwanted response disappeared. The resulting system response is discussed in the following verification and validation testing section.

4.2. Verification and Validation Testing

The simulated aircraft dynamics and the four flight control designs were ground tested to verify the implementation accuracy, from 9 September 1996 through 20 September 1996. During this time the previous mentioned implementation problems were addressed. In addition, two verification flights were flown by a CALSPAN safety pilot and a USAF Test Pilot School staff pilot prior to actual flight test of the designs. Model validation testing was accomplished on the four flight control system designs while flying to and from Palmdale Airport, on the flight test sorties. Only one design was examined on a single sortie. Heavy weight data were obtained flying to Palmdale Airport and light weight data during the return trip to Edwards AFB. Programmed Test Inputs (PTI) provided the required frequency sweeps and step inputs. The frequency sweeps provided data for Frequency Response Analysis (FRA). Data were recorded using the VSS II onboard system in a MATLAB™ format. The sampling rate was 50 Hz. Recorded data parameters are listed in Table D1, in Appendix D. All model validation testing occurred between 4,000 and 6,000 feet MSL. The aircraft was flown at final approach speed (125 to 135 KAS) with gear down and 20-degree flaps. The frequency range of the programmed sweeps was from .1 to 10 Hz. The amplitude was 0.25 degree. Duration was 25 seconds which provided approximately 1250 data points. The FRA was performed using PC-FRA, Version 1.01, developed by High Planes Engineering. Step inputs were used to compare predicted time histories. The steps were 1 inch of stick deflection in magnitude for 3 seconds duration. Time histories and bode plots were then compared to predicted responses simulated in MATLAB™.

Model validation analysis was performed using the data shown in Appendix E. Bode plots generated from MATLAB™ and flight test data for the closed loop transfer functions alpha output to stick

displacement and pitch rate output to stick displacement were analyzed for each design method. The flight test data were limited in frequency range from 0.1 radians per second (r/s) to approximately 30 to 40 r/s, based on the frequency sweep used. The higher frequency content was not considered significant since this was beyond the frequency range that affects handling qualities and most of the system outputs in the flight control systems were attenuated above 30 r/s. Lower frequency data would be desired, down to at least 0.01 r/s, to validate the low frequency response of the closed-loop system and to compare it to the predicted model since there were some dynamics predicted at lower frequencies. Model validation testing should be conducted with frequency sweeps that provide a lower frequency content.

For the classical flight control system design, the magnitude gain over the frequency range tested matched well with predicted values. The H_2 design frequency plots showed significant differences between the predicted gain levels and the flight test data. The H_∞ design frequency plots were inconclusive due to scatter, and were marginal at best. The mixed design frequency plots had the best comparison with the predicted model, but still contained some additional gain above 10 r/s. The phase content of the closed-loop system, for all the designs, consistently showed additional phase lag, as much as approximately 20 degrees from predicted. This could degrade the predicted handling qualities, based on RSmith criteria [SG79], as much as one to two Cooper-Harper ratings [CH69].

Flight test time histories of alpha and pitch rate (q) resulting from a step programmed test input (PTI) were compared to MATLAB™ generated model predictions (Figures E9 through E12). The predictions used a 3-second step input, while the duration of the PTI lasted from 5 to 6 seconds. Response trend comparisons could still be made. The flight test pitch rate response was representative of the predicted response for all the designs except the H_2 design, which deviated from predicted. The classical and the mixed designs exhibited some additional pitch rate response delay, compared to the predicted model. The alpha flight test response for all the designs was similar in character to predicted for the first 1 to 2 seconds, although the classical design displayed more initial delay. The alpha response had significant deviations which can be seen in Appendix E, Figures E9 through E12.

The close matches between the classical predicted curves and the flight test data, for both frequency response and time histories, tend to indicate that the unaugmented aerodynamics simulated by the VSS II

Learjet were similar to the model used in design, although the classical system exhibited significant additional lag. This in-flight simulated aerodynamic model was used for all the configurations flown. The marginal at best (mixed), inconclusive to marginal (H_{∞}), and mismatched (H_2) comparisons between predicted curves and flight test data indicate a problem in the implementation of these designs in the VSS II Learjet. Although there is a mismatch between the design predicted time histories and the model validation flight test results, for the purpose of demonstrating the design process through flight test implementation of these methods, the difference was not significant enough to invalidate the results. Analysis of the VSS II Learjet system capabilities and the limitations when implementing these flight control designs are beyond the scope of this thesis, but should be considered in future flight tests of similar systems. It should also be noted that these factors may contribute to but do not fully explain the undesirable aircraft response during the flare through landing roll-out, exhibited by some of the flight control systems described in the following results sections.

The deviations between the predicted time histories and the flight test results make drawing conclusions concerning comparisons between design methods questionable. This was not an objective of this research. The model verification and validation testing results were considered sufficient to demonstrate the successful implementation of these flight control design methods.

V. Flight Test Results

This chapter presents the results of a limited handling qualities evaluation of the four longitudinal flight control systems designed during this research. Three of the flight control systems were designed using modern state-space optimization techniques. The fourth was designed using classical techniques. The flight test phase of this project was labeled HAVE INFINITY. The purpose of the HAVE INFINITY flight test was to evaluate the handling qualities of these four longitudinal flight control systems during the approach and landing phase of flight. Flight tests were conducted using the CALSPAN Variable Stability Simulator II (VSS II) aircraft from 30 September to 3 October 1996 at Edwards AFB and Palmdale Airport, California. The HAVE INFINITY test team consisted of members of USAF Test Pilot School Class 96A. Team members flew 9 practice sorties, requiring 12 flight hours, and 6 test sorties, requiring 8 flight hours. Testing was requested by Wright Laboratory, Wright-Patterson AFB, Ohio.

5.1. Test Objective

The test objective was to evaluate the handling qualities of the four HAVE INFINITY longitudinal flight control systems during the approach and landing phase of flight. Each flight control system was evaluated using an offset landing task as described in the Test Procedures section of this chapter. Cooper-Harper (CH) and PIO ratings were assigned by the project test pilots after each offset landing task. Analysis of CH and PIO ratings, as well as pilot comments, allowed the determination of a final handling quality level for each flight control system design. One of three levels was assigned based upon the following guidance.

Level I: Satisfactory, no improvement necessary, CH 1-3

Level II: Unsatisfactory but tolerable, deficiencies warrant improvement, CH 4-6

Level III: Unacceptable, deficiencies require improvement, CH 7-9

These final criteria were based on information described in "The Use of Pilot Ratings in the Evaluation of Aircraft Handling Qualities"[CH69] and in USAF TPS Flying Qualities Phase Text Vol. IV, Flying Qualities Testing [TPS95].

5.2. Test Procedures

The HAVE INFINITY test program was conducted from 30 September to 3 October 1996 at Edwards AFB and Palmdale Airport, California. It consisted of six flights and 8 hours of flight test. The handling qualities of four different longitudinal flight control systems were evaluated during the approach and landing phase of flight using an offset landing task. The task was performed by four evaluation pilots with a broad range of flying experience. Table 5.1 summarizes each pilot's previous weapon system experience.

Evaluation Pilot	Weapon System Experience
1	C-141B
2	B-1B
3	F-16
4	F-18

Table 5.1. Evaluation Pilots' Flying Experience

Each of the four evaluation pilots rated the flight control system designs using the CH and PIO rating scales (Appendix F). Prior to the actual flight test, each pilot practiced the offset landing task in a variety of different aircraft. This allowed the pilots to become familiar with the task over a broad range of aircraft handling qualities. The practice aircraft included the F-15, F-16, T-38, and C-23.

5.2.1 Methods and Conditions

The test team aircrew onboard the VSS II included a CALSPAN safety pilot, a HAVE INFINITY evaluation pilot, a test conductor, and a CALSPAN system operator who reconfigured the flight control systems. The CALSPAN safety pilot was the aircraft commander. The test conductor duties were performed by a HAVE INFINITY test team engineer or a second evaluation pilot. Flight tests were limited to a maximum head-wind of 20 knots, a maximum tailwind of 10 knots, and a maximum crosswind of 10 knots for flight safety and data quality considerations. The ground test team consisted of two spotters stationed beside the landing runway at Palmdale Airport. These spotters maintained VHF radio contact with both the Palmdale control tower and the test team aircrew.

The flight test was structured into test blocks. Each test block represented one of the four flight control system configurations and consisted of three approaches. The three approaches had to be flown sequentially on a single flight in order to complete the test block. Each test block was reserved for a single pilot/flight control configuration pairing. Only the CALSPAN safety pilot and the test conductor knew which flight control system was actually being tested. Evaluation pilots performed blind testing throughout the test program.

The first approach of each test block was a straight-in to a touch and go. If the flight control configuration under test was controllable, as defined in MIL-STD-1797A [Mil90], the test proceeded to the offset landing task. The offset landings were accomplished as described in the next section. The evaluation pilot provided comments and CH/PIO ratings for each offset landing performed. If a CH rating of 8 or better was obtained on the first offset landing of a test block, the evaluation pilot repeated the offset landing task and again provide comments and CH/PIO ratings. A third offset landing was accomplished if the comments and ratings from the first two were inconsistent. The test conductor determined if the ratings were consistent and when the test block was complete. Data from any additional landings were also included in the final analysis of the appropriate control system design.

5.2.2 Offset Landing Task:

The offset landing task was performed at Palmdale Airport, Runway 25. The VSS II aircraft was configured with the appropriate flight control system on downwind at approximately 150 KCAS and the variable stability system was then engaged. The aircraft was configured with gear and 20-degree flaps and turned to final to intercept the 3-degree ILS glideslope. On final, the aircraft was offset 300 feet to the left of centerline and slowed to final approach speed. The safety pilot called altitude above the ground in 50-foot increments off of the radar altimeter. At 200 feet AGL, the safety pilot called "maneuver". The evaluation pilot aggressively maneuvered the aircraft using 30 to 45 degrees of bank to capture the runway centerline. A simultaneous longitudinal correction was made to intercept a visual glidepath to touchdown. The pilot attempted to land in the middle of the desired box described in the next paragraph at a touchdown speed 10 knots less than approach speed (+10/-5 knots).

5.2.2.1. Landing Zone

Specialized runway markings used to determine desired and adequate task performance were painted on Runway 25 at Palmdale Airport. Standard 18-inch wide white paint lines were used for all markings. The landing zone markings are depicted in Figure 5.1. The leading edge of the desired box corresponded to the ILS glideslope point of impact. Standard runway distance markers were used as a backup in case the lines became obscured or a runway change was necessary.

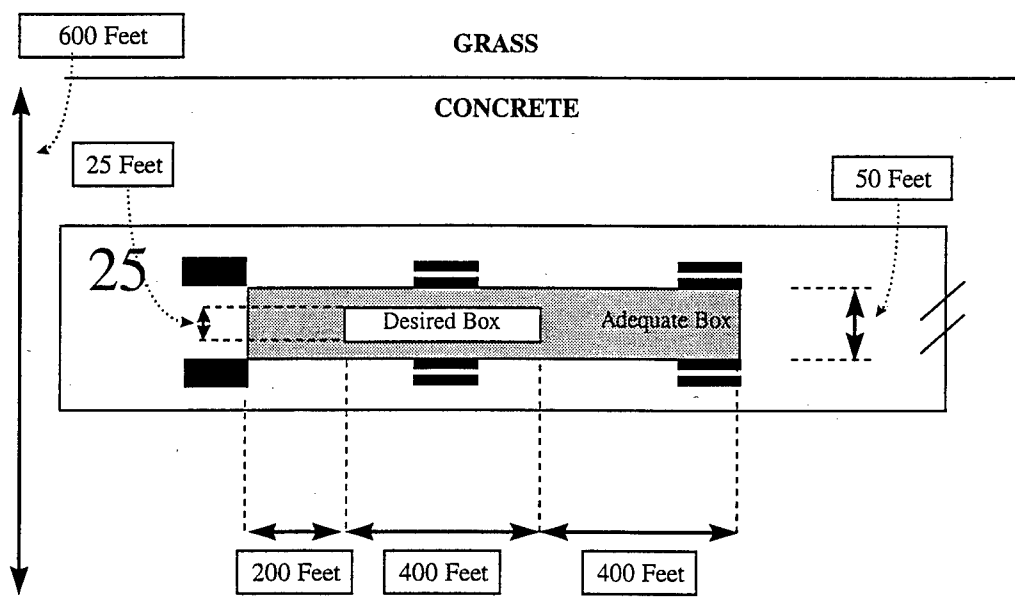


Figure 5.1. Landing Zone Markings and Dimensions

5.2.2.2. Landing Task Evaluation

Following the touch and go, the safety pilot took control of the aircraft. The evaluation pilot received a performance rating from the ground spotters over the VHF radio based on the aircraft's touchdown position. For a landing to be considered in a particular zone, both main landing gear were required to be on or inside the respective white line. The evaluation pilot determined whether airspeed and lateral touchdown criteria were met. Based on this information, the evaluation pilot assigned a performance rating of desired, adequate, or inadequate. The test conductor then stepped the evaluation pilot through the

CH and PIO rating scales. Evaluation pilots assigned a CH and PIO rating to each offset landing task accomplished. Evaluation pilots also gave qualitative comments on handling qualities, workload, and problems effecting task performance. The comment card used is shown in Appendix F.

An 8mm camcorder onboard the VSS II recorded all landings and associated pilot comments. A ground based camera also recorded Sortie No. 2 from final approach to roll out. Post-flight analysis of cockpit videotape and the test card comments was used to construct a database of pilot comments for each of the flight control system designs. A summary of these pilot comments can be found in Appendix G.

5.3. Results and Analysis

The next four sub-sections describe the flight test results for the four design configurations based on the flight test team's analysis of the flight test data. The focus of the HAVE INFINITY test team was to determine a handling qualities rating for each design. The test team's perspective and evaluation is included even though it was not limited to the design point used in the controllers' design. All of the figures referenced in these next four sub-sections are presented in Appendix H, and are as they were presented in the flight test report. The overall results section, however, interprets these results as they apply to this thesis.

5.3.1. Classical Flight Control Configuration

The four evaluation pilots performed four straight in approaches and ten offset landing tasks with the classical flight control design. See Figures H.1. and H.2. for CH and PIO ratings. Evaluation pilot 4 did not provide PIO ratings for two approaches. All the pilots stated that the classical flight control design flew nicely throughout the landing task. The aircraft was predictable, responsive and had good sensitivity. One pilot indicated that quick abrupt inputs were required to maintain glide-path, and that there was a tendency to over flare the aircraft. A second pilot stated that he got a slight bobble upon the initial glide-slope capture and that the stick was a bit too heavy. The third pilot stated that excessive aft stick was required in the flare. A fourth pilot stated that the aircraft flew nicely without additional qualifications. Overall, this configuration was considered Level II.

5.3.2. H₂ Flight Control Configuration

The four evaluation pilots performed four straight in approaches and twelve offset landing tasks with the H₂ flight control design. See Figures H.3. and H.4. for CH and PIO ratings. The comments indicated that the aircraft felt heavy and unresponsive. One pilot called the aircraft jittery. The aircraft required low gain inputs in order to fly acceptably. Of the 12 landings, 11 had desired touchdown performance, and one was inadequate. All pilots indicated that the aircraft was acceptably flown down to touchdown. The aircraft exhibited an uncommanded nose up after touch down requiring extensive forward stick input to maintain control. On one occasion the aircraft became unexpectedly airborne after touchdown. The aircraft performance after touchdown drove the higher CH ratings. Overall, the H₂ flight control configuration was considered to have Level III handling qualities due to the unacceptable motions after touchdown.

5.3.3. H_∞ Flight Control Configuration

The four evaluation pilots performed five straight in approaches and thirteen offset landing tasks with the H_∞ flight control design. See Figures H.5. and H.6. for CH and PIO ratings. The comments indicated that the aircraft flew predictably until the pilot increased his input gains when the aircraft exhibited a jittery motion. Of the 13 landings, 6 had desired touchdown performance, 3 were adequate, and 4 were inadequate. Evaluation pilot 4 did not provide PIO ratings for two approaches. One pilot noticed a lightening in control forces with reduction in airspeed for all four of his landings. For all pilots the aircraft behaved unpredictably upon flare initiation. The aircraft tended to float and all pilots noted the need to apply forward stick right after the initiation of the flare to arrest the pitch-up motion. After the main gear touchdown, the nose could not be lowered even with full forward stick input. On at least one occasion the aircraft unintentionally ballooned and became airborne after touchdown. The aircraft performance after the initiation of the flare through landing roll out resulted in the high CH ratings. Overall, the H_∞ flight control configuration was considered to have Level III handling qualities due to the unacceptable motions after the flare initiation through landing roll-out.

5.3.4. *Mixed H₂/H_∞ Flight Control Configuration*

The four evaluation pilots performed a total of four straight in approaches and ten offset landings with the mixed flight control design. See Figures H.7. and H.8. for CH and PIO ratings. The comments indicated that the aircraft felt sluggish and heavy on approach with a somewhat slow initial response. Two of the pilots indicated that the aircraft was somewhat unpredictable, while the other two considered the aircraft predictable. All four pilots stated that the aircraft handling qualities prior to the initiation of the flare were acceptable. For the 10 offset landings, 6 resulted in desired touchdown performance, 2 resulted in adequate, and 2 were inadequate. The flight control configuration had unacceptable behavior from flare initiation through landing roll-out. All pilots commented on a heave and float tendencies, and on at least four occasions, the aircraft became airborne after the initial touchdown. On every landing, all pilots required one-half to full forward stick to arrest an unanticipated pitch-up motion after touchdown. Overall, the mixed flight control configuration was considered to have Level III handling qualities due to the unacceptable motions after flare through landing roll.

5.3.5. *Overall Results:*

The HAVE INFINITY flight test team concluded that the classical longitudinal flight control design exhibited Level II handling qualities for the approach and landing phase of flight. Furthermore, all three state-space designs exhibited undesirable motion at some point between flare and the landing roll, resulting in Level III ratings. However, the landing roll-out was not included in the design phase. The changes in stability derivatives due to ground effect and airspeed reduction during landing roll; the effects of a sensed pitch rate change due to the gear impacting the ground; the shift in the center of rotation once the gear are in contact with the ground; and the thrust effects on pitching moment as the throttles are retarded to idle are some of the factors which were not included in the design point used to define the controllers synthesized in this thesis. While it is interesting that the classical controller did not exhibit the undesirable characteristics on landing roll and the modern controllers did, the landing roll handling qualities were not the target objectives of the designs.

The flight control designs were solely designed for the approach phase of flight and intended to be analyzed from approach to the touchdown point. The pilot ratings that were given were mostly based on the

disturbing handling characteristics after touchdown. Therefore the ratings given were not directly applicable to the desired evaluation objective. Pilot comments did indicate the three state-space designs exhibited acceptable handling qualities on final approach although no precise task was defined for this portion of the approach. Additionally, many of the spot landings met the desired objective criteria. While it is not appropriate to alter the flight test handling qualities ratings after the fact, the data does support the conclusion that all designs were 'acceptable' on approach. The term 'acceptable' must be used loosely since there is insufficient data (i.e. no pilot ratings given just for the approach portion of the flight) to determine a handling qualities level for the approach flight phase separate from the landing roll. It can be concluded that the four flight controller designs were successfully implemented, safely flown during approach to the touchdown point, and although the handling qualities level rating data was inconclusive for the objective flight condition, the pilots did not find the handling qualities objectionable during the approach phase of flight.

VI. Conclusions and Recommendations

6.1. Summary

The main objective of this thesis was to apply modern control theory, specifically H_2 , H_∞ , and mixed H_2/H_∞ control synthesis, to an actual aircraft system, starting from an aircraft's stability derivatives and progressing through implementation to flight test of the systems. That objective was successfully met.

The stability derivatives of a fictitious aircraft with unstable airframe aerodynamics was the starting point for this research. Those stability derivatives were used to create an aircraft model in both transfer function and state-space form. Four longitudinal flight control system controllers were design for this fictitious aircraft. These designs applied not only classical design methods, but also optimal flight control design methods, specifically H_2 , H_∞ , and mixed H_2/H_∞ control synthesis. The TPS Flight Control System project was the basis for the structure used to design the feedback control systems. These designs were analyzed for handling qualities, noise rejection properties, and stability margins. Controller designs were obtained that met the design analysis criteria.

The classical controller was primarily included as a control case for comparison and to help verify proper implementation of the un-augmented aerodynamics simulated by the VSS II system. This base-line design applied the design techniques commonly used to design flight control systems, including root locus and bode plot analysis, to synthesize the controller. This method was tedious, but the physical interpretation of the controller states made the process easy to analyze and improving the predicted handling qualities ratings was intuitive. There was no way, except trial and error, to optimize the controller for noise rejection or stability margins, or to quantify trade-offs between performance objectives.

The H_2 design problem was set-up as a one degree of freedom, angle of attack command controller in the feed-forward loop. The H_2 design technique was very capable at both wind gust and measurement noise rejection, but difficult to use when handling qualities was an objective. The use of a pseudo-integrator to improve tracking was not effective. Setting up the system as a model matching problem, and investigating the closed loop system pole locations as a function of the design weightings, might provide insights to the missing physical interpretation of the controller states and make designing for handling qualities more intuitive.

The H_∞ design problem was set-up as a one degree of freedom, angle of attack command controller in the feed-forward loop. This method was less cumbersome than the H_2 technique, but also fails to provide physical interpretation to the controller states. Systematic changes in weightings does not systematically improve the handling qualities predictions.

The mixed H_2/H_∞ control synthesis optimally traded off properties of an H_2 controller solely designed for noise rejection and an H_∞ controller designed to obtain both good margins and reasonable handling qualities with a weighting only on complementary sensitivity. Again, the resulting mixed controller lacked physical interpretations of the controller states and any correlation between handling qualities predictions and controller selection.

The four flight control designs were then implemented in the Calspan Variable Stability Simulator II (VSS II) Learjet. This aircraft has the capability to simulate the fictitious aircraft's aerodynamics and implement the controller designs. The modern designs were difficult to implement since those methods tended to create controllers with high frequency poles, which were not realistically meaningful. Also, the resulting controllers were unstable, and although unstable controllers can and were implemented, internal stability can become a problem. Unstable controllers are not ideal in applied systems. The implementation of the fictitious aircraft aerodynamics appeared correct, based on the classical design verification testing results. The verification and validation testing of the closed loop systems indicated significant variations between the predicted flight control system response and the flight test results. This would limit conclusions comparing the design methods and the resulting controllers, since the systems tested did not accurately represent the flight control systems designed. However, such comparisons were not a thesis objective. The variations in predicted versus flight test results were not significant enough to invalidate the implementation of these designs. The modern designs were intended to accommodate uncertainty, and this was effectively demonstrated. A better understanding of the VSS II system capabilities and limitations would improve future flight testing results utilizing this system.

The four controllers were evaluated during a limited handling qualities flight test, named HAVE INFINITY. The classical design was rated level II, while all three modern designs were rated level III. The resulting pilot ratings were influenced by the handling characteristics after touchdown through landing roll.

This was not part of the flight condition the controllers were designed to handle. Pilot comments regarding the handling qualities prior to touch down indicate 'acceptable' handling qualities for all designs tested. The flight control designs were safely implemented and flown, but the flight test was inconclusive in determining the handling qualities rating for the controllers in the intended flight condition.

This study encompassed aerodynamic modeling, aircraft equations of motion and dynamics, linear control theory, optimal flight control design methods, aircraft stability and control analysis, handling qualities analysis, principles of flight test, and flight test project management. In the process of putting all of these disciplines together, issues were raised and areas of further research were discovered. This thesis was accomplished in three major phases: Set-Up and Design; Implementation; and Flight Test and Analysis. The remainder of this chapter will discuss recommendations arising from each of these phases.

6.2. Recommendations

- Examine and flight test these design methods using full state feedback. The controllers designed in this thesis were limited by feeding back only angle of attack and pitch rate. Full state feedback does not complicate the optimization process, but would improve control of the states.
- Set-up the system as a model matching problem. First choose an aircraft model that exhibits solid level 1 handling qualities. Then apply H_2 synthesis to design a controller that optimizes noise rejection while minimizing the difference between the system output and the 'level 1' aircraft model. This set-up was not used during this thesis, but might prove to be a more efficient approach to the problem, should noise rejection be a primary objective of the flight control design
- Investigate how the closed loop system poles are affected by variations in design weights. The physical interpretation of controller states and the effects of weighting changes on handling qualities predictions could be explored by a systematic investigation of the effects on pole locations due to variations in design weights. Creating a 'root locus' of the closed loop poles as a function of design weighting might provide insights into these areas.

- Include problem constraints in the mixed design which limit the controller's poles to a realistic frequency range. Some acceptable controllers were eliminated since they were not implementable due to high frequency poles. The mixed design process is capable of multiple constraints of various types.
- Investigate constraints which would define the handling qualities criteria boundaries for use with mixed control synthesis. If the handling qualities criteria could be part of the constraints on the mixed problem, the handling qualities issue would be eliminated from the process.
- Use a known design method as a control case, like the classical design, to verify and validate the implementation and help isolate contributing factors of the experiment. The classical controller also aided in the blind evaluations during the flight test.
- Either design the controllers to include landing roll-out as a design criteria, or limit the flight test evaluation to the flight condition used in the design process. The point design used in the design phase of this research did not include landing roll characteristics, but the pilots included this phase of flight in the ratings given. As a result the ratings did not reflect the condition the controllers were designed to accommodate. The only applicable flight test data were general pilot comments concerning the approach phase, insufficient for determining a handling qualities level.

Appendix A
Aircraft Model Data

The following was provided by Calspan:

AIRCRAFT DATA					
Flight Condition					
Altitude	=	1000	ft	TAS	= 214.2 ft/sec
KCAS	=	125	knots	Mach	= 0.1926
				α_0	= 6.69 degrees
Aircraft Geometry					
S	=	232	ft ²	b	= 34.1 ft
				cbar	= 7.0 ft
Mass Properties					
Weight	=	11,000	lbs	I_{xx}	=28,000 slug-ft ²
I_{zz}	=	47,000	slug-ft ²	I_{yy}	=22,000 slug-ft ²
Longitudinal Stability Derivatives					
C_{D0}	=	0.0486		C_{L0}	= 0.36
C_{di}	=	0.0792		C_{Lu}	= 0.0
C_{du}	=	0.0		C_{La}	= 5.04
C_{txu}	=	-0.3255		C_{Lad}	= 0.0
C_{Dde}	=	0.0		C_{Lq}	= 0.0
C_{Dlq}	=	0.02		C_{Lde}	= 0.2438
				C_{m0}	= - 0.004
				C_{mu}	= 0.0
				C_{ma}	= 0.2
				C_{mad}	= 0.0
				C_{mq}	= - 6.0
				C_{mde}	= - 0.7314

The following is a MATLAB™ script file which uses the above aircraft data and calculates the state-space representation of the aircraft dynamics.

```
function [A,B,C,D]= cspanmod
% function [A,B,C,D]=cspanmod
% Returns a 4th-order wind axis state-space model
% of a Learjet N102VS @ 125 KIAS and 1000 feet
% The states (x) are:
% 1 q                               deg/sec
% 2 alpha                            deg
% 3 V (true)                          feet/sec
% 4 gamma                             deg
% Inputs (u) are:
% 1 de                                deg
% 2 dz                                deg
% 3 dx                                deg
% Outputs (y) are:
% 1 q                               deg/sec
% 2 alpha                            deg
% 3 V (true)                          feet/sec
% 4 gamma                             deg
% 5 q_dot                             deg/sec/sec
% 6 alpha_dot                          deg/sec
% 7 V_dot                             feet/sec/sec
% 9 Nz                                g's
% 10 theta                            deg
% Constants
g=32.2;                               %ft/sec
r2d=180/pi;                            %deg/rad
d2r=pi/180;                             %rad/deg
% Flight condition
V_indicated=125;                        % KIAS
h=1000;                                  %ft
```

```

% Mass properties
lyy=22000; % (slug feet^2)
weight=11,000; % lbs
m=weight/32.2; % slugs

% Geometry
b=34.1; %ft
S=232; %ft^2
c=7; %ft
tail_to_cg=21; %ft
ar=b/c;
e=0.84;

% Atmosphere model
rho_0=0.0023769; % slug/ft^3
rho=rho_0*(1-(.0019812*h/288.15))^(1/(.0019812*96.034))-1); %
slug/ft^3

V=V_indicated/sqrt(rho/rho_0)*6080/3600; % feet per sec
q_bar=1/2 * rho *V^2;

% Non-dimensional derivatives (per radian)
cm0= -0.004;
cma= 0.2;
cmde=-0.7314;
cmad= 0;
cmq= -6;
cm= 0;
cl0= 0.36;
cla= 5.04;
clde=-cmde*c/tail_to_cg;
cl=weight/(q_bar*S);
alpha0=(cl-cl0)/cla;
cd0= 0.0486;
cda=(2*cl0*cla+2*cla*cla*alpha0)/(pi*ar*e);
cdi= 0.0792*r2d;
cdlg= 0.02;
cd=cd0+cda*alpha0+cdlg;

% Dimensional derivatives
Mq=rho*S*V*c/(4*lyy)*(cmq+cmad);
M_alpha=rho*S*V*c/(2*lyy)*cma;
Mu=0.0;
Zq=0.0;
Zw=rho*S*V/(2*m)*(-cla);
Z_alpha=Zw*V;
Zu=-2*g/V;
Xq=0.0;
Xw=rho*S*V/(2*m)*(-cda);
X_alpha=Xw*V;
Xu=rho*S*V/m*(-cd);
M_de=rho*S*V*c/(2*lyy)*cmde;
Z_de=rho*S*V/(2*m)*(-clde);
X_de=0;

A=[ Mq M_alpha Mu 0
    1+ZqV Z_alpha/V Zu/V*57.3 0
    0 X_alpha/57.3 Xu -g/57.3
    0 -Z_alpha/V -Zu/V*57.3 0 ];

B=[ M_de
    Z_de/V
    X_de
    Z_de/V ];

C=[ eye(size(A))
    A
    A(4,:)*(V*d2r/g)
    0 1 0 1];

D=[ zeros(size(B))
    B
    B(4,:)*(V*d2r/g)
    0 ];

```

Appendix B

Design Evaluation Script Files

The following is a MATLAB™ script file which calculates the vector stability margins given a state-space representation of the system [Asys, Busys, Cysys, Dysys] and the controller [Ak, Bk, Ck, Dk].

```

%
% Margins          1-input vector margins
%                 2-output (alfa loop broken) vector margins
%                 3-output (q loop broken) vector margins
%                 4-multi variable output vector margins

[akg,bkg,ckg,dkg]=series(Asys,Busys,Cysys,Dysys,Ak,Bk,Ck,Dk);
[akgs,bkgs,ckgs,dkgs]=feedback(akg,-bkg,ckg,-dkg,1);
[akgt,bkgt,ckgt,dkgt]=feedback(akg,-bkg,ckg,-dkg,2);
[svs1,ws1]=sigma(akgs,bkgs,ckgs,dkgs);
[svt1,wt1]=sigma(akgt,bkgt,ckgt,dkgt);
alphao1=1/max(svs1);
ao1=1/max(svt1);
vgms1lo=(1/(1+alphao1));
vgms1hi=(1/(1-alphao1));
if vgms1hi < 1e-10; vgms1hi=1e-10;end;
vgmt1lo=(1-ao1);
if vgmt1lo < 1e-10; vgmt1lo=1e-10;end;
vgmt1hi=(1+ao1);
vgm1lo=min([vgms1lo vgms1hi vgmt1lo vgmt1hi]);
vgm1hi=max([vgms1lo vgms1hi vgmt1lo vgmt1hi]);
vgm1=20*log10([vgm1hi vgm1lo]);
vpms1=2*asin(alphao1/2)*180/pi;
vpmt1=2*asin(ao1/2)*180/pi;
vpm1=max([vpms1 vpmt1]);
fprintf('a:\margins.m', '\nInput VGM = [%4.2f %4.2f]dB\n',vgm1);
fprintf('a:\margins.m', 'Input VPM = + %4.2f deg\n',vpm1);

[agk,bgk,ckg,dkg]=series(Ak,Bk,Ck,Dk,Asys,Busys,Cysys,Dysys);

acl2=(agk+bgk(:,2)*cgk(2,:));
bcl2=bgk(:,1);
ccl2=cgk(1,:);
dcl2=dgk(1,1);
[agk2s,bgk2s,ckg2s,dgk2s]=feedback(acl2,-bcl2,ccl2,-dcl2,1); %feedback defined for
[agk2t,bgk2t,ckg2t,dgk2t]=feedback(acl2,-bcl2,ccl2,-dcl2,2); % negative feedback
[svs2,ws2]=sigma(agk2s,bgk2s,ckg2s,dgk2s);
[svt2,wt2]=sigma(akgt,bkgt,ckgt,dkgt);
alphao2=1/max(svs2);
ao2=1/max(svt2);
vgms2lo=(1/(1+alphao2));
vgms2hi=(1/(1-alphao2));
if vgms2hi < 1e-10; vgms2hi=1e-10;end;
vgmt2lo=(1-ao2);
if vgmt2lo < 1e-10; vgmt2lo=1e-10;end;
vgmt2hi=(1+ao2);
vgm2lo=min([vgms2lo vgms2hi vgmt2lo vgmt2hi]);
vgm2hi=max([vgms2lo vgms2hi vgmt2lo vgmt2hi]);
vgm2=20*log10([vgm2hi vgm2lo]);
vpms2=2*asin(alphao2/2)*180/pi;
vpmt2=2*asin(ao2/2)*180/pi;
vpm2=max([vpms2 vpmt2]);

acl3=(agk+bgk(:,1)*cgk(1,:));
bcl3=bgk(:,2);
ccl3=cgk(2,:);
dcl3=dgk(2,2);
[agk3s,bgk3s,ckg3s,dgk3s]=feedback(acl3,-bcl3,ccl3,-dcl3,1); %feedback defined for

```

```

[agk3t,bgk3t,cgk3t,dgk3t]=feedbk(acl3,-bcl3,ccl3,-dcl3,2); % negitive feedback
[svs3,ws3]=sigma(agk3s,bgk3s,cgk3s,dgk3s);
[svt3,wt3]=sigma(agk3t,bgk3t,cgk3t,dgk3t);
alphao3=1/max(svs3);
ao3=1/max(svt3);
vgms3lo=(1/(1+alphao3));
vgms3hi=(1/(1-alphao3));
if vgms3hi < 1e-10; vgms3hi=1e-10;end;
vgmt3lo=(1-ao3);
if vgmt3lo < 1e-10; vgmt3lo=1e-10;end;
vgmt3hi=(1+ao3);
vgm3lo=min([vgms3lo vgms3hi vgmt3lo vgmt3hi]);
vgm3hi=max([vgms3lo vgms3hi vgmt3lo vgmt3hi]);
vgm3=20*log10([vgm3hi vgm3lo]);
vpms3=2*asin(alphao3/2)*180/pi;
vpmt3=2*asin(ao3/2)*180/pi;
vpm3=max([vpms3 vpmt3]);
fprintf('a:\margins.m','1st loop VGM = [ %4.2f %4.2f ]dB\n',vgm2);
fprintf('a:\margins.m','1st loop VPM = + %4.2f deg\n',vpm2);
fprintf('a:\margins.m','2nd loop VGM = [ %4.2f %4.2f ]dB\n',vgm3);
fprintf('a:\margins.m','2nd loop VPM = + %4.2f deg\n',vpm3);

```

```

[agks,bgks,cgks,dgks]=feedbk(agk,-bgk,cgk,-dgk,1);
[agkt,bgkt,cgkt,dgkt]=feedbk(agk,-bgk,cgk,-dgk,2);
[svs4,ws4]=sigma(agks,bgks,cgks,dgks);
[svt4,wt4]=sigma(agkt,bgkt,cgkt,dgkt);
alphao4=1/max(max(svs4));
ao4=1/max(max(svt4));
vgms4lo=(1/(1+alphao4));
vgms4hi=(1/(1-alphao4));
if vgms4hi < 1e-10; vgms4hi=1e-10;end;
vgmt4lo=(1-ao4);
if vgmt4lo < 1e-10; vgmt4lo=1e-10;end;
vgmt4hi=(1+ao4);
vgms4=20*log10([vgms4hi vgms4lo]);
vgmt4=20*log10([vgmt4hi vgmt4lo]);
vpms4=2*asin(alphao4/2)*180/pi;
vpmt4=2*asin(ao4/2)*180/pi;
vpm4=max([vpms4 vpmt4]);
fprintf('a:\margins.m','mv s-VGM = [ %4.2f %4.2f ]dB\nmv t-VGM = [ %4.2f %4.2f ]dB\n',vgms4,vgmt4);
fprintf('a:\margins.m','mv VPM = + %4.2f deg\n',vpm4)

```

The following is a MATLAB™ script file which calculates and plots the singular values versus frequency of GK and KG where G is given by [Asys, Busys, Cysys, Dysys] and K is the controller [Ak, Bk, Ck, Dk].

```
figure(fa);subplot(2,1,1)
[as,bs,cs,ds]=series(Asys,Busys,Cysys,Dysys,Ak,Bk,Ck,Dk);
[sv,w]=sigma(as,bs,cs,ds);
kgsv=20*log10(sv);
semilogx(w,kgsv,'r');
hold;grid;title('SV plot of KG, H2, Design #3r, RWM');xlabel('Frequency (rad/sec)'),ylabel('Singular Values dB')
axis([5e-3,1e3,-50,30])

subplot(2,1,2);
[askg,bskg,cskg,dskg]=series(Ak,Bk,Ck,Dk,Asys,Busys,Cysys,Dysys);
[sv,w]=sigma(askg,bskg,cskg,dskg);
gksv=20*log10(sv);
semilogx(w,max(gksv),'r');
hold;grid;title('SV plot of GK, H2, Design #3r, RWM');xlabel('Frequency (rad/sec)'),ylabel('Singular Values dB')
axis([5e-3,1e3,-50,30])
```

Appendix C

Design Phase Time Histories

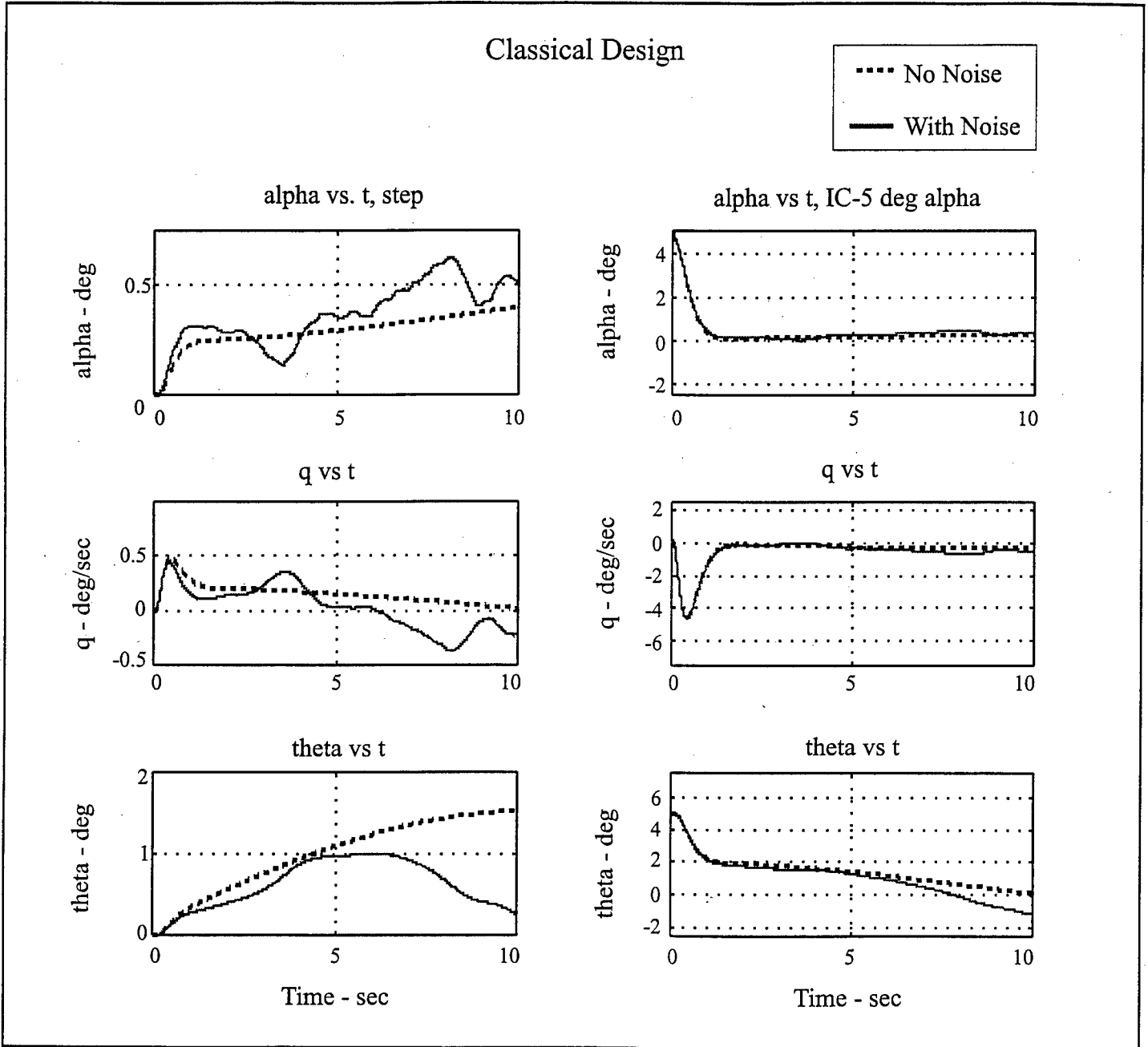


Figure C.1. Classical Design Time Histories (Set 1 of 2)

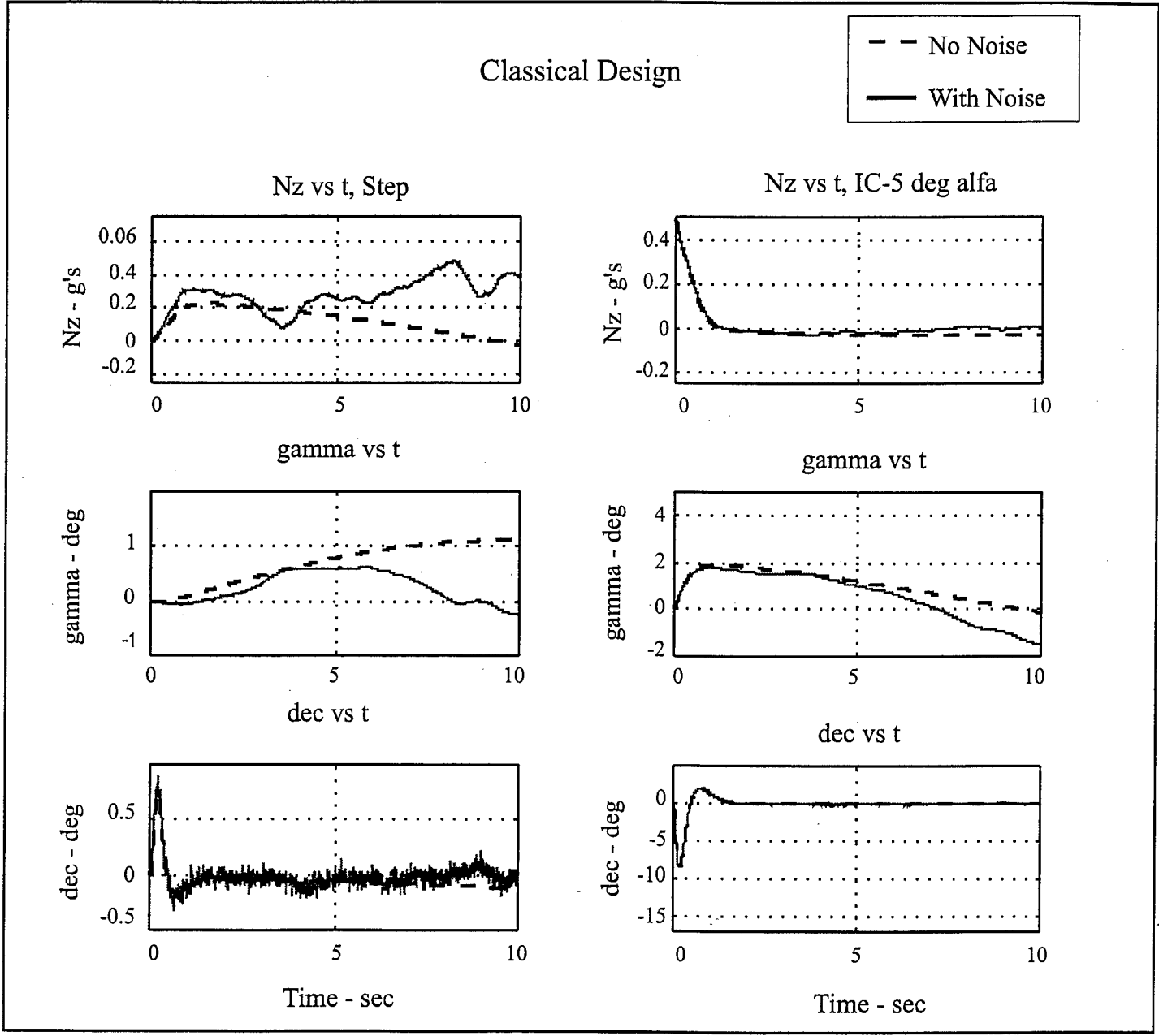


Figure C.2. Classical Design Time Histories (Set 2 of 2)

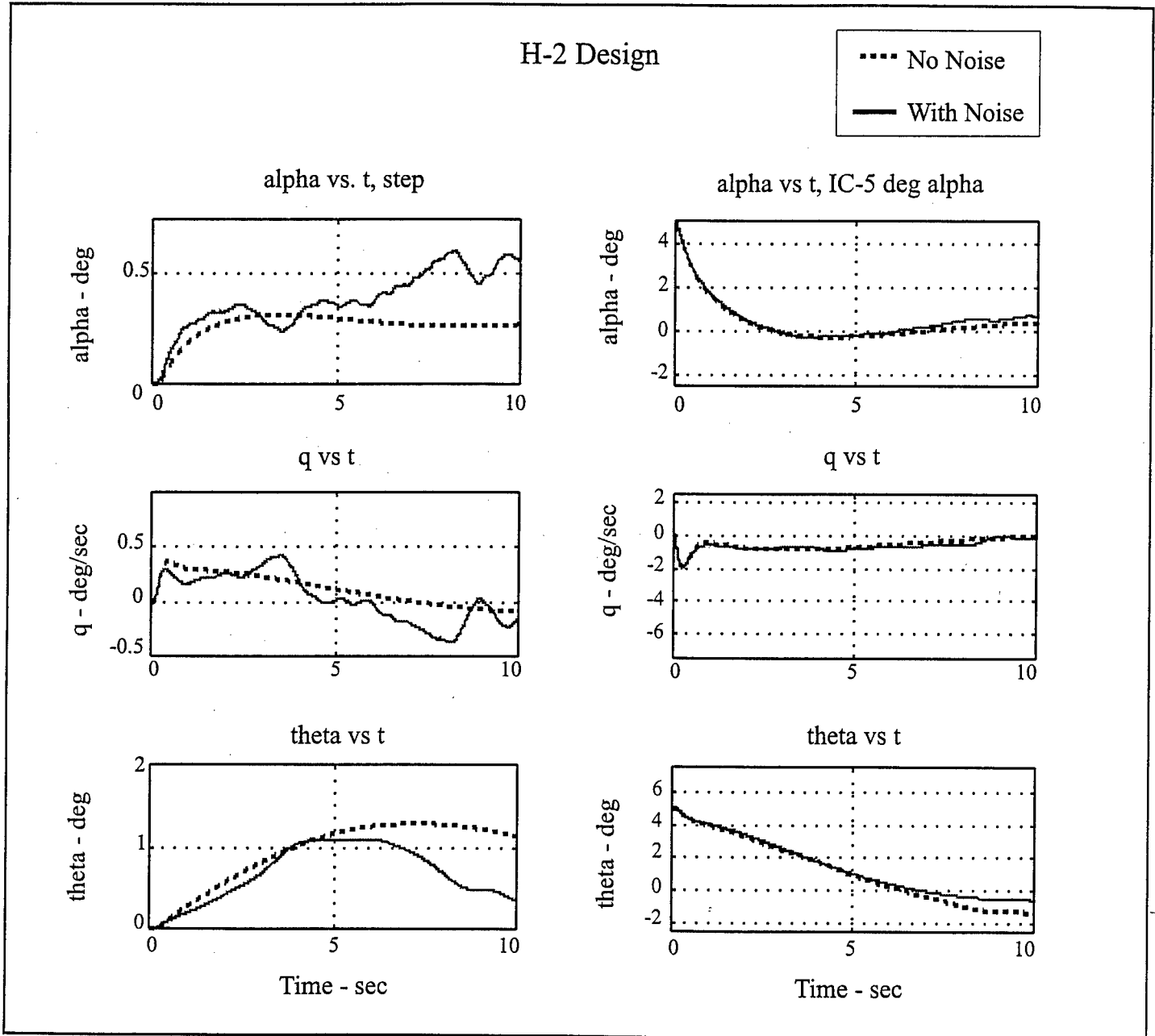


Figure C.3. H-2 Design Time Histories (Set 1 of 2)

H-2 Design

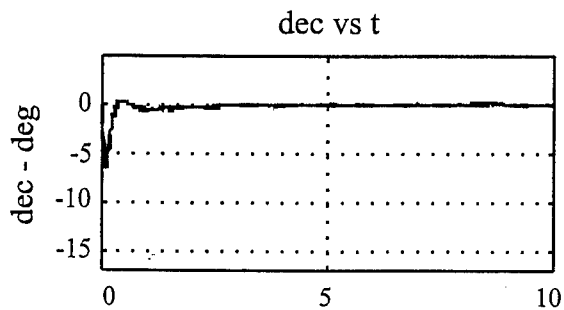
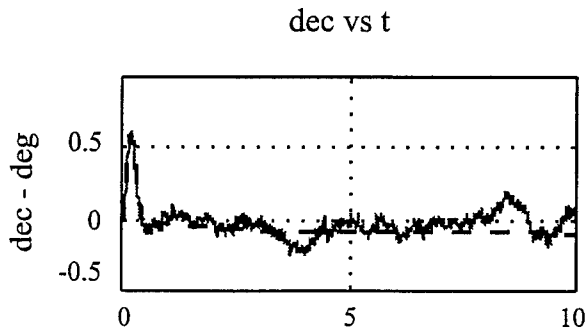
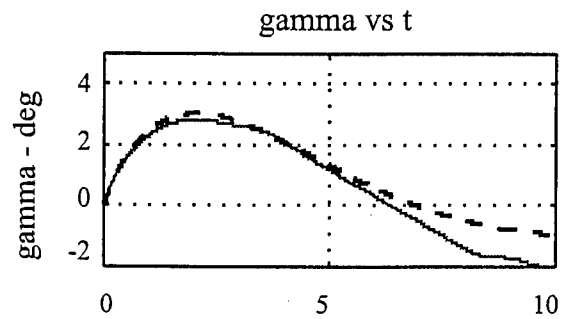
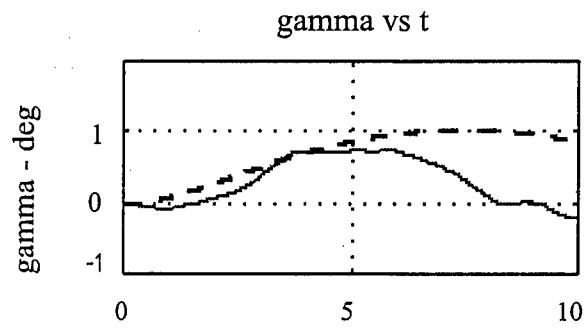
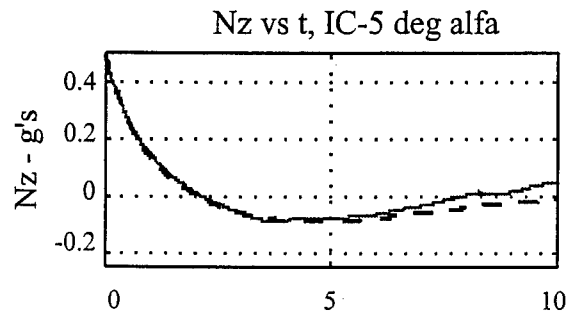
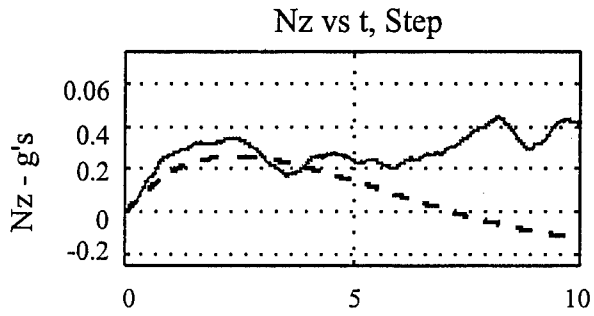
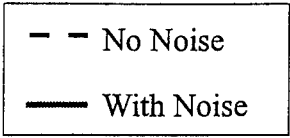
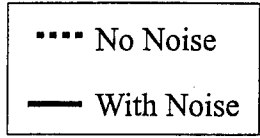
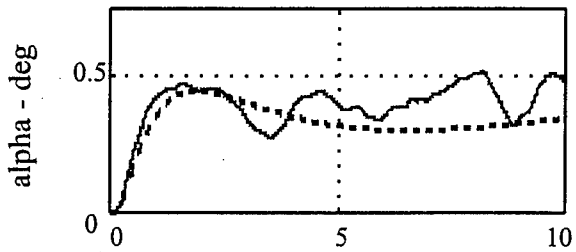


Figure C.4. H-2 Design Time Histories (Set 2 of 2)

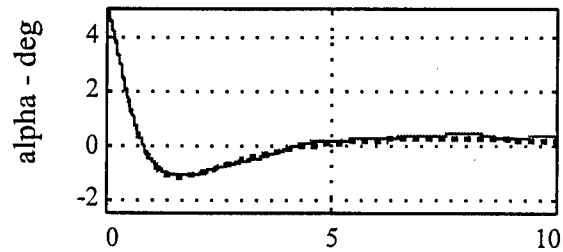
H-infinity Design



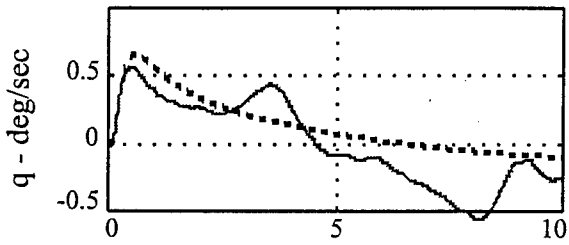
alpha vs. t, step



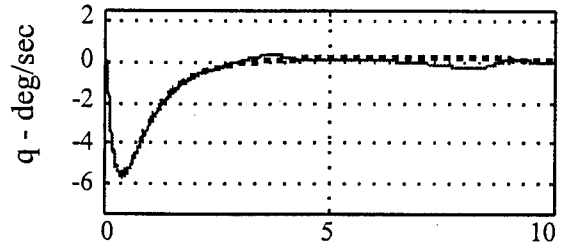
alpha vs t, IC-5 deg alpha



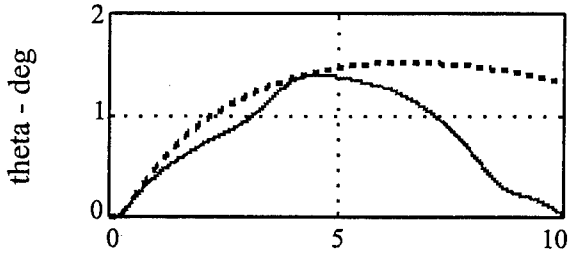
q vs t



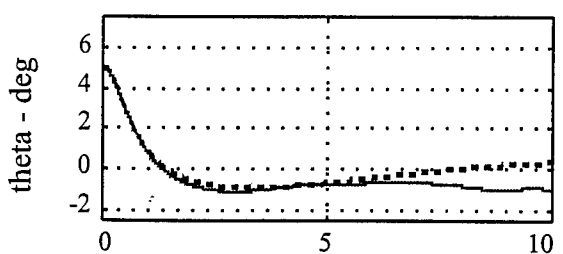
q vs t



theta vs t



theta vs t



Time - sec

Time - sec

Figure C.5. H-infinity Design Time Histories (Set 1 of 2)

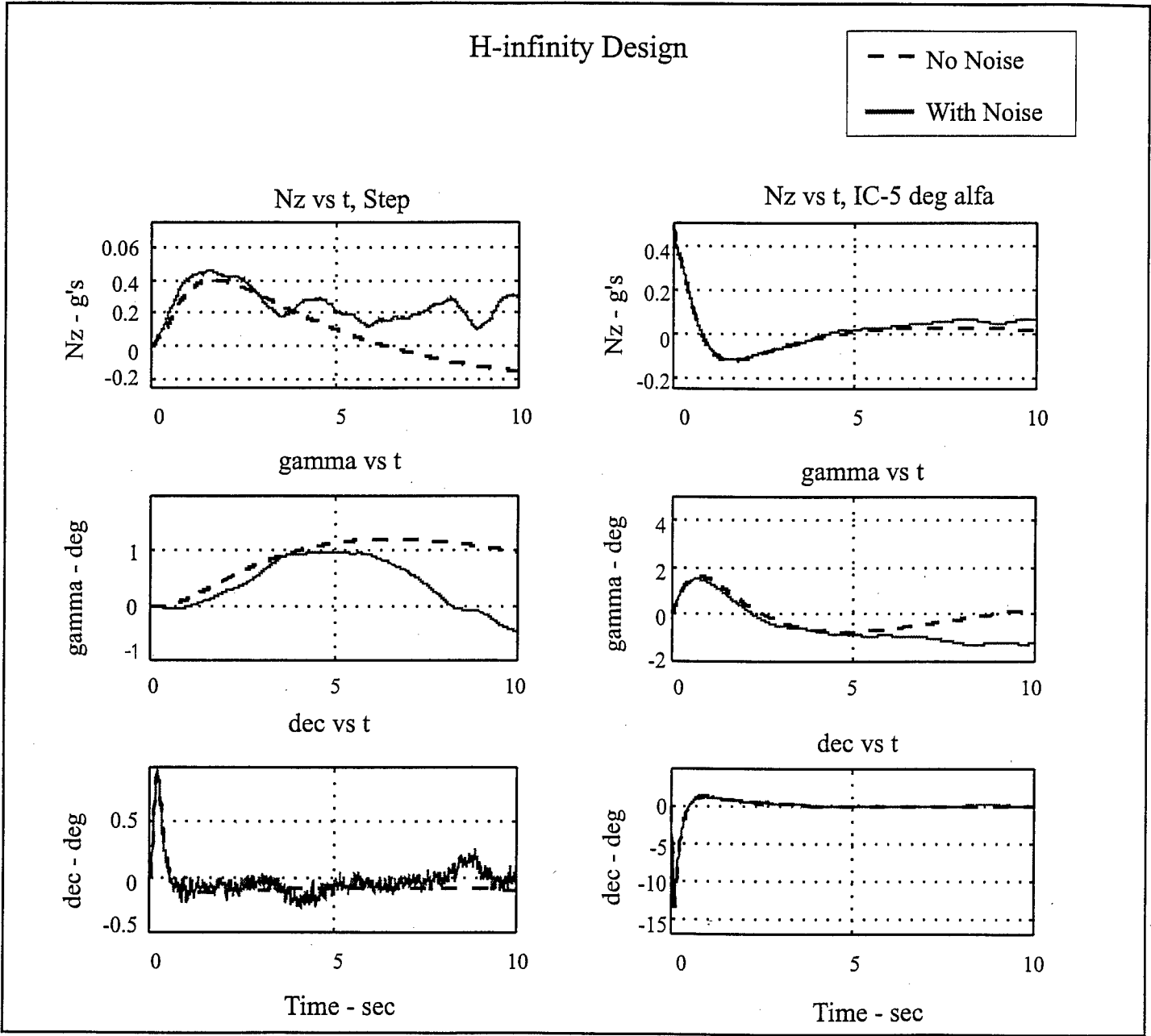


Figure C.6. H-infinity Design Time Histories (Set 2 of 2)

Mixed Design

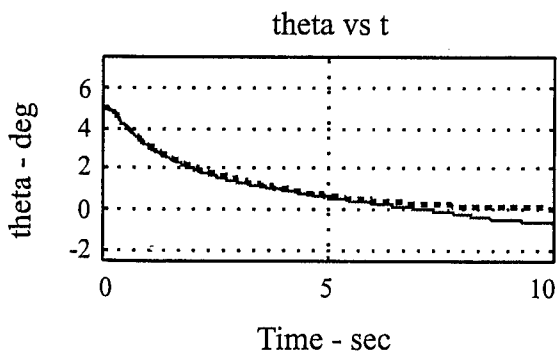
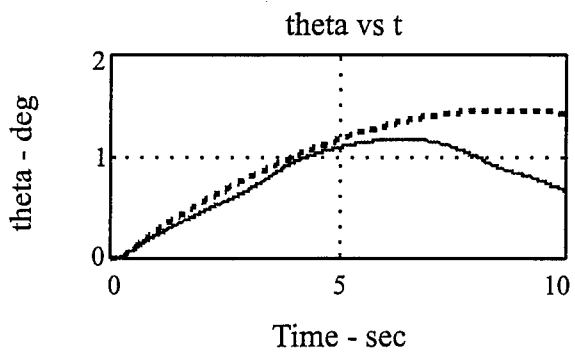
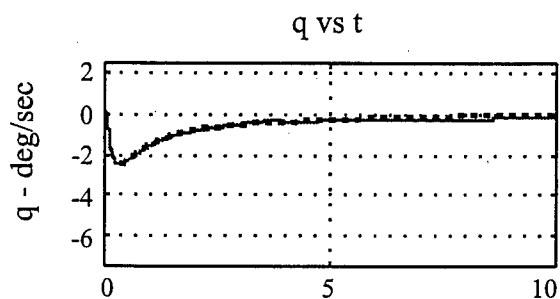
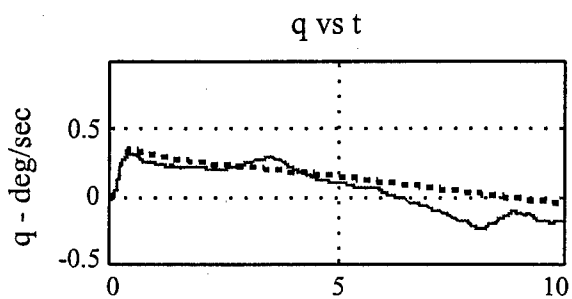
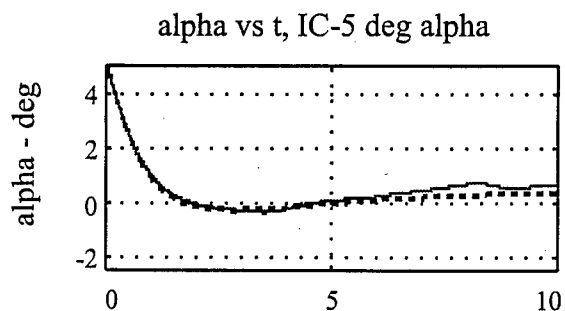
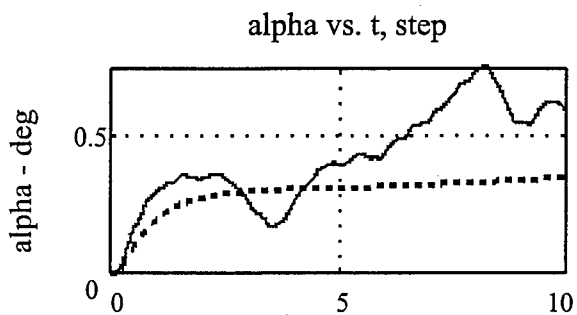
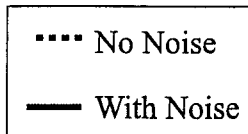


Figure C.7. Mixed Design Time Histories (Set 1 of 2)

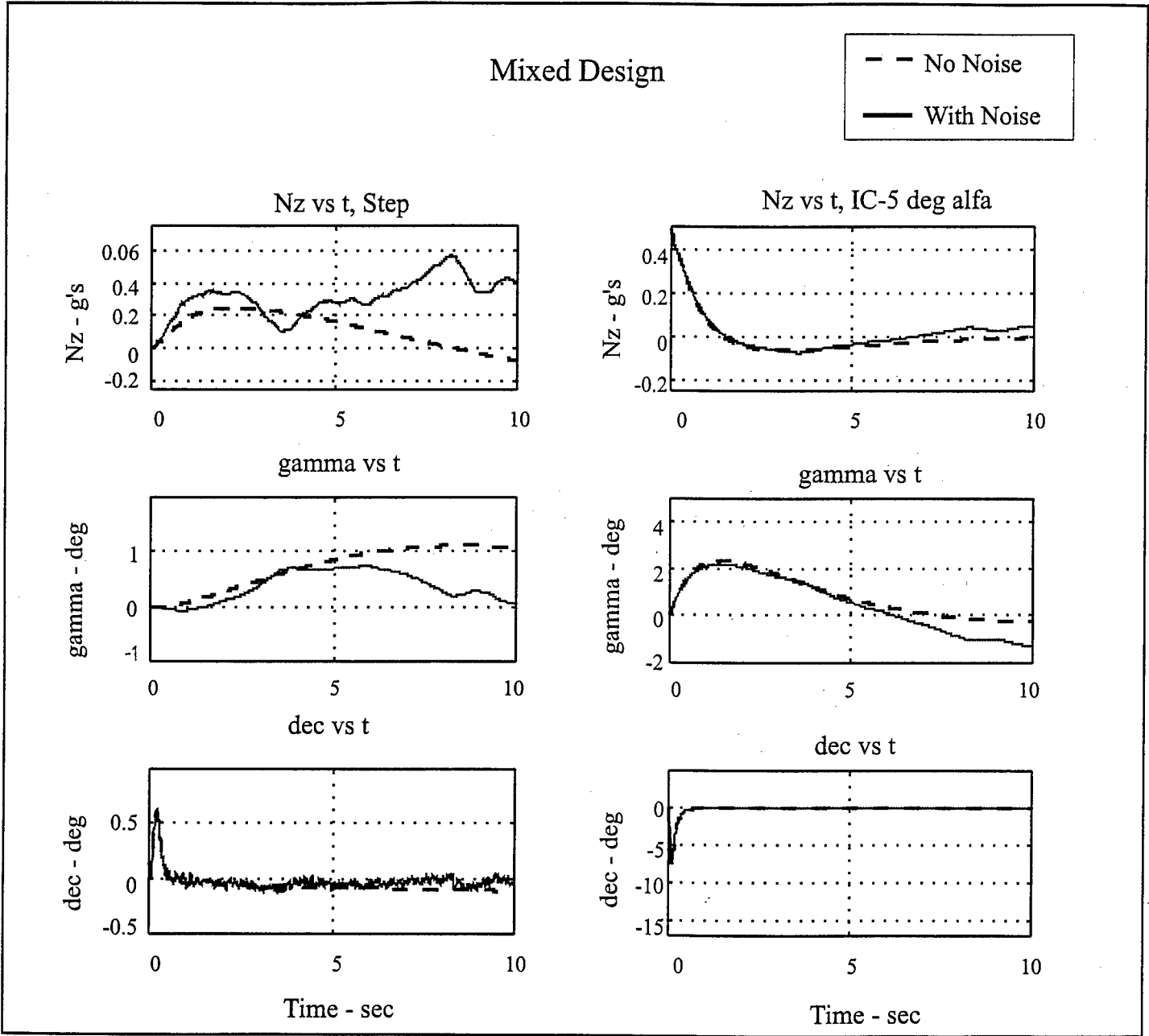


Figure C.8. Mixed design Time Histories (Set 2 of 2)

Classical, H2, Hinf, & Mixed - No Noise

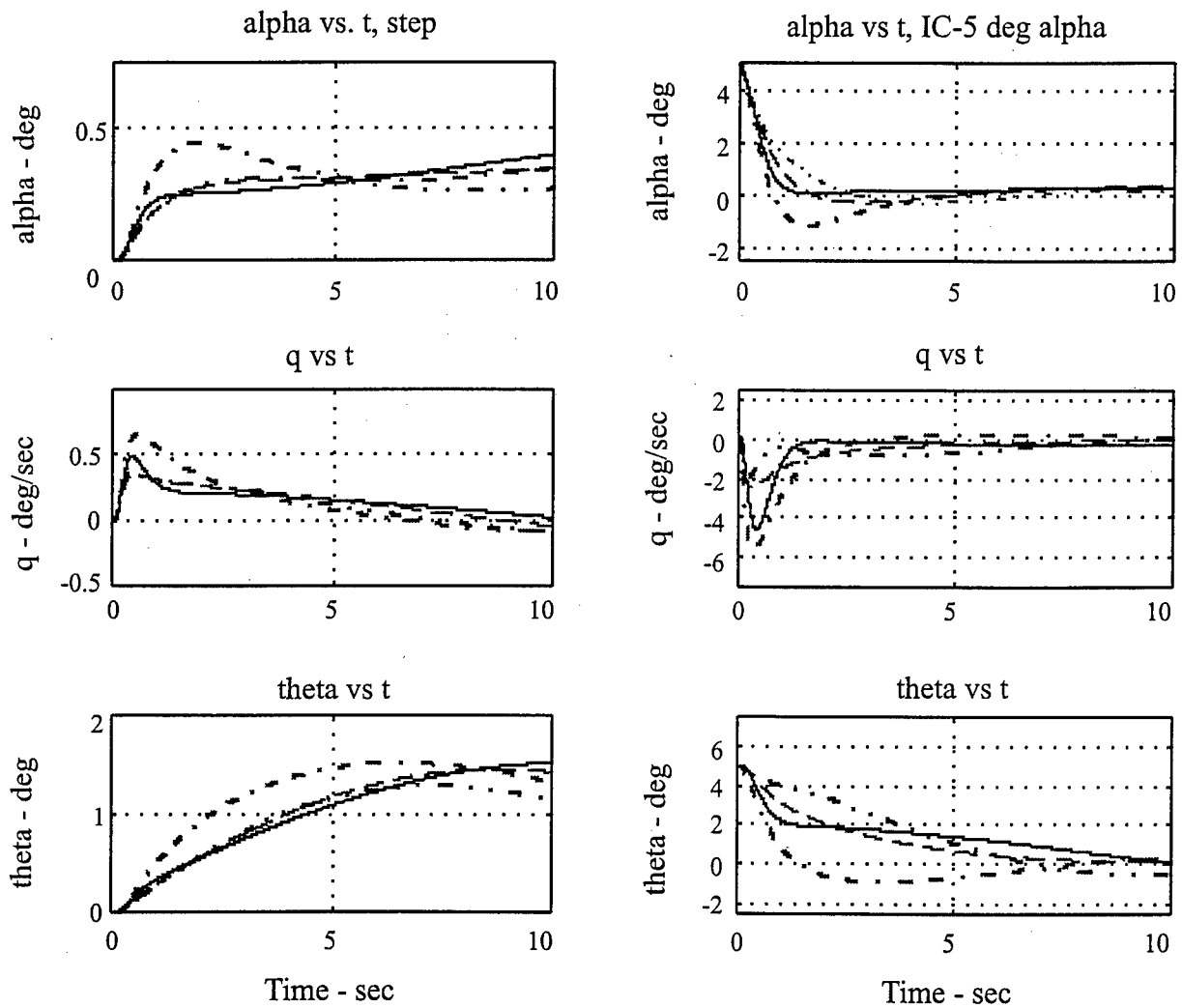
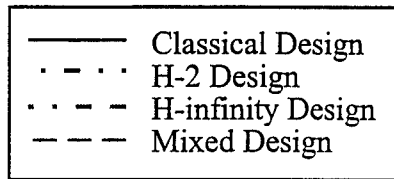


Figure C.9. All Designs Time Histories (Set 1 of 2)

Classical, H2 ,Hinf, & Mixed - No Noise

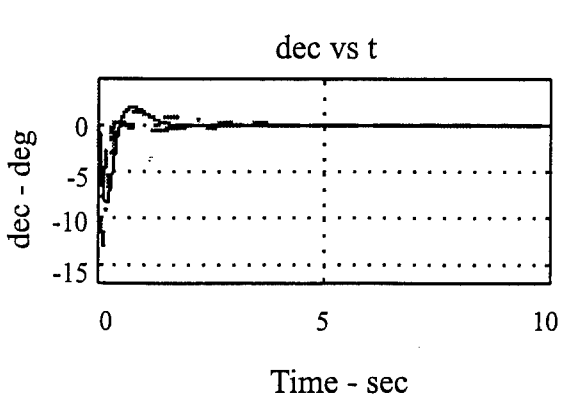
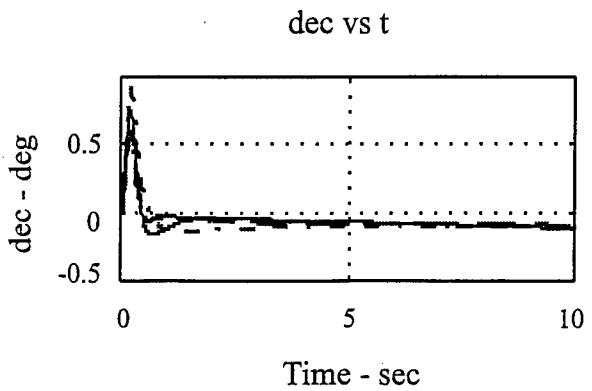
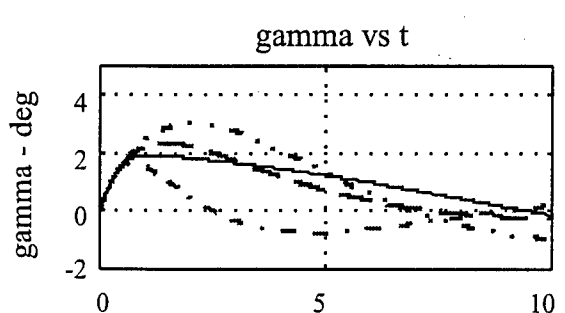
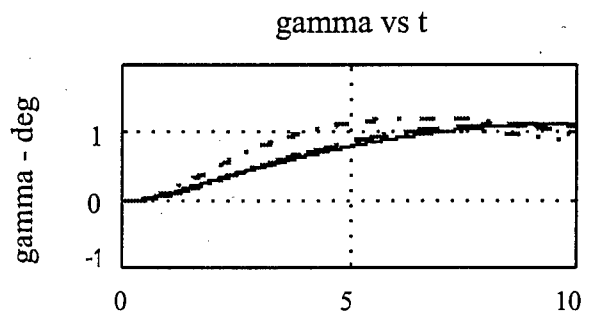
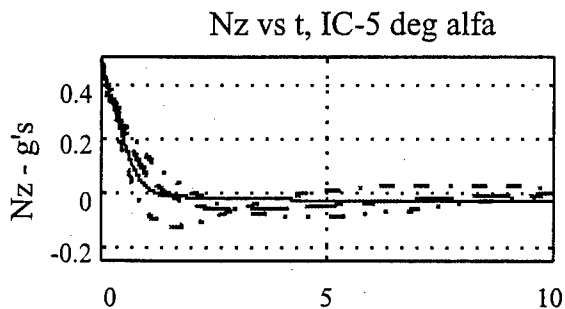
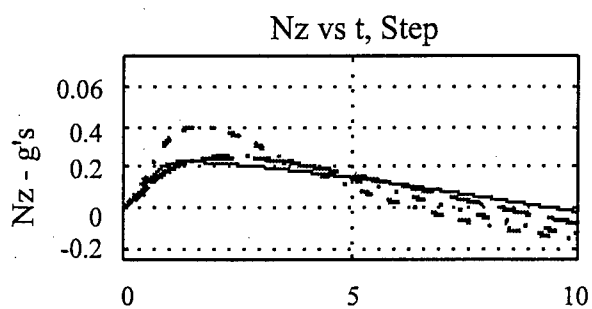
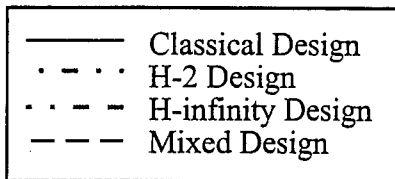


Figure C.10. All Designs Time Histories (Set 2 of 2)

Classical, H2 ,Hinf, & Mixed - No Noise

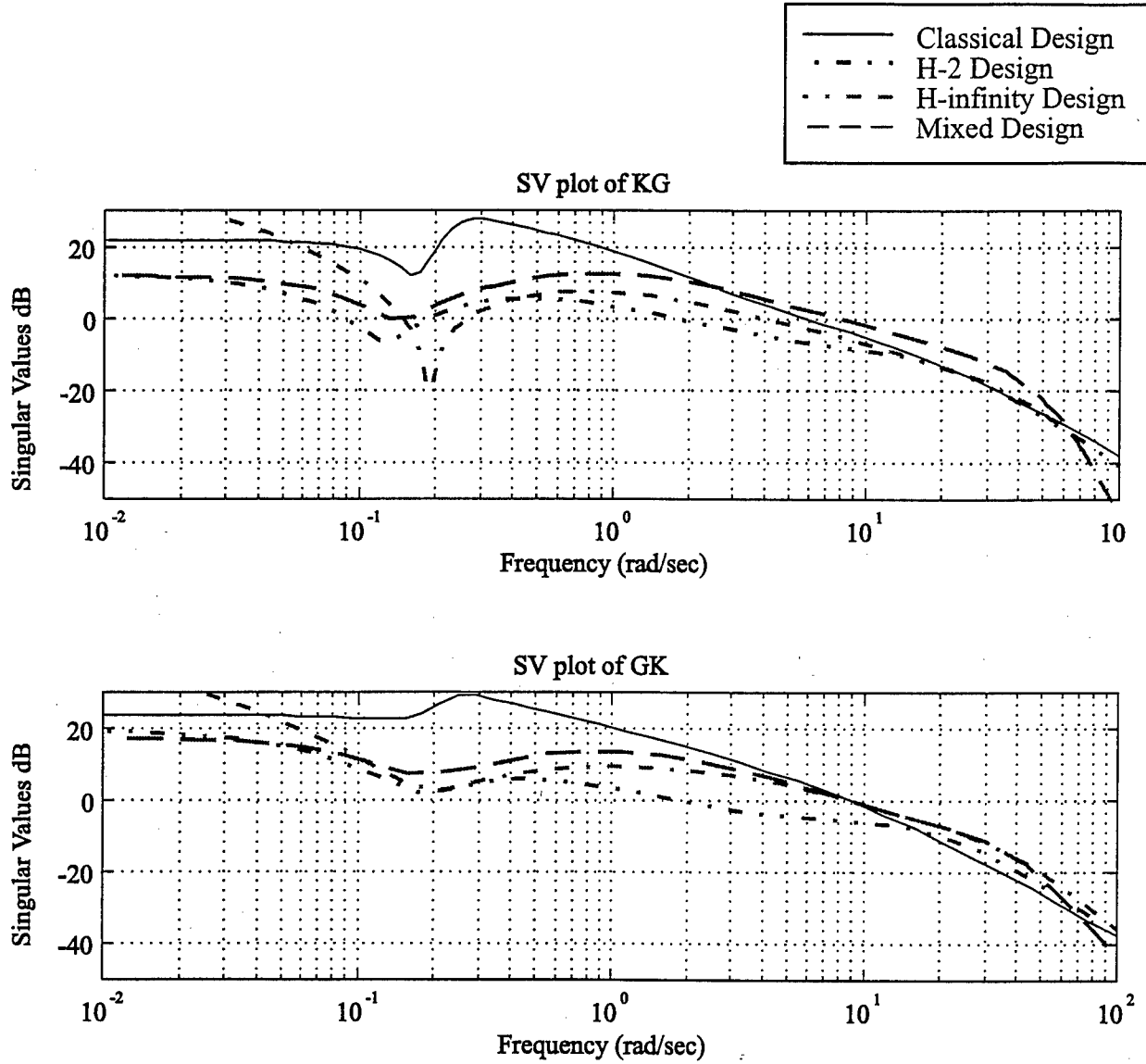


Figure C.11. All Designs Singular Value Plots

Appendix D

Data Acquisition Parameters

Parameter	Units	Parameter	Units
HOURS		alpha_c	deg
MINUTES		alphadot	deg/s
SECONDS		beta_cf	deg
MSECONDS		beta_c	deg
engaged		hp	ft
fes	lb	h_dot	ft/sec
fas	lb	l_thrust	lb
frp	lb	r_thrust	lb
des	in	fuel_tot	lb
das	deg	fuel_fus	lb
drp	in	oat	deg
dec	deg	pti	deg
dac	deg	des_in	inch
drc	deg	de_virt	deg
de	deg	dec_fb	deg
ds	deg	de_test	deg
da	deg	de_augm	deg
dr	deg	de_virt2	deg
theta	deg	dec_m	deg
phi	deg	dec_lj	deg
psi	deg	alpha_in	deg
p	deg/sec	q_in	deg/s
q	deg/sec	kout	deg
r	deg/sec	x1	deg
nx	G	x2	deg
ny	G	x3	deg
nz	G	x4	deg
nzp	G	x5	deg
vi	knots	x6	deg
ve	knots	f16_q	deg/sec
vt	ft/sec	f16_alpha	deg
alpha_cf	deg	fcs_confignond	1-4

Table D.1. Data Acquisition Parameters Recorded During Testing

Appendix E

Data Analysis Plots

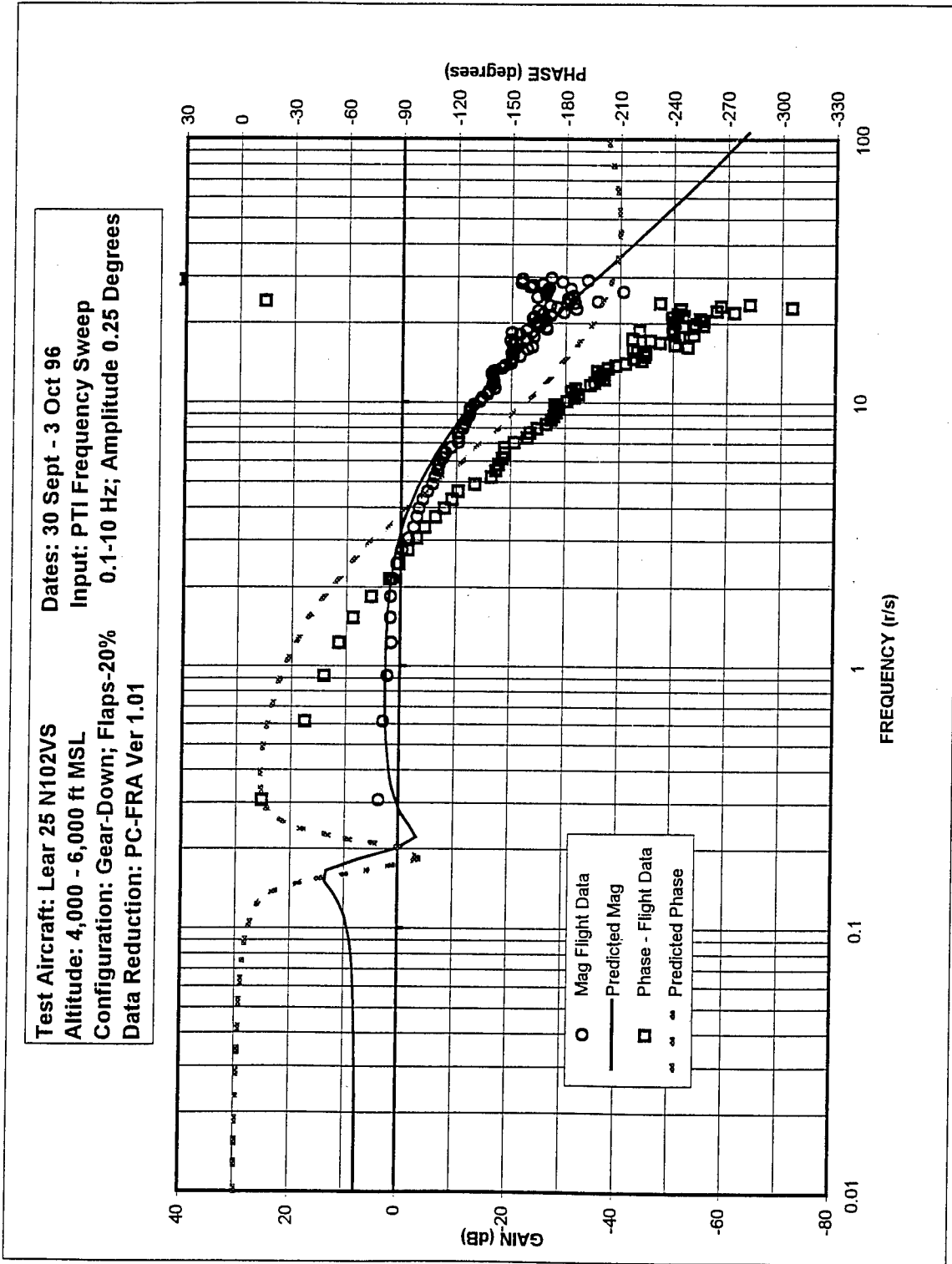


Figure E-1: Classical Design Bode Plot, Closed Loop, Alpha/PTI Sweep

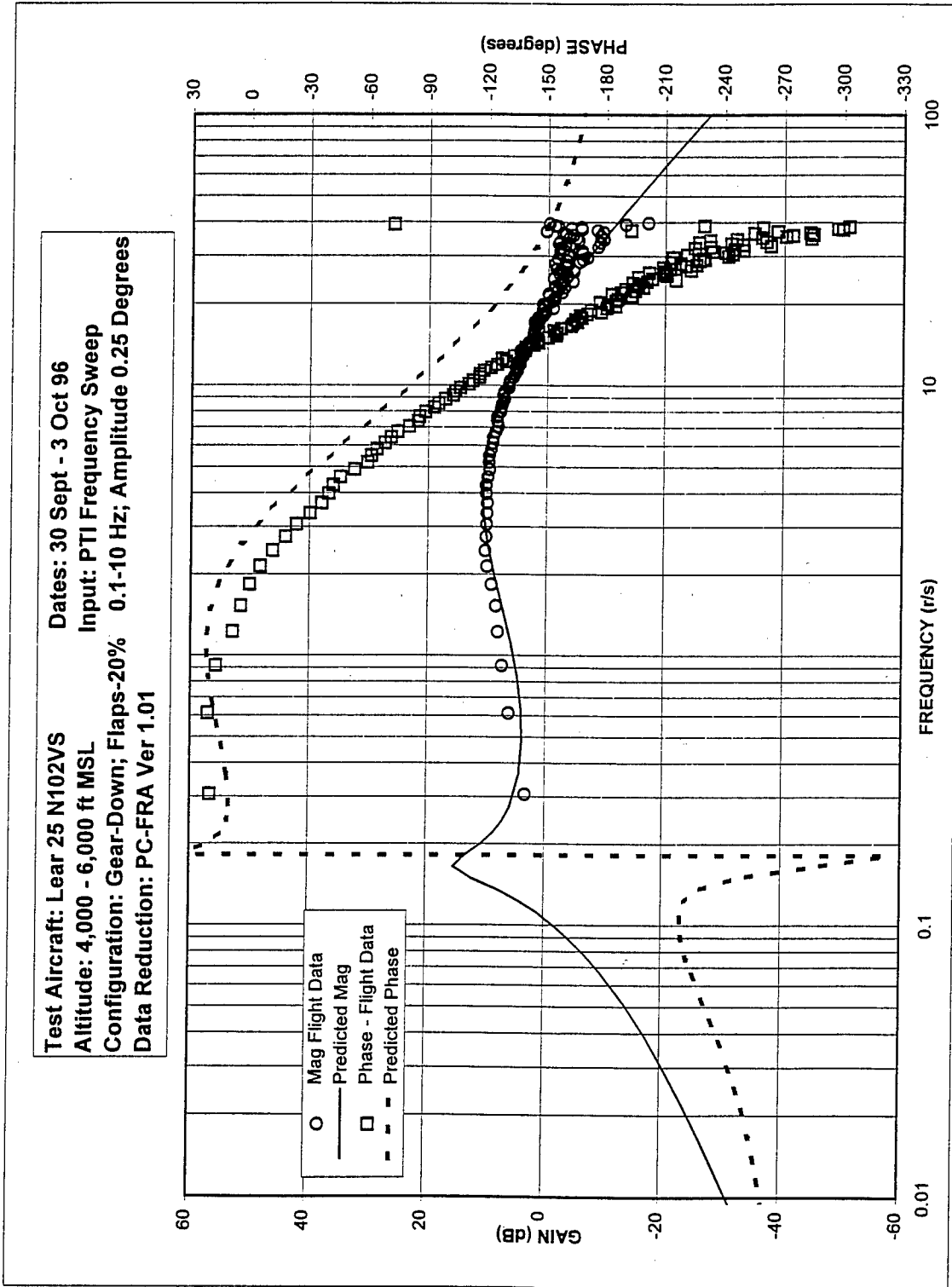


Figure E-2: Classical Design Bode Plot, Closed Loop, Pitch Rate/PTI Sweep

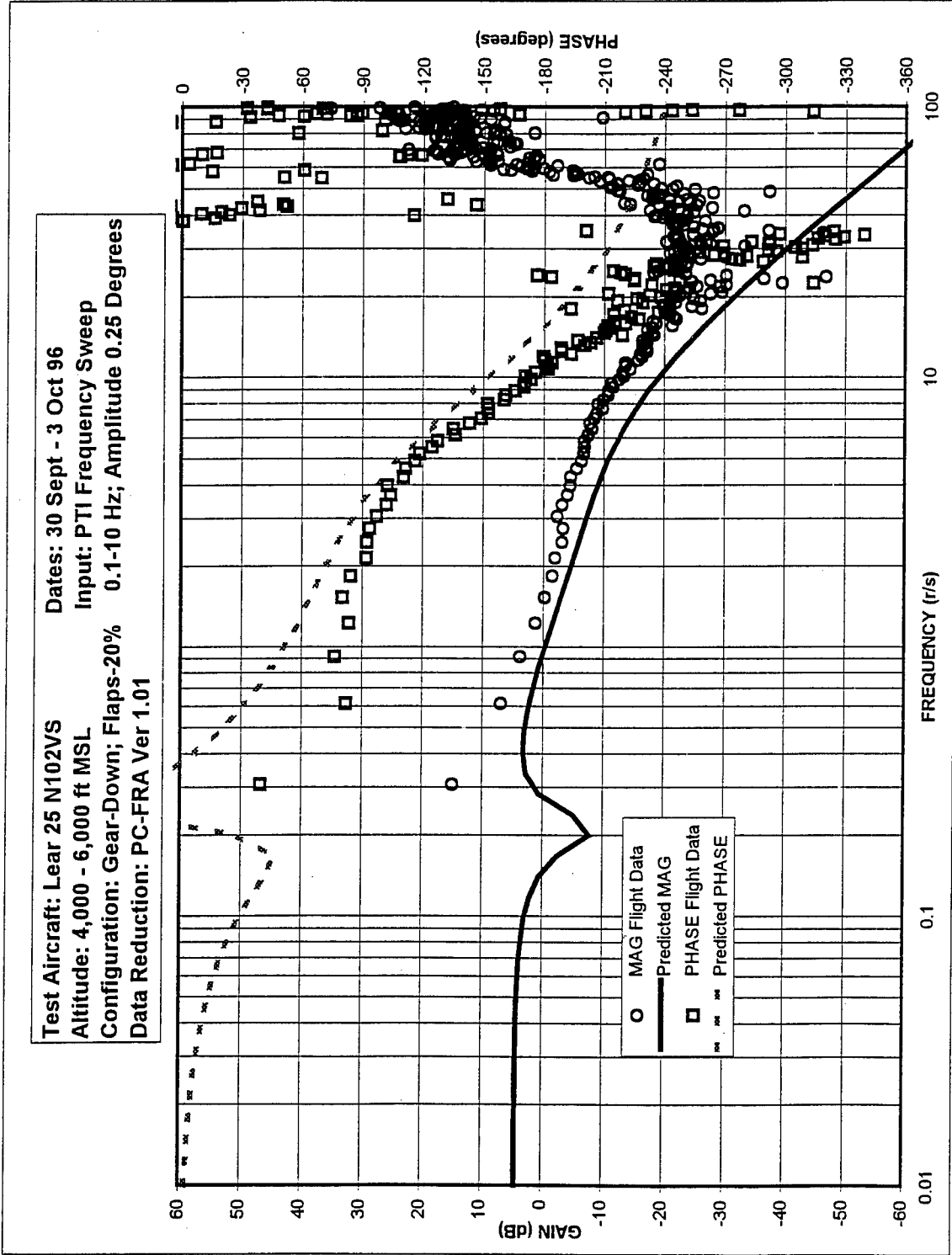


Figure E-3: H-2 Design Bode Plot, Closed Loop, Alpha/PTI Sweep

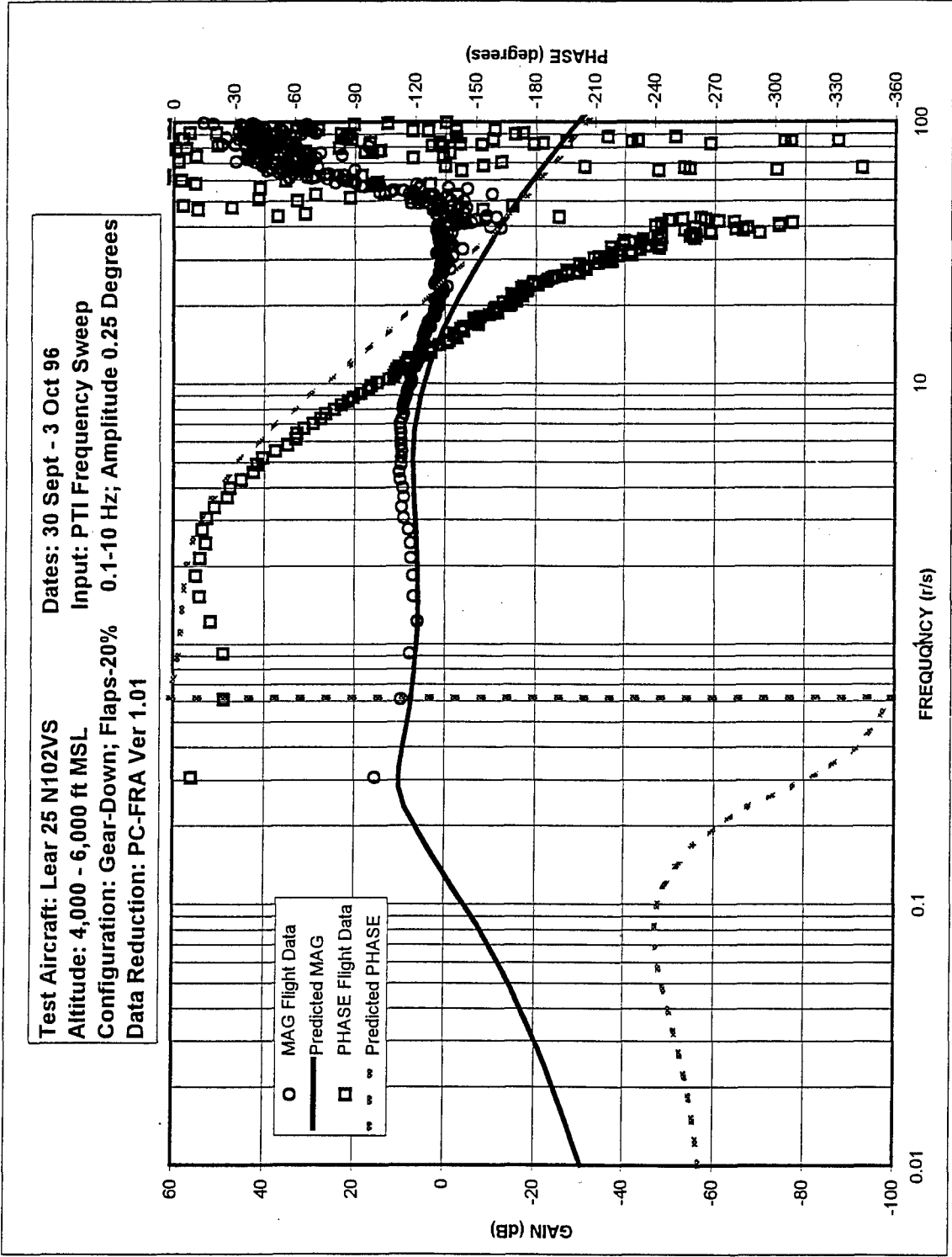


Figure E-4: H-2 Design Bode Plot, Closed Loop, Pitch Rate/PTI Sweep

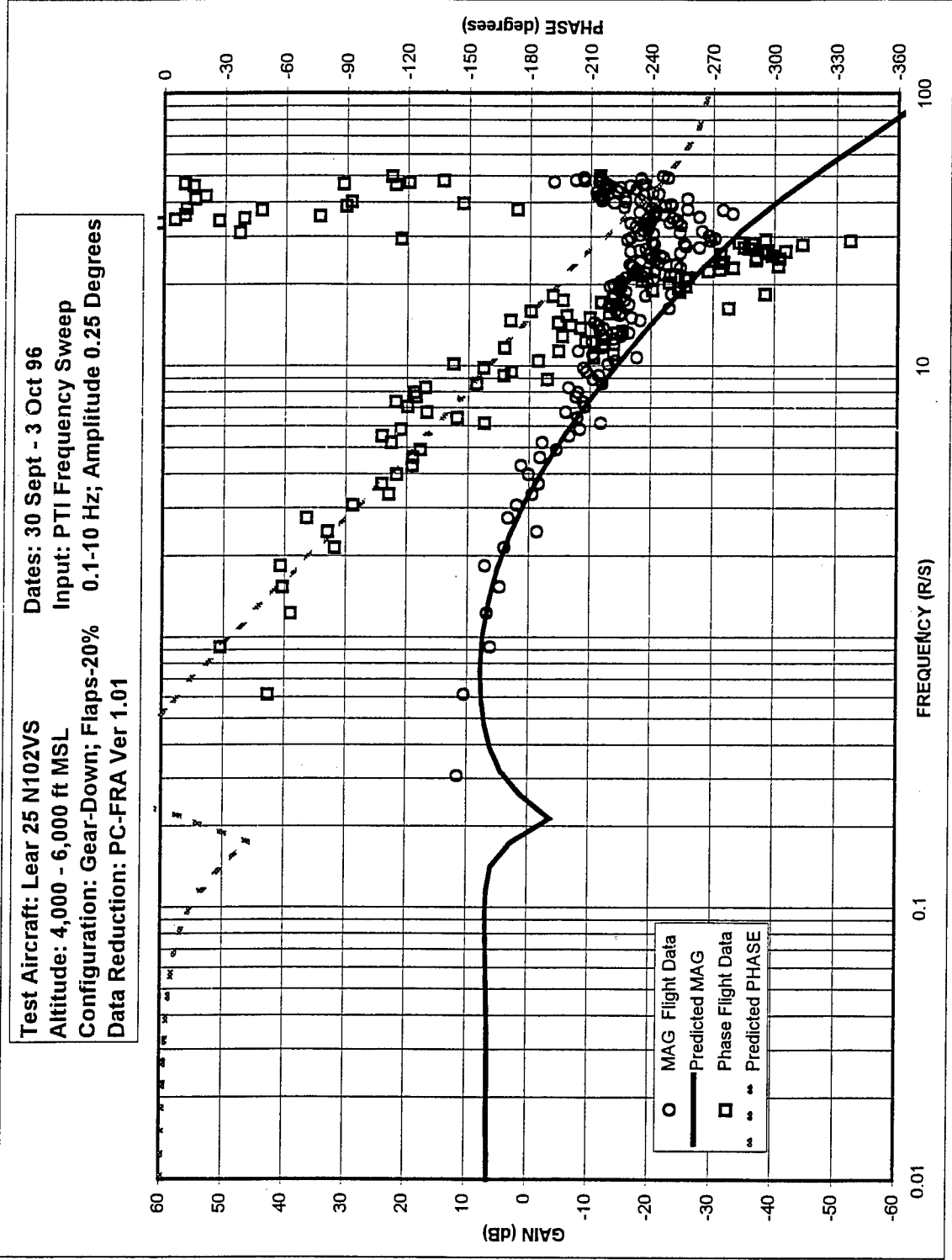


Figure E-5: H-Infinity Design Bode Plot, Closed Loop, Alpha/PTI Sweep

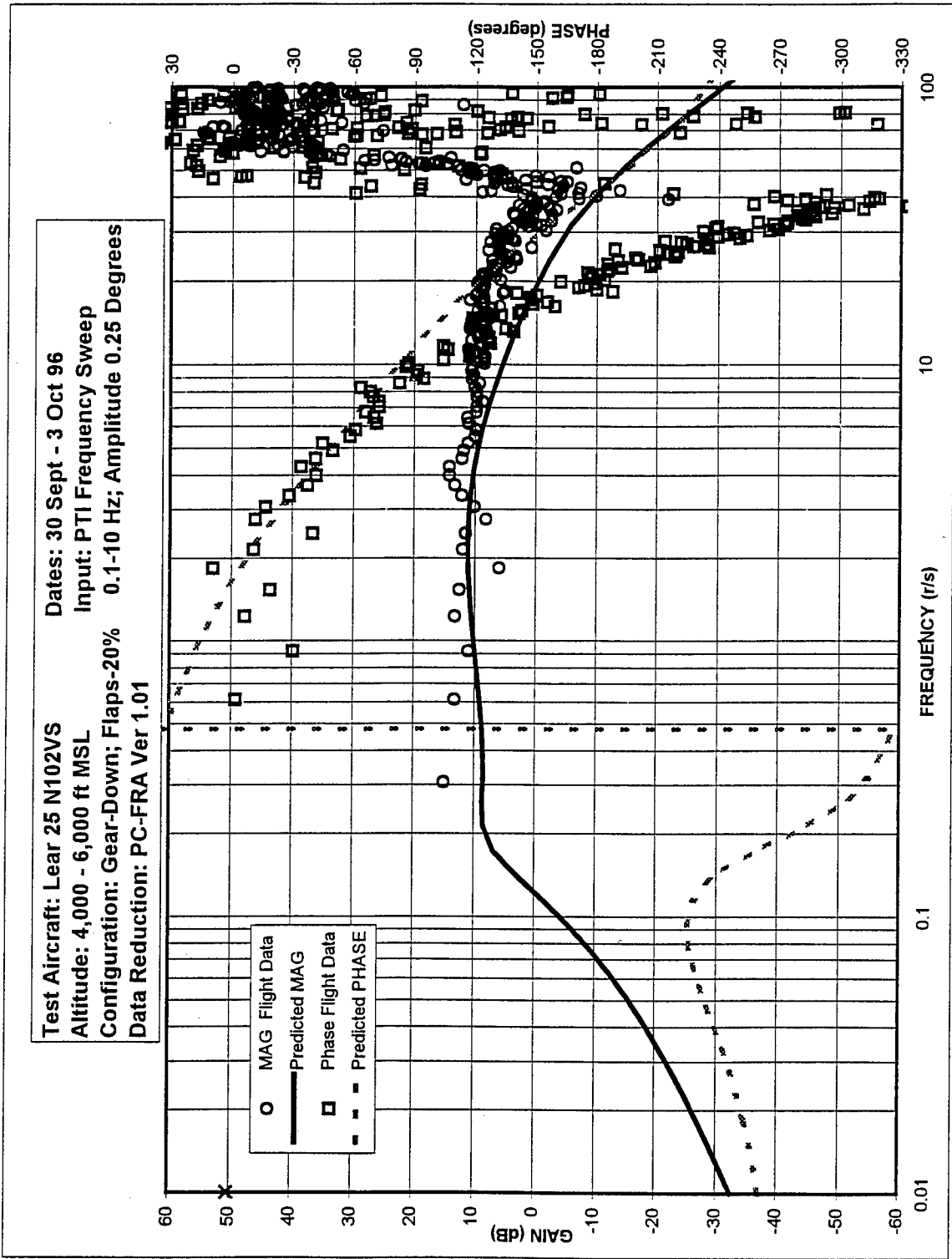


Figure E-6: H-Infinity Design Bode Plot, Closed Loop, Pitch Rate/PTI Sweep

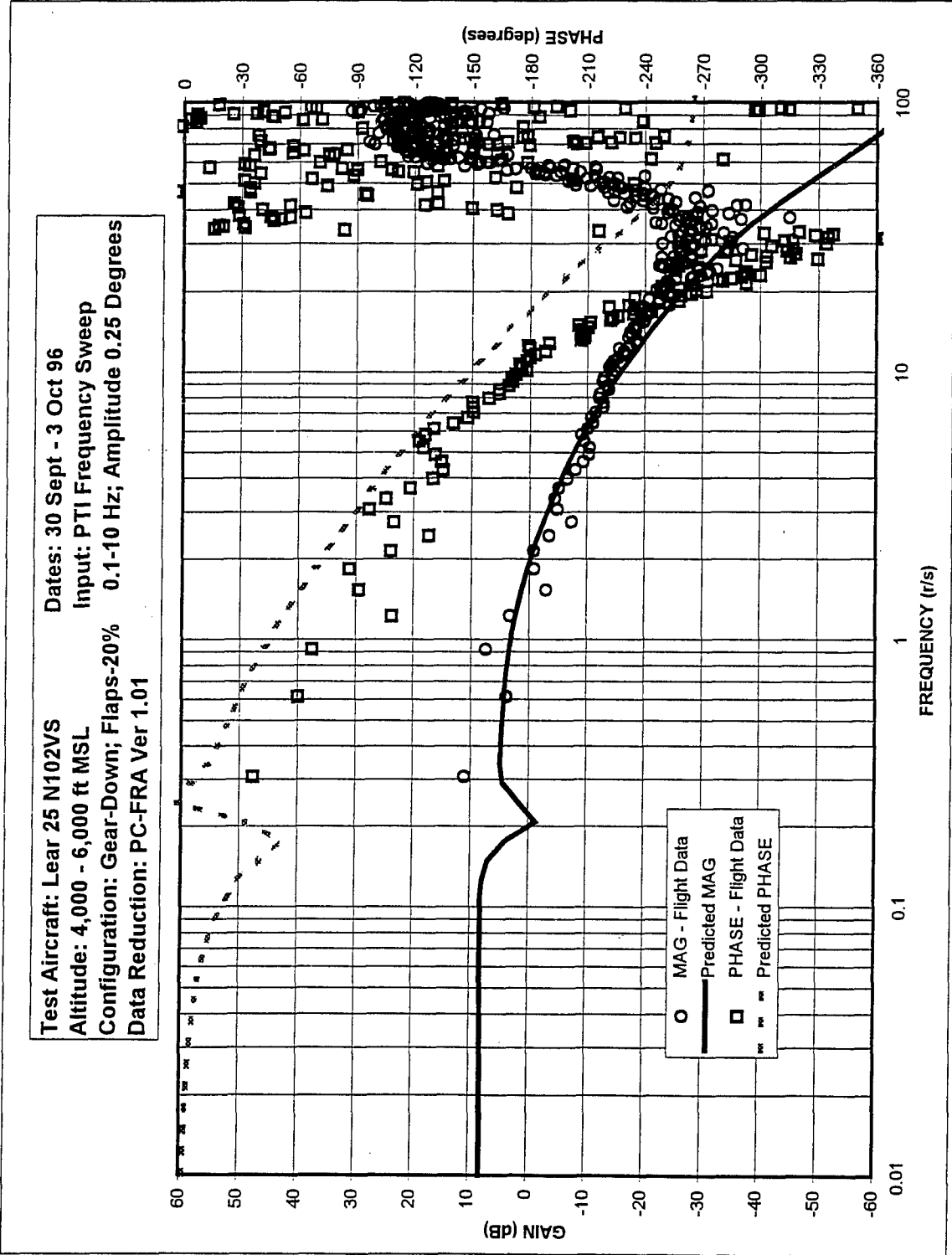


Figure E-7: Mixed Design Bode Plot, Closed Loop, Alpha/PTI Sweep

Test Aircraft: Lear 25 N102VS **Dates:** 30 Sept - 3 Oct 96
Altitude: 4,000 - 6,000 ft MSL **Input:** PTI Frequency Sweep
Configuration: Gear-Down; Flaps-20% **0.1-10 Hz; Amplitude 0.25 Degrees**
Data Reduction: PC-FRA Ver 1.01

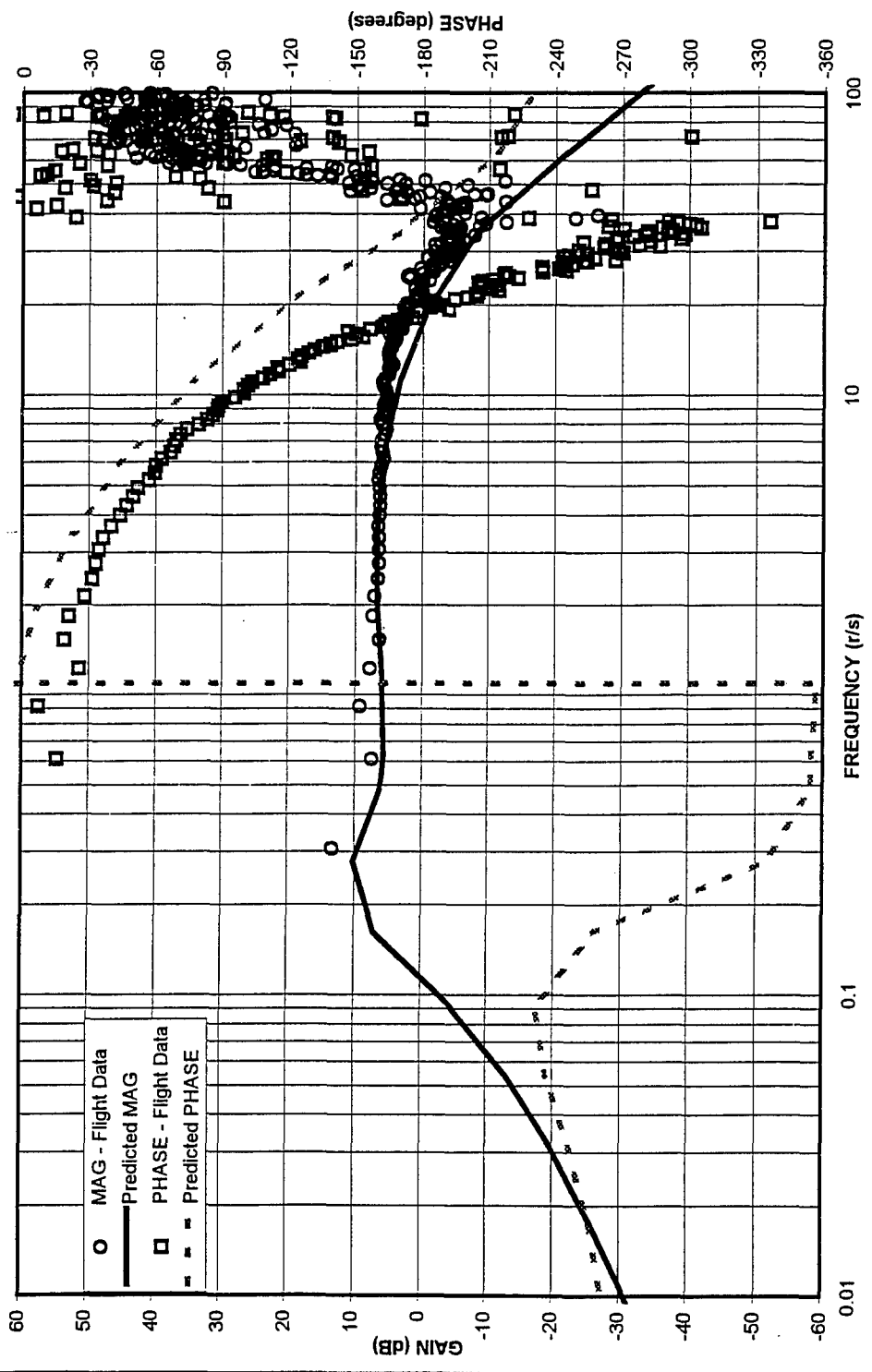


Figure E-8: Mixed Design Bode Plot, Closed Loop, Pitch Rate/PTI Sweep

Test Aircraft: Lear 25 N102VS	Date: 3 Oct 96
Altitude: 4,000 - 6,000 ft MSL	Input: Step, 1" stick displacement
Configuration: Gear - Down; Flaps - 20 %	— Flight Test Data
MATLAB Model Prediction

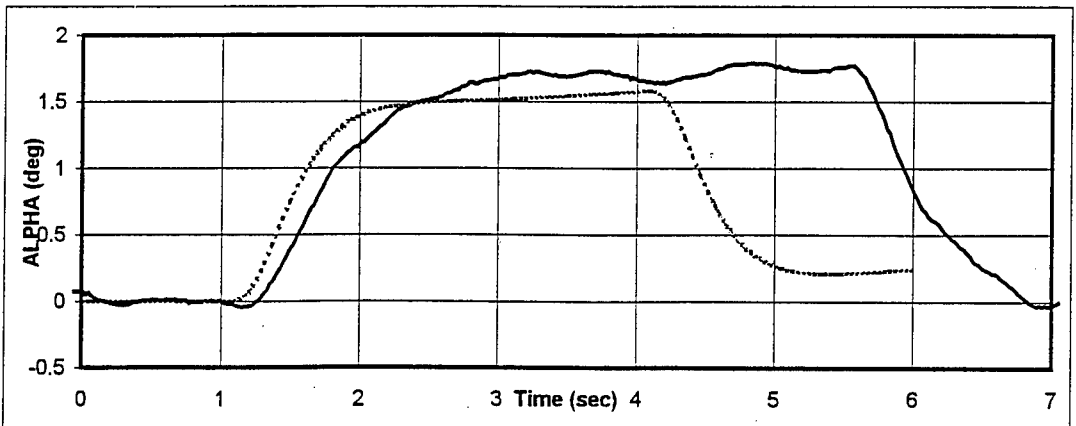
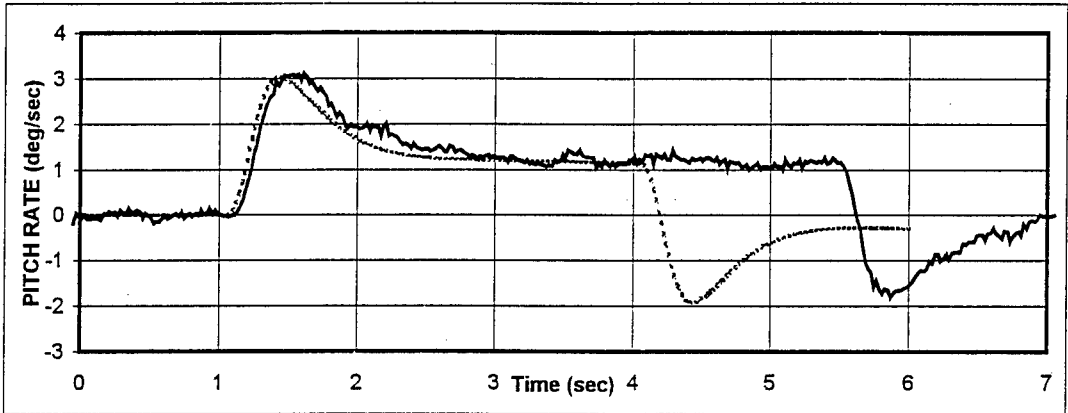
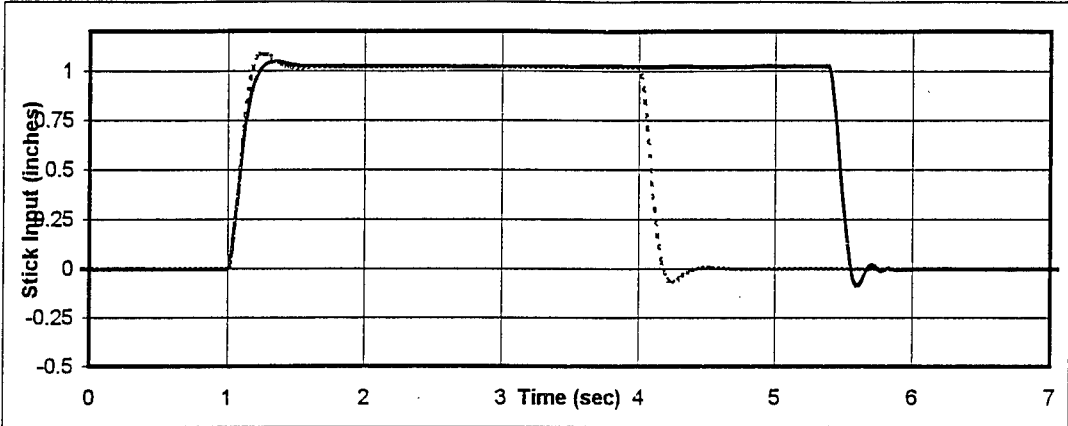


Figure E-9: Step Input Time Histories, Classical Design

Test Aircraft: Lear 25 N102VS	Date: 3 Oct 96
Altitude: 4,000 - 6,000 ft MSL	Input: Step, 1" stick displacement
Configuration: Gear - Down; Flaps - 20 %	— Flight Test Data
 MATLAB Model Prediction

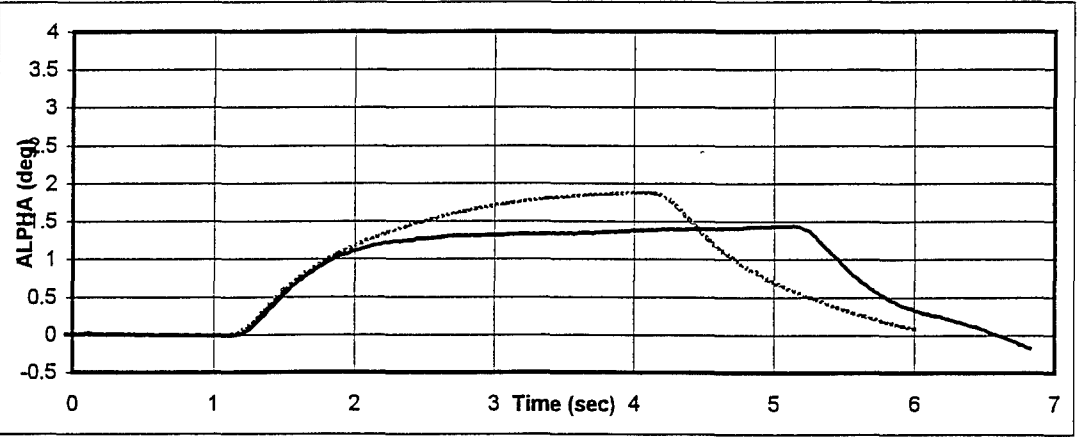
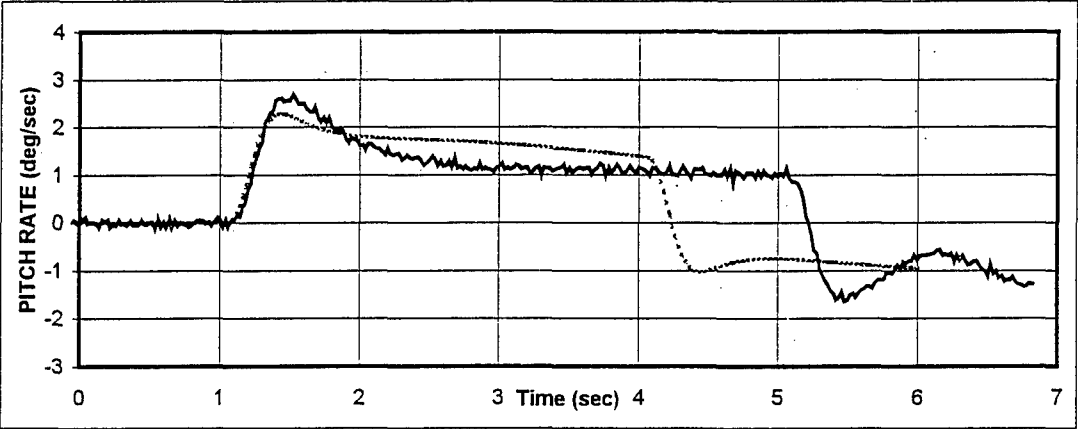
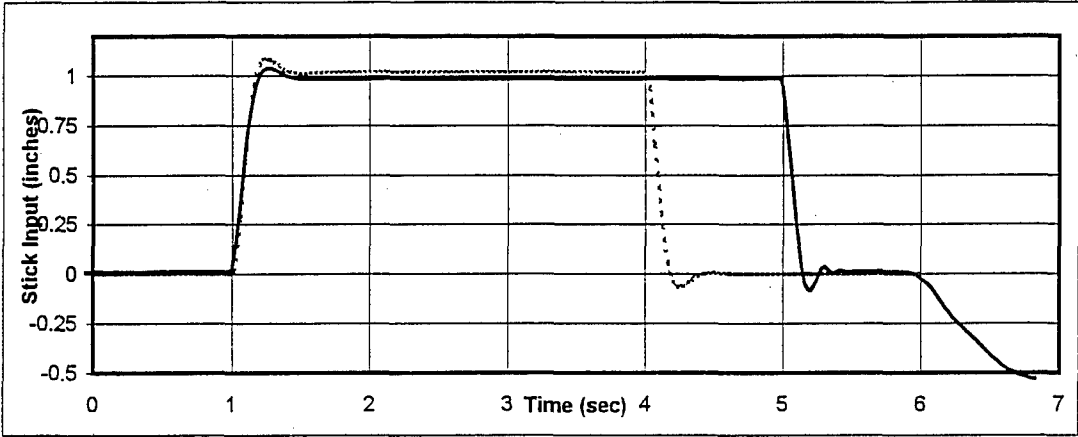


Figure E-10: Step Input Time Histories, H-2 Design

Test Aircraft: Lear 25 N102VS	Date: 3 Oct 96
Altitude: 4,000 - 6,000 ft MSL	Input: Step, 1" stick displacement
Configuration: Gear - Down; Flaps - 20 %	— Flight Test Data
MATLAB Model Prediction

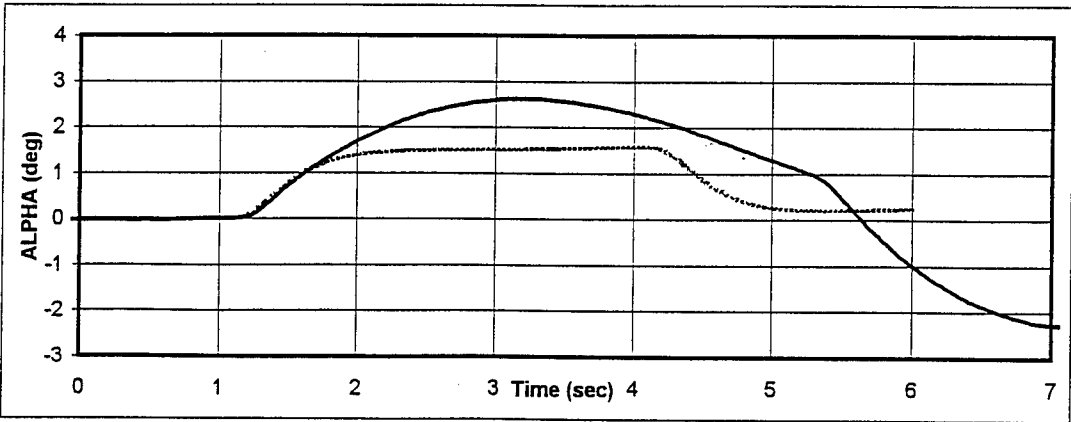
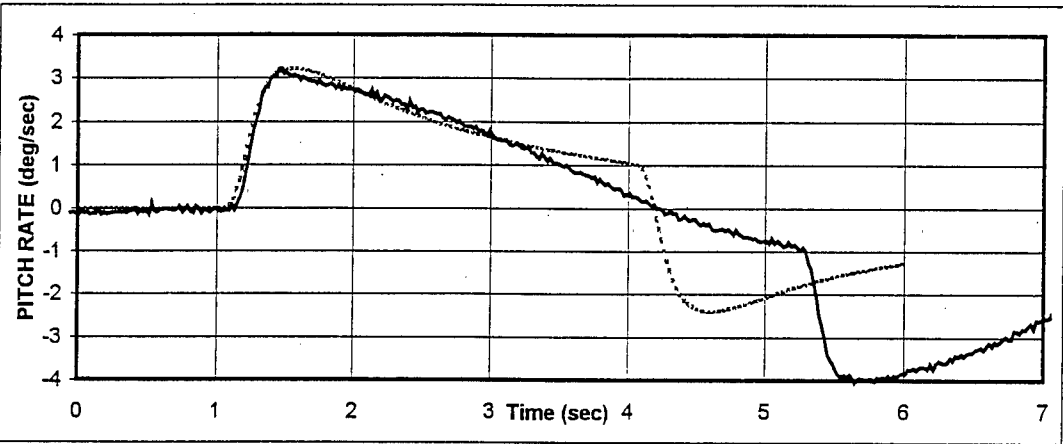
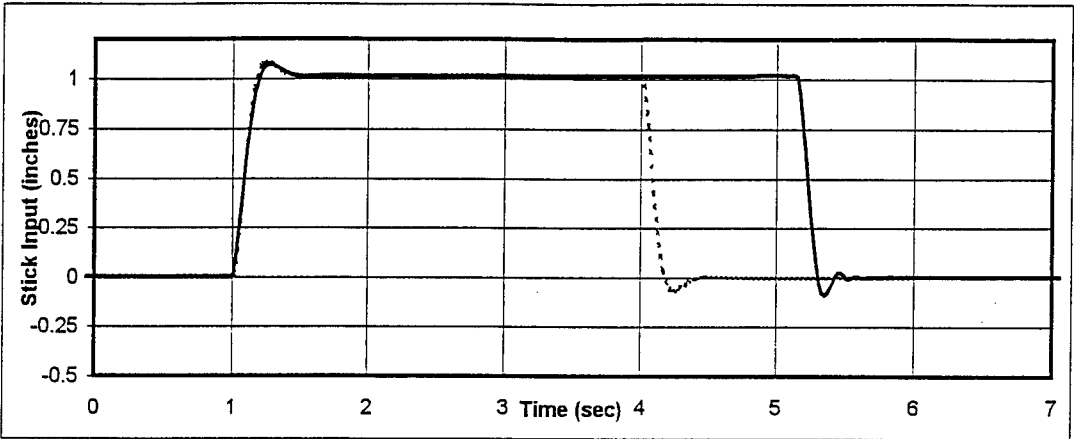


Figure E-11: Step Input Time Histories, H-Infinity Design

Test Aircraft: Lear 25 N102VS	Date: 3 Oct 96
Altitude: 4,000 - 6,000 ft MSL	Input: Step, 1" stick displacement
Configuration: Gear - Down; Flaps - 20 %	— Flight Test Data
	---- MATLAB Model Prediction

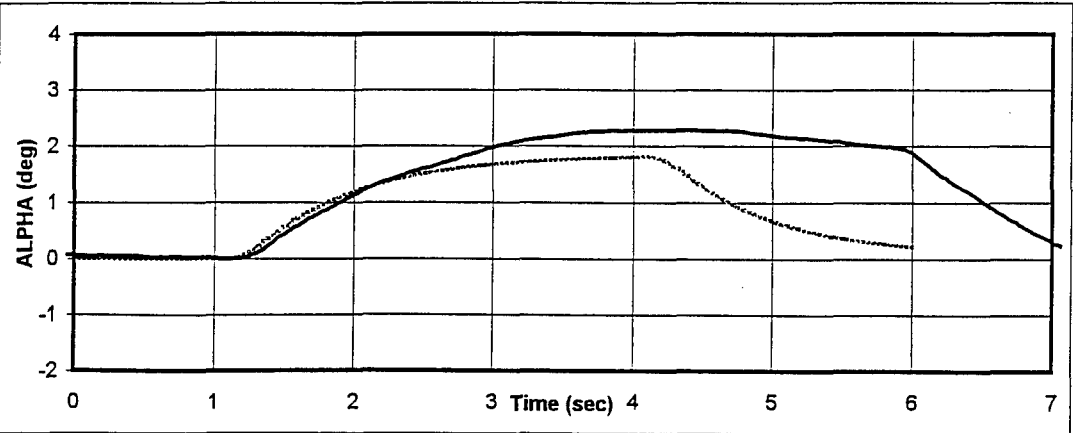
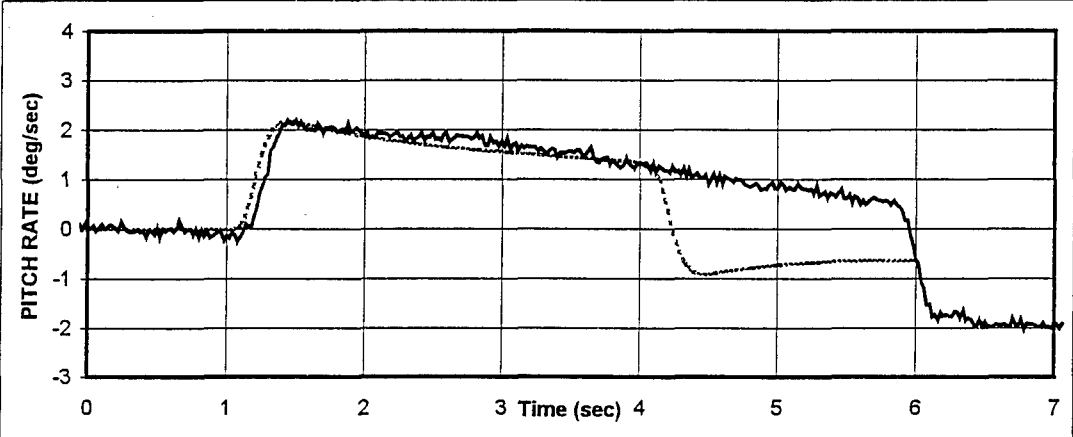
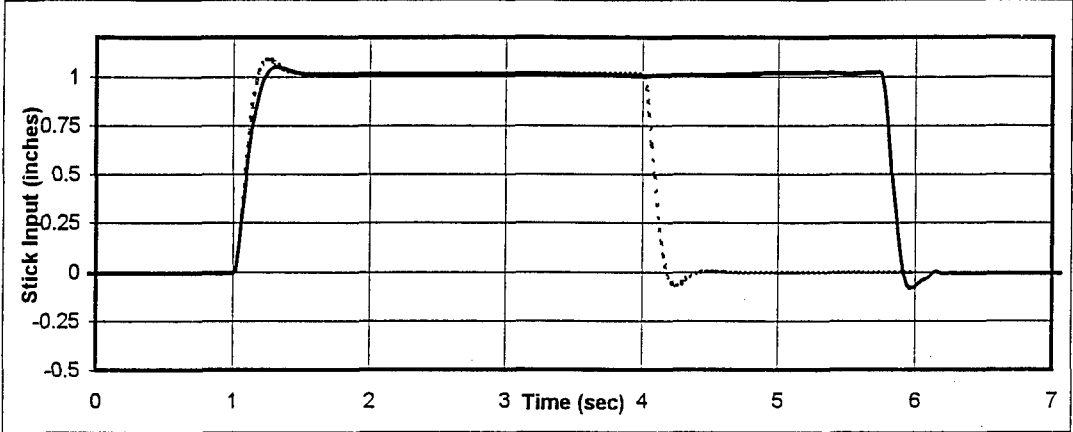


Figure E-12: Step Input Time Histories, Mixed Design

APPENDIX F

Test Card and Rating Scales

∞ HAVE INFINITY TEST CARD		DATE:	CARD#:
EVAL PILOT:		TEST BLOCK:	
SAFETY PILOT:		TEST PT:	
TEST CONDUCTOR:		CONFIG:	
WINDS:	TURB:	RWY:	
FUEL:	APP SPEED:	TD SPEED:	
/			
TASK: Intercept ILS glideslope and offset 300' laterally. At 200' AGL, correct to centerline by 100' AGL using 30 to 45 degrees of bank. Intercept a visual glidepath to touchdown in desired box.			
CH:		PIO:	
LANDING:	Desired	Adequate	No Good
INITIAL RESPONSE:	SLOW	-----	
SENSITIVITY:	LOW	-----	
PREDICTABILITY:	BAD	-----	
WORKLOAD:	LOW	-----	
QUICK			
HIGH			
GOOD			
HIGH			
COMPENSATION (Type):			
UNDESIRABLE MOTIONS (When/Type):			
PROBLEMS EFFECTING TASK:			
Wind			
Turbulence			
Offset			
Glideslope			
Correction			
Lateral Control			
Flare			
Power Control			
Touchdown			
VSS Trip			
GEN HANDLING QUALITIES:			

Figure F1 Sample Test Card

COOPER-HARPER RATING SCALE

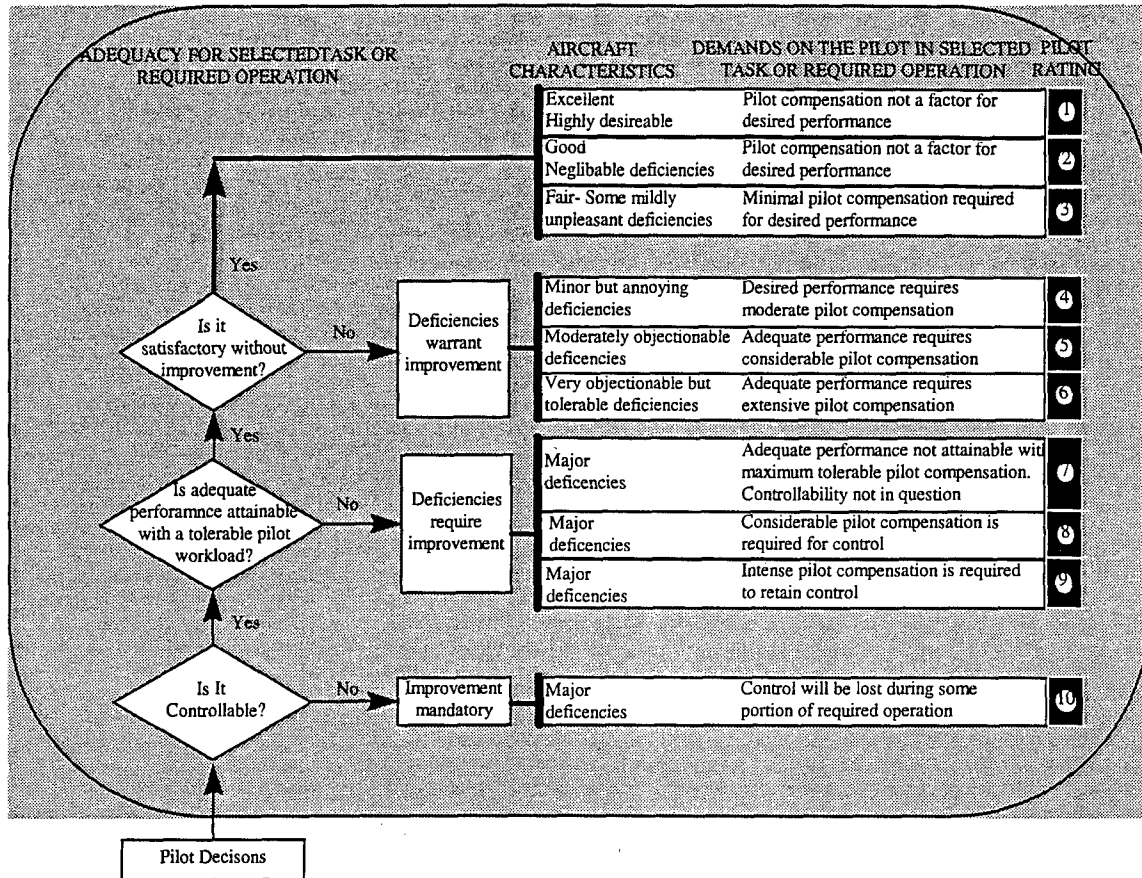


Figure F2 Cooper Harper Rating Scale

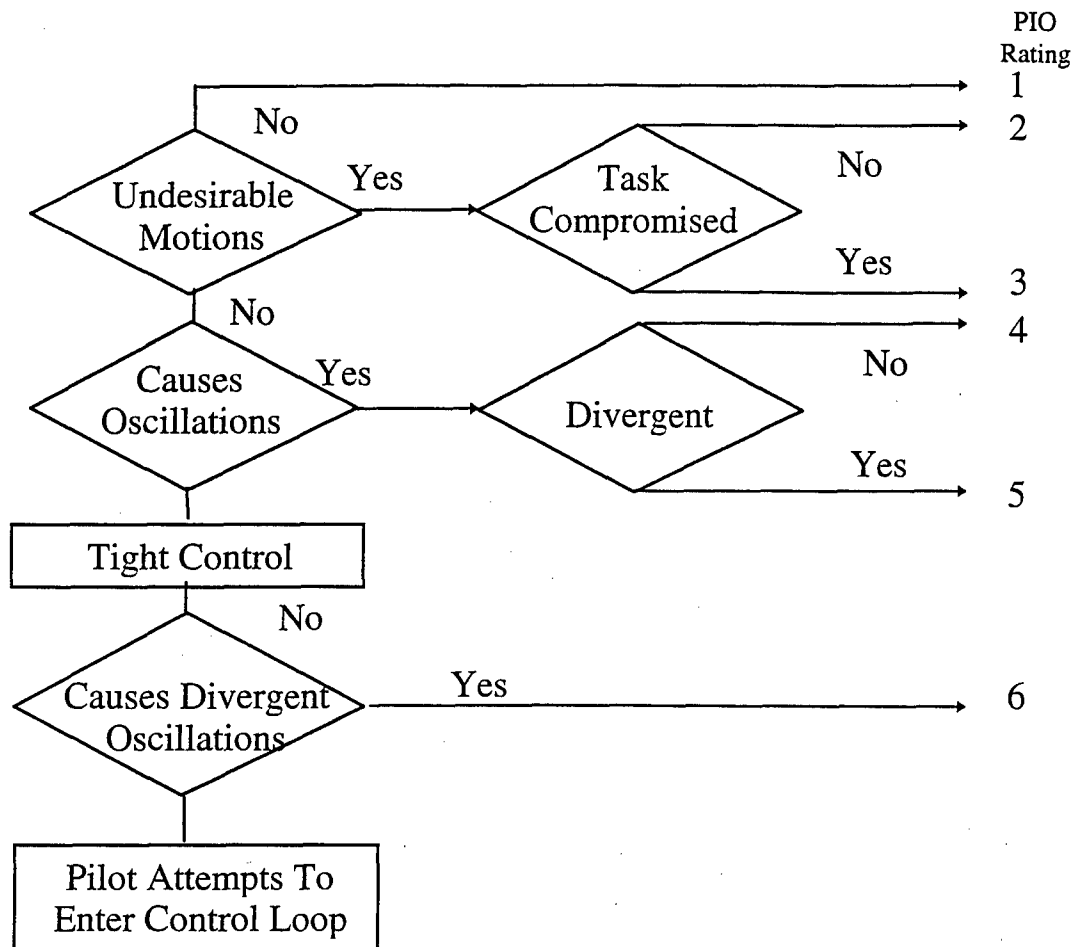


Figure F3 PIO Rating Decision Tree

PIO 1 – No tendency for pilot to induce undesirable motion.

PIO 2 – Undesirable motion tends to occur when pilot initiates abrupt maneuvers or attempts tight control. These motions can be prevented or eliminated by pilot technique.

PIO 3 – Undesirable motions easily induced when pilot initiates abrupt maneuvers or attempts tight control. These motions can be prevented or eliminated, but only at sacrifice to task performance or through considerable pilot attention and effort.

PIO 4 – Oscillations tend to develop when pilot initiates abrupt maneuvers or attempts tight control. Pilot must reduce gain or abandon task to recover.

PIO 5 – Divergent oscillations tend to develop when pilot initiates abrupt maneuvers or attempts tight control. Pilot must reduce gain or abandon task to recover.

PIO 6 – Disturbance or normal control may cause divergent oscillation. Pilot must open control loop by releasing or freezing the stick.

Appendix G

Pilot Comments Data Base

CONFIGURATION ID Classical

Mission date: 30 Sep 96

Eval pilot: Fittante

Flight # 1

Handling qualities: The aircraft was responsive and predictable. Overall the pilot stated that this configuration had nice handling qualities.

Landing: The nose tracked well and the task was easy to perform.

Appr	Landing zone	Turb	Wind	C-H Rating	PIO Rating
1	Desired	none	calm	3	1
2	Desired	none	calm	3	1
3	Desired	none	calm	3	1

Notes on C-H: All four had desired performance and minimal workload.

Notes on PIO Rating: No undesirable motions were noted.

Mission date: 1 Oct 96

Eval pilot: Edwards

Flight # 2

Handling qualities: The aircraft had a quick response and was fairly predictable with moderate to high sensitivity.

Landing: There was no tendency to balloon or bounce with this configuration.

Appr	Landing zone	Turb	Wind	C-H Rating	PIO Rating
1	Desired	Light	vrbl/4	4	2
2	Desired	Light	vrbl/4	4	1

Notes on C-H: Moderate workload was required because the response of this configuration required the pilot to make quick, abrupt inputs to maintain glide path.

Notes on PIO Rating: There was a tendency to over flare for the first approach and no unwanted motions were perceived on the second approach.

CONFIGURATION ID Classical

Mission date: 2 Oct 96

Eval pilot: Malacrida

Flight # 3

Handling qualities: The aircraft predictability was good and the sensitivity was nice. The stick was a bit heavy.

Landing: No problems noted on landing.

Appr	Landing zone	Turb	Wind	C-H Rating	PIO Rating
1	Desired	none	180/3	4	2
2	Desired	none	180/3	4	2

Notes on C-H: The pilot described his workload as moderate, but also commented that this is a borderline level one design.

Notes on PIO Rating: A slight bobble resulted during the ILS glideslope capture and resulted in a PIO 2.

Mission date: 2 Oct 96

Eval pilot: Fittante

Flight # 4

Handling qualities: The aircraft had good response with fairly light stick forces.

Landing: The aircraft nose stayed down after landing.

Appr	Landing zone	Turb	Wind	C-H Rating	PIO Rating
1	Desired	none	vr/b/5	3	1

Notes on C-H: Minimal workload was required.

Notes on PIO Rating: No unwanted motions were observed.

Mission date: 3 Oct 96

Eval pilot: Bouchard

Flight # 5

Handling qualities: The aircraft had moderate to slow initial response, with moderate sensitivity, predictability and workload.

Landing: The pilot felt he flared a little to high which resulted in a firm landing for the first approach and the aircraft had excessive aft stick required for flare.

Appr	Landing zone	Turb	Wind	C-H Rating
1	Adequate	none	220/6	5
2	Desired	none	220/6	4

Notes on C-H: A CH 5 was given for the first approach because of adequate performance, but the pilot commented that the handling qualities were more representative of CH 3. The second approach was given a CH 4 because of moderate compensation in the form of excessive aft stick required to flare.

CONFIGURATION ID H₂

Mission date: 30 Sep 96

Eval pilot: Fittante

Flight # 1

Handling qualities: The aircraft had heavy stick forces and didn't want to move. It was very stable with a dead beat response, and was unresponsive. Sharp inputs caused a slight pitch bobble.

Landing: The aircraft was not evaluated for control after touchdown since the evaluation pilot tripped off the VSS.

Appr	Landing zone	Turb	Wind	C-H Rating	PIO Rating
1	Desired	none	calm	4	2
2	Desired	none	calm	4	2
3	Desired	none	calm	4	2

Notes on C-H: On the second approach the initial correction was input with the aircraft one dot above glideslope causing a third approach.

Notes on PIO Rating: The rating of 2 was given due to the slight pitch bobble.

Mission date: 1 Oct 96

Eval pilot: Edwards

Flight # 2

Handling qualities: The aircraft was very quick in response, jittery, and required low gain smooth inputs to obtain the desired results.

Landing: During the flare the stick had to be rapidly brought forward to lower the nose.

Appr	Landing zone	Turb	Wind	C-H Rating	PIO Rating
1	Desired	Light	160/3	5	3
2	Desired	Light	230/6	4	1

Notes on C-H: Sensitivity to control inputs made the aircraft unpredictable which increased workload for the first approach. For the second approach workload decreased due to a learning curve.

Notes on PIO Rating: Undesirable motions caused the rating of 3 for the first approach, but were not perceived on the second approach which was given a rating of 1.

CONFIGURATION ID H₂

Mission date: 2 Oct 96

Eval pilot: Malacrida

Flight # 3

Handling qualities: The aircraft had poor pitch predictability for higher gain inputs. The initial response of the aircraft was slow and sensitivity was low.

Landing: The pilot needed small pulse inputs to flare. The aircraft was barely controllable on the ground requiring high pilot compensation.

Appr	Landing zone	Turb	Wind	C-H Rating	PIO Rating
1	Desired	none	280/6	8	4
2	Desired	none	280/6	8	4

Notes on C-H: The pilot had full forward stick applied at touchdown and still had difficulty keeping the aircraft on the ground.

Notes on PIO Rating: Significant non oscillatory, undesirable motions were seen on the ground.

Mission date: 2 Oct 96

Eval pilot: Fittante

Flight # 4

Handling qualities: The aircraft had heavy stick forces and was sluggish. The heavier forces and delayed response produced a little oscillation on final.

Landing: At approximately two seconds after touchdown full forward stick was required to keep the nose from pitching up.

Appr	Landing zone	Turb	Wind	C-H Rating	PIO Rating
1	Desired	none	vrh/5	6	3
2	Desired	none	vrh/5	8	3

Notes on C-H: Compensation was mainly required for the sluggish pitch response and the pitch up after landing. On the second approach controllability was in question after touchdown.

Notes on PIO Rating: The rating of 3 was given for the undesired motion on final.

Mission date: 3 Oct 96

Eval pilot: Bouchard

Flight # 5

Handling qualities: The aircraft had low sensitivity, bad predictability and high workload. On final approach the aircraft seemed to handle fine.

Landing: On the straight in at touchdown the aircraft bounced and began an uncontrollable pitch up maneuver upon which the safety pilot disengaged the VSS and initiated a go around.

Notes on C-H: Although this test did not consider the straight in an operational task with regards to Cooper Harper ratings, the configuration was deemed uncontrollable.

CONFIGURATION ID H₂

Mission date: 3 Oct 96

Eval pilot: Malacrida

Flight # 6

Handling qualities: The initial response of the aircraft was good but the sensitivity was low to moderate and the predictability was bad.

Landing: At approximately two seconds after touchdown full forward stick was required to keep the nose from pitching up.

Appr	Landing zone	Turb	Wind	C-H Rating	PIO Rating
1	Not adequate	none	vrb/5	7	4

Notes on C-H: The CH 7 was based on the long landing and the problems in the flare.

Notes on PIO Rating: The task was abandon due to pitch bobble and uncommanded pitch up.

Mission date: 3 Oct 96

Eval pilot: Bouchard

Flight # 6

Handling qualities: The aircraft had good initial response with slightly low sensitivity and bad predictability.

Landing: Forward stick required in flare and landing to keep the aircraft from ballooning.

Appr	Landing zone	Turb	Wind	C-H Rating	PIO Rating
1	Desired	none	vrb/5	10	1
2	Desired	none	vrb/5	9	1

Notes on C-H: The aircraft was uncontrollable after touch down for the first approach and with full stick on the second approach the aircraft marginal control on roll out.

CONFIGURATION ID H.

Mission date: 1 Oct 96

Eval pilot: Edwards

Flight # 2

Handling qualities: The stick inputs were sensitive with a quick initial response, glidepath was not difficult to maintain

Landing: The aircraft wanted to float in the flare. During the flare the stick had to be brought forward to prevent ballooning.

Appr	Landing zone	Turb	Wind	C-H Rating	PIO Rating
1	Safety trip	Light	190/5	7	2
2	Adequate	Light	190/5	7	2

Notes on C-H: On the first rated approach the safety pilot took control prior to touchdown due to a high sink rate. On the second approach touched down in the adequate box with the aircraft ballooning.

Notes on PIO Rating: A PIO of 2 was given due to unwanted motion in the flare.

Mission date: 2 Oct 96

Eval pilot: Malacrida

Flight # 3

Handling qualities: The aircraft was predictable and had good pitch response until the pilot gains were increased.

Landing: The aircraft had a tendency to float on the runway. Too much forward stick was required during the flare.

Appr	Landing zone	Turb	Wind	C-H Rating	PIO Rating
1	Not Adequate	none	280/6	7	3
2	Adequate	none	280/6	5	3
3	Not Adequate	none	280/6	7	3

Notes on C-H: Workload was not an issue, poor performance drove the CH 5 and 7's.

Notes on PIO Rating: The unwanted motion of the heave and float at flare resulted in a PIO 3.

CONFIGURATION ID H.

Mission date: 2 Oct 96

Eval pilot: Fittante

Flight # 4

Handling qualities: The aircraft had good aircraft response through the correction to centerline with light pitch forces.

Landing: The aircraft wanted to float and forward stick was required for touchdown. Full forward stick was required to keep the nose on the runway.

Appr	Landing zone	Turb	Wind	C-H Rating	PIO Rating
1	Desired	none	vrh/5	8	3
2	Desired	none	vrh/5	8	3

Notes on C-H: The aircraft was just barely controllable for both landings after touchdown.

Notes on PIO Rating: A PIO rating of 3 was assigned for the easily induced jittery aircraft response during the flare as stick forces became lighter.

Mission date: 2 Oct 96

Eval pilot: Edwards

Flight # 4

Handling qualities: The lateral correction was easily accomplished with heavy stick forces.

Landing: The aircraft had a tendency to balloon in the flare and full forward stick was required to keep the aircraft on the ground.

Appr	Landing zone	Turb	Wind	C-H Rating	PIO Rating
1	Desired	none	200/5	8	2
2	Desired	none	200/5	7	2

Notes on C-H: Pilot workload to prevent the aircraft from pitching up drove the CH ratings.

Notes on PIO Rating: A PIO of 2 was given due to unwanted motion during and after touchdown.

Mission date: 3 Oct 96

Eval pilot: Bouchard

Flight # 5

Handling qualities: The aircraft had moderate to quick initial response, with moderate to highly sensitive, slightly unpredictable and moderate workload.

Landing: Forward stick was required to keep the nose down.

Appr	Landing zone	Turb	Wind	C-H Rating
1	Desired	none	220/6	7
2	Desired	none	220/6	9

Notes on C-H: The design was considered level 3 because of the roll out characteristics. The first received a CH 7 because of extensive pilot compensation without questionable controllability. The second received a CH 9 because controllability was in question after touchdown.

CONFIGURATION ID H.

Mission date: 3 Oct 96

Eval pilot: Malacrida

Flight # 6

Handling qualities: The aircraft had adequate initial response and sensitivity but it had bad predictability.

Landing: A forward stick was required at flare to keep the aircraft from ballooning.

Appr	Landing zone	Turb	Wind	C-H Rating	PIO Rating
1	Not adequate	none	vrb/5	7	3

Notes on C-H: The aircraft landed long.

Notes on PIO Rating: The rating of 3 was given for the undesired motion on final.

Mission date: 3 Oct 96

Eval pilot: Bouchard

Flight # 6

Handling qualities: The aircraft had adequate initial response with low sensitivity and bad predictability.

Landing: After touchdown forward stick was required to keep the nose from pitching up.

Appr	Landing zone	Turb	Wind	C-H Rating	PIO Rating
1	Adequate	none	vrb/5	6	1

Notes on C-H: The aircraft landed in the adequate zone with high workload.

CONFIGURATION ID Mixed H₂/H_∞

Mission date: 1 Oct 96

Eval pilot: Edwards

Flight # 2

Handling qualities: The aircraft handled well coming down final and during the offset task. The aircraft initial response seemed slow.

Landing: During the flare the stick had to be brought forward to prevent ballooning.

Appr	Landing zone	Turb	Wind	C-H Rating	PIO Rating
1	Desired	none	230/6	5	2
2	Desired	none	230/6	8	2

Notes on C-H: On the first approach a CH 5 was given due to high workload. On the second approach a CH 8 was given due to unpredictable aircraft motion after touchdown

Notes on PIO Rating: A PIO of 2 was given due to unwanted motion after touchdown.

Mission date: 2 Oct 96

Eval pilot: Malacrida

Flight # 3

Handling qualities: The aircraft felt heavy with a sluggish response and was not terribly predictable.

Landing: The aircraft exhibited a heave with the flare.

Appr	Landing zone	Turb	Wind	C-H Rating	PIO Rating
1	Adequate	none	280/6	7	3
2	Not adequate	none	280/6	7	3

Notes on C-H: The pilot gave CH 7 because of the high workload and extensive compensation. The pilot had to consciously lower his gains and apply his inputs early.

Notes on PIO Rating: The unwanted motion of the heave at flare resulted in a PIO 3.

Mission date: 2 Oct 96

Eval pilot: Fittante

Flight # 4

Handling qualities: The aircraft had slightly high stick forces and pitch control was solid during transition to landing until just prior to touchdown.

Landing: At touchdown there was a sudden reversal in pitch force, requiring full forward stick to keep the nose on the runway.

Appr	Landing zone	Turb	Wind	C-H Rating	PIO Rating
1	Desired	none	vr/5	8	1
2	Desired	none	vr/5	8	1

Notes on C-H: CH 8 was given for controllability during and after touchdown.

Notes on PIO Rating: The PIO rating of 1 was given because there was no longer a jittery response during the transition to landing.

CONFIGURATION ID Mixed H₂/H₁

Mission date: 2 Oct 96

Eval pilot: Edwards

Flight # 4

Handling qualities: The initial response was good with adequate sensitivity and bad predictability.

Landing: Full forward stick was applied after touchdown, but the aircraft became airborne again after both landings.

Appr	Landing zone	Turb	Wind	C-H Rating	PIO Rating
1	Desired	none	vrbl/5	8	2
2	Desired	none	vrbl/5	8	2

Notes on C-H: Considerable pilot compensation was required.

Notes on PIO Rating: A PIO of 2 was given due to unwanted motion after touchdown.

Mission date: 3 Oct 96

Eval pilot: Bouchard

Flight # 5

Handling qualities: The aircraft had moderate initial response, with low to moderate sensitivity, bad predictability and high workload.

Landing: At touchdown, during the straight in, the aircraft bounced and began an uncontrollable pitch up maneuver similar to configuration L. At this time the pilot requested the safety pilot to take control of the aircraft.

Notes on C-H: Although this test did not consider the straight in an operational task with regards to Cooper Harper ratings, the configuration was deemed uncontrollable.

Mission date: 3 Oct 96

Eval pilot: Malacrida

Flight # 6

Handling qualities: The aircraft had adequate initial response but moderately low sensitivity and bad predictability.

Landing: After touchdown forward stick was required to keep the nose from pitching up.

Appr	Landing zone	Turb	Wind	C-H Rating	PIO Rating
1	Not adequate	none	vrbl/5	7	3

Notes on C-H: The aircraft landed long.

Notes on PIO Rating: The rating of 3 was given for the undesired motion on final.

CONFIGURATION ID Mixed H₂/H_∞

Mission date: 3 Oct 96

Eval pilot: Bouchard

Flight # 6

Handling qualities: The aircraft had adequate initial response and sensitivity and bad predictability.

Landing: After touchdown full forward stick was required to keep the nose from pitching up.

Appr	Landing zone	Turb	Wind	C-H Rating	PIO Rating
1	Adequate	none	vrbl/5	6	1

Notes on C-H: Landed in the adequate zone and had high workload.

Appendix H

Flight Test Data

Cooper-Harper and PIO Ratings

Classical Design:

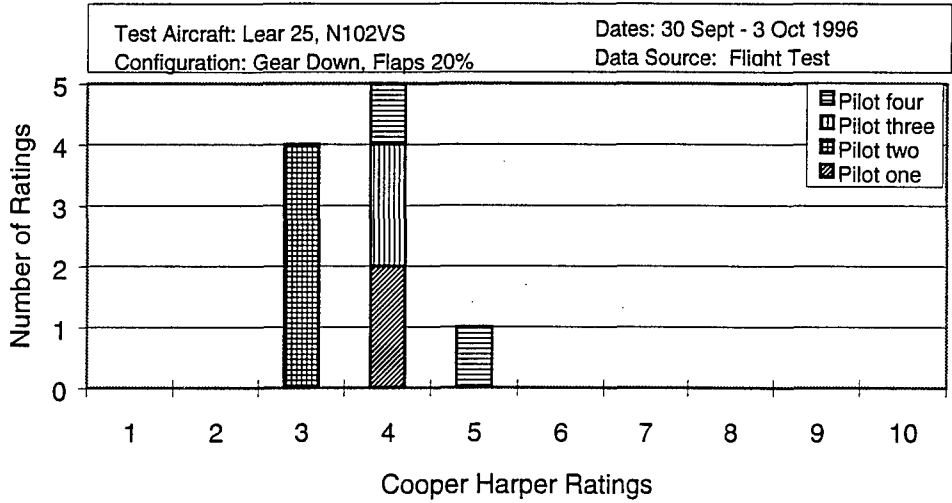


Figure H.1. Classical Flight Control Design Handling Quality Ratings

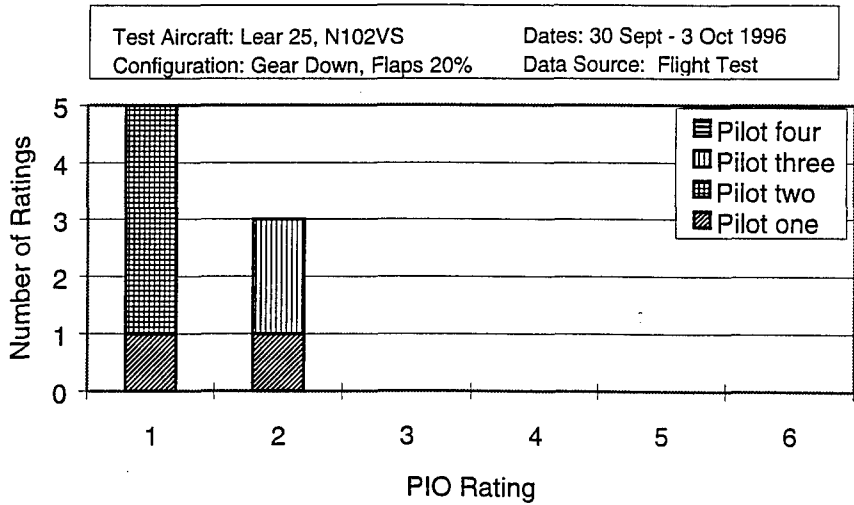


Figure H.2. Classical Flight Control Design Pilot Induced Oscillation Ratings

H₂ Design:

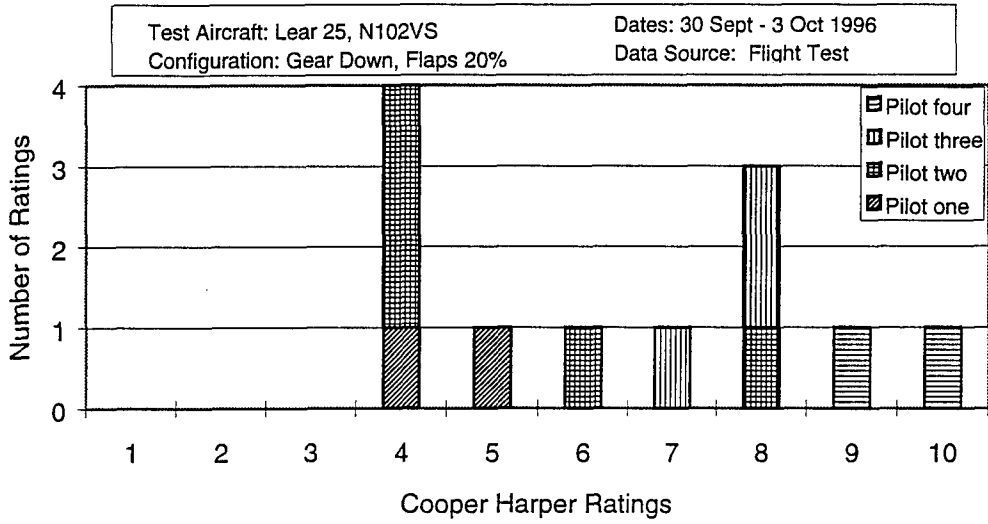


Figure H.3. H₂ Flight Control Design Handling Quality Ratings

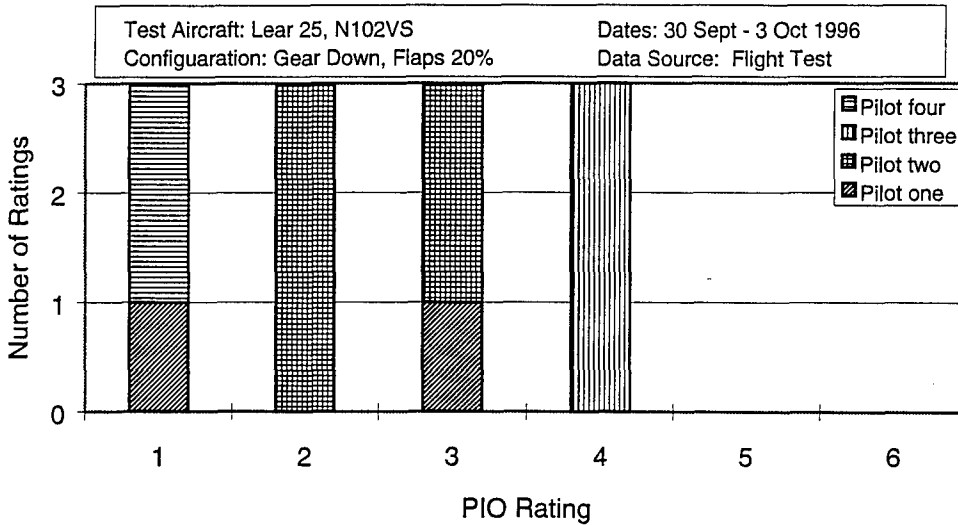


Figure H.4. H₂ Flight Control Design Pilot Induced Oscillation Ratings

H_∞ Design:

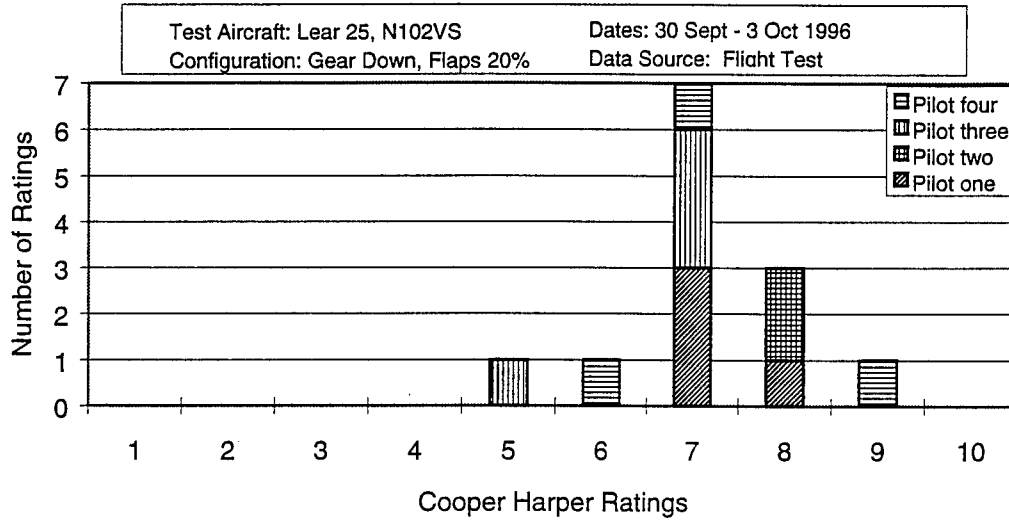


Figure H.5. H_∞ Flight Control Design Handling Quality Ratings

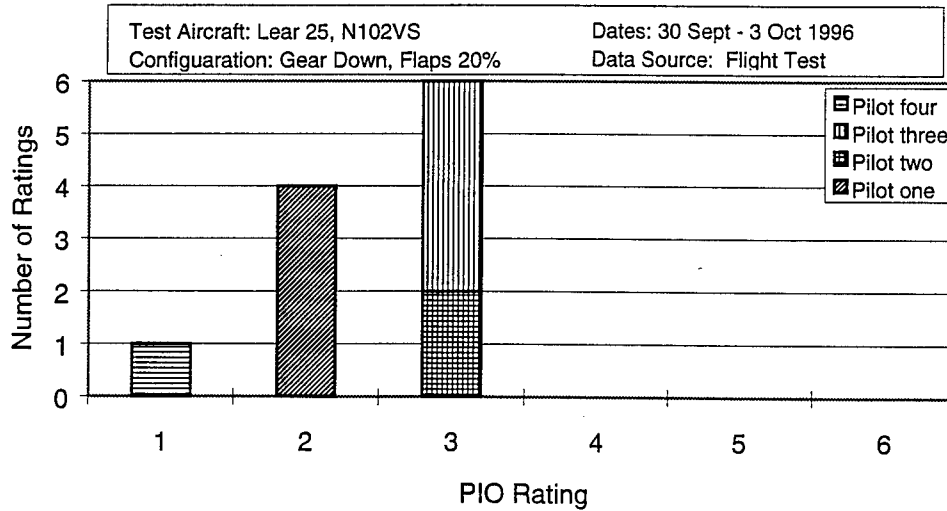


Figure H.6. H_∞ Flight Control Design Pilot Induced Oscillation Ratings

Mixed Design:

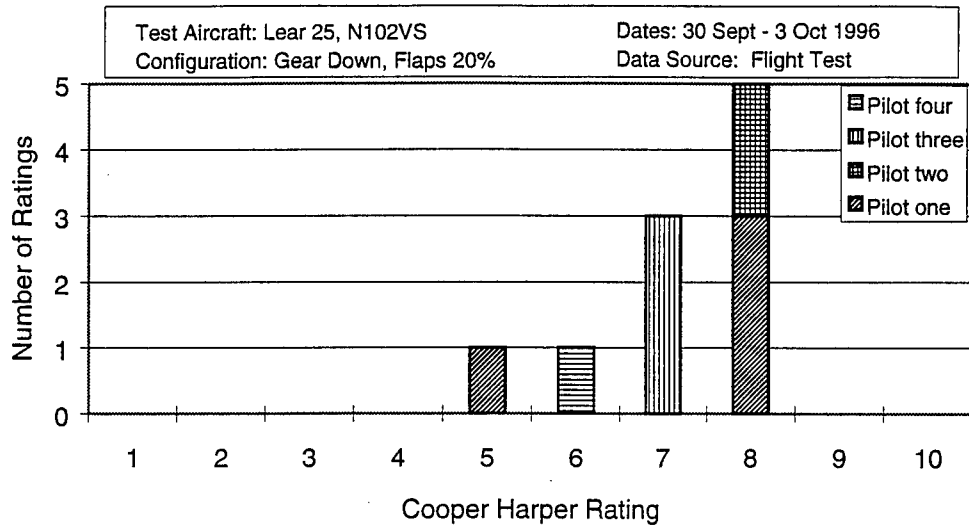


Figure H.7. Mixed Flight Control Design Handling Quality Ratings

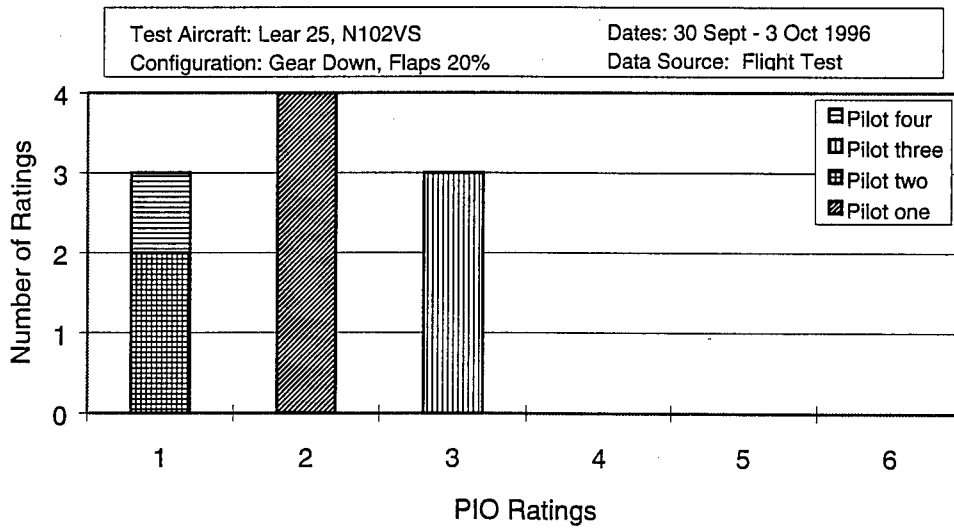


Figure H.8. Mixed Flight Control Design Pilot Induced Oscillation Ratings

Bibliography

- Bal93 Ball, J., et al., *Learjer Flight Syllabus abd Background Material for the U.S. Air Force/U.S. Navy Test Pilot School Variable Stability Programs*, Calspan Corporation, Buffalo NY, July 1993.
- Ber88 Berthe, C.J., et al., *Fly-By-Wire Design Considerations*, Presentation at The Society of Experimental Test Pilots 20th Annual European Symposium, Linkoping, Sweden, June 1988
- CH69 Cooper, George E., and Robert P. Harper, *The Use of Pilot Rating in the Evaluation of Aircraft Handling Qualities*, NASA Technical Note D-5153, National Aeronautics and Space Administration, Washington DC, April 1969.
- Dec94 Decker, Douglas D., *Flight Control Design using Mixed H_2/μ Optimization*, Master's Thesis, Air Force Institute of Technology, Dayton OH, December 1994.
- Doy89 Doyle, John C., et al., "State-Space Solutions to Standard H_2 and H_∞ Control Problems," in *IEEE Transactions on Automatic Control*, Vol. 34, No. 8, August 1989, pp 831-847.
- DFT92 Doyle, John C., Bruce A. Francis, and Allen R. Tannenbaum, *Feedback Control Theory*, Macmillan Publishing Company, New York NY, 1992.
- FPE91 Franklin, Gene F., J. David Powell, and Abbas Emami-Naeini, *Feedback Control of Dynamic Systems* (Third Edition), Addison-Westly Publishing Company, New York, 1994.
- Gan86 Gangsaas, Dagfinn, et al., "Application of Modern Synthesis to Aircraft Control: Three Case Studies," in *IEEE Transactions on Automatic Control*, Vol. AC-31, No. 11, November 1986, pp 995-1013.
- Hoh96 Hoh, Roger H., Class Lecture, "Highly Augmented Airplane Handling Qualities," USAF Test Pilot School, Edwards AFB CA, May 1996.
- Hoh81 Hoh, Roger H., et al., *Development of Flying Quality Criteria for Aircraft with Independent Control of Six Degrees of Freedom*, AFWAL-TR-81-3027, Wright-Patterson AFB OH, AFFDL, April 1981.
- MIL90 Military Standard, *Flying Qualities of Piloted Aircraft*, MIL-STD-1797A, 30 January 1990.
- MH90 Mitchell, David G. and Roger Hoh, *Concepts for a Mission-Oriented Flying Qualities Mil Standard*, Technical Report No. 1279-1, Hawthorne CA, Systems Technology Inc., July 1990.
- RB86 Ridgely, D. Brett, and Siva S. Banda, *Introduction To Robust Multivariable Control*, AFWAL-TR-85-3102, AFWAL/FIGC, Wright-Patterson AFB OH, February 1986
- Rid91 Ridgely, D. Brett, *A Nonconservative Solution to the General Mixed H_2/H_∞ Optimization Problem*, PhD Dissertation, Massachusetts Institute of Technology, Cambridge MA, 1991.
- RW95 Ridgely, D. Brett, and David E. Walker, "The General Mixed H_2/H_∞ Control Problem," July 1995, Submitted to *Automatica*
- SG79 Smith, Ralph H., and Norman D. Geddes, *Handling Qualities Requirements For Advanced Aircraft Design: Longitudinal Mode*, AFFDL-TR-86-44, AFFDL, Wright-Patterson AFB OH, August 1979

- TPS95 *USAF TPS Flying Qualities Phase Text Vol. IV, Flying Qualities Testing*, USAF TPS/EDF, Edwards AFB CA, June 1995.
- Wal94 Walker, D.E., *H₂ Optimal Control With H_∞, μ , and L₁ Constraints*, PhD Dissertation, Air Force Institute of Technology, AFIT/DS/AA/94-2, Wright-Patterson AFB OH, June 1994.
- WR94 Walker, D.E. and D.B. Ridgely, "Reduced Order Mixed H₂/H_∞ Optimization With a Singular H_∞ Constraint," in *Proceedings of the 1994 American Control Conference*, Baltimore MD, June 1994, pp 1,128-1,132.

Vita

Captain Phillip T. Edwards [REDACTED]. He graduated from Oak Park and River Forest High School, Oak Park, Illinois in 1983. He was appointed to the U. S. Air Force Academy where he earned his commission and a Bachelor of Science degree in Aeronautical Engineering in 1987. Captain Edwards attended Undergraduate Pilot Training at Vance AFB, OK, where he received his wings in September, 1988. He was assigned to the 18th Military Airlift Squadron (MAS), Military Airlift Command (MAC), McGuire AFB, NJ, flying the C-141B Starlifter. While at McGuire AFB, he became a flight evaluator and served as Assistant Chief, Airlift Training Section, 21 AF Standardization, Evaluation and Training. Captain Edwards was selected for the Joint Air Force Institute of Technology / USAF Test Pilot School program, and graduated from the Experimental Test Pilot course in December 1996. Upon completion of his studies, he will be assigned to the 418th Flight Test Squadron at Edwards AFB, California, flight testing the C-130J.

Permanent Address: 1123 N. Marion St
Oak Park, IL 60302

REPORT DOCUMENTATION PAGE

Form Approved
OMB No. 0704-0188

Public reporting burden for this collection of information is estimated to average 1 hour per response, including the time for reviewing instructions, searching existing data sources, gathering and maintaining the data needed, and completing and reviewing the collection of information. Send comments regarding this burden estimate or any other aspect of this collection of information, including suggestions for reducing this burden, to Washington Headquarters Services, Directorate for Information Operations and Reports, 1215 Jefferson Davis Highway, Suite 1204, Arlington, VA 22202-4302, and to the Office of Management and Budget, Paperwork Reduction Project (0704-0188), Washington, DC 20503.

1. AGENCY USE ONLY (Leave blank)	2. REPORT DATE March 1997	3. REPORT TYPE AND DATES COVERED Master's Thesis	
4. TITLE AND SUBTITLE MODERN FLIGHT CONTROL DESIGN, IMPLEMENTATION AND FLIGHT TEST		5. FUNDING NUMBERS JON: M96J0200 PEC: 65807F	
6. AUTHOR(S) Phillip T. Edwards, Captain, USAF		7. PERFORMING ORGANIZATION NAME(S) AND ADDRESS(ES) Air Force Institute of Technology, WPAFB OH 45433-6583	
8. PERFORMING ORGANIZATION REPORT NUMBER AFIT/GAE/ENY/97M-01		9. SPONSORING / MONITORING AGENCY NAME(S) AND ADDRESS(ES) WL/FIGC 2210 Eighth Street, Bldg 146, Suite 21 Wright-Patterson AFB, OH 45433-7531	
10. SPONSORING / MONITORING AGENCY REPORT NUMBER N/A		11. SUPPLEMENTARY NOTES	
12a. DISTRIBUTION / AVAILABILITY STATEMENT Approved for public release; distribution is unlimited		12b. DISTRIBUTION CODE A	
13. ABSTRACT (Maximum 200 words) This thesis addresses the application issues raised implementing flight control designs derived from optimal control theory and the challenges in obtaining acceptable handling qualities when using these techniques. Using the USAF TPS FCS project as the controller architecture, four controllers were designed using classical methods, and H_2 , H_∞ , and mixed H_2/H_∞ optimal control theory. These designs were implemented in the Calspan VSS II Learjet, simulating unstable aircraft longitudinal dynamics and a limited handling qualities flight test evaluation was performed. The design phase found the optimal control techniques, as applied, difficult to design to handling qualities specifications. The H_2 , H_∞ , and mixed H_2/H_∞ controllers were unstable and often contained high frequency poles, which were difficult to implement. The flight test rated the designs acceptable on approach, but no handling qualities level for approach was determined.			
14. SUBJECT TERMS handling qualities variable stability H_∞ Optimization		flight control systems optimal control theory Mixed H_2/H_∞ Optimization	VSS II Learjet H_2 Optimization
15. NUMBER OF PAGES 139		16. PRICE CODE	
17. SECURITY CLASSIFICATION OF REPORT UNCLASSIFIED	18. SECURITY CLASSIFICATION OF THIS PAGE UNCLASSIFIED	19. SECURITY CLASSIFICATION OF ABSTRACT UNCLASSIFIED	20. LIMITATION OF ABSTRACT SAR

GENERAL INSTRUCTIONS FOR COMPLETING SF 298

The Report Documentation Page (RDP) is used in announcing and cataloging reports. It is important that this information be consistent with the rest of the report, particularly the cover and title page. Instructions for filling in each block of the form follow. It is important to *stay within the lines* to meet *optical scanning requirements*.

Block 1. Agency Use Only (Leave blank).

Block 2. Report Date. Full publication date including day, month, and year, if available (e.g. 1 Jan 88). Must cite at least the year.

Block 3. Type of Report and Dates Covered. State whether report is interim, final, etc. If applicable, enter inclusive report dates (e.g. 10 Jun 87 - 30 Jun 88).

Block 4. Title and Subtitle. A title is taken from the part of the report that provides the most meaningful and complete information. When a report is prepared in more than one volume, repeat the primary title, add volume number, and include subtitle for the specific volume. On classified documents enter the title classification in parentheses.

Block 5. Funding Numbers. To include contract and grant numbers; may include program element number(s), project number(s), task number(s), and work unit number(s). Use the following labels:

C - Contract	PR - Project
G - Grant	TA - Task
PE - Program Element	WU - Work Unit Accession No.

Block 6. Author(s). Name(s) of person(s) responsible for writing the report, performing the research, or credited with the content of the report. If editor or compiler, this should follow the name(s).

Block 7. Performing Organization Name(s) and Address(es). Self-explanatory.

Block 8. Performing Organization Report Number. Enter the unique alphanumeric report number(s) assigned by the organization performing the report.

Block 9. Sponsoring/Monitoring Agency Name(s) and Address(es). Self-explanatory.

Block 10. Sponsoring/Monitoring Agency Report Number. (If known)

Block 11. Supplementary Notes. Enter information not included elsewhere such as: Prepared in cooperation with...; Trans. of...; To be published in.... When a report is revised, include a statement whether the new report supersedes or supplements the older report.

Block 12a. Distribution/Availability Statement. Denotes public availability or limitations. Cite any availability to the public. Enter additional limitations or special markings in all capitals (e.g. NOFORN, REL, ITAR).

DOD - See DoDD 5230.24, "Distribution Statements on Technical Documents."

DOE - See authorities.

NASA - See Handbook NHB 2200.2.

NTIS - Leave blank.

Block 12b. Distribution Code.

DOD - Leave blank.

DOE - Enter DOE distribution categories from the Standard Distribution for Unclassified Scientific and Technical Reports.

NASA - Leave blank.

NTIS - Leave blank.

Block 13. Abstract. Include a brief (*Maximum 200 words*) factual summary of the most significant information contained in the report.

Block 14. Subject Terms. Keywords or phrases identifying major subjects in the report.

Block 15. Number of Pages. Enter the total number of pages.

Block 16. Price Code. Enter appropriate price code (*NTIS only*).

Blocks 17. - 19. Security Classifications. Self-explanatory. Enter U.S. Security Classification in accordance with U.S. Security Regulations (i.e., UNCLASSIFIED). If form contains classified information, stamp classification on the top and bottom of the page.

Block 20. Limitation of Abstract. This block must be completed to assign a limitation to the abstract. Enter either UL (unlimited) or SAR (same as report). An entry in this block is necessary if the abstract is to be limited. If blank, the abstract is assumed to be unlimited.